



**PARAMETER STUDY FOR OPTIMIZING THE MASS  
OF A SPACE NUCLEAR POWER SYSTEM RADIATION SHIELD**

THESIS

Benjamin R. Kowash, 2<sup>nd</sup> Lieutenant, USAF  
AFIT/GNE/ENP/02M-04

**DEPARTMENT OF THE AIR FORCE  
AIR UNIVERSITY  
AIR FORCE INSTITUTE OF TECHNOLOGY**

---

---

Wright-Patterson Air Force Base, Ohio

APPROVED FOR PUBLIC RELEASE; DISTRIBUTION UNLIMITED.

The views expressed in this thesis are those of the author and do not reflect the official policy or position of the United States Air Force, Department of Defense, or the U. S. Government.

**PARAMETER STUDY FOR OPTIMIZING THE MASS  
OF A SPACE NUCLEAR POWER SYSTEM RADIATION SHIELD**

**THESIS**

Presented to the Faculty of the School of Engineering and Management  
of the Air Force Institute of Technology

Air University

In partial fulfillment of the requirements for the degree of  
Master of Science in Nuclear Engineering

Benjamin R. Kowash, B.S.

2<sup>nd</sup> Lieutenant, USAF

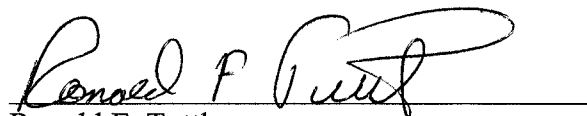
March 2002

APPROVED FOR PUBLIC RELEASE; DISTRIBUTION UNLIMITED.

**PARAMETER STUDY FOR OPTIMIZING THE MASS  
OF A SPACE NUCLEAR POWER SYSTEM RADIATION SHIELD**

Benjamin R. Kowash, B.S.  
2<sup>nd</sup> Lieutenant, USAF

Approved:



Ronald F. Tuttle  
Associate Professor of Engineering Physics  
Research Advisor

8 MAR 2002  
date



Kirk A. Mathews  
Professor of Nuclear Engineering

8 March 2002  
date



Shankar Mall  
Professor of Aerospace Engineering

3/8/02  
date

## **Acknowledgements**

My appreciation and thanks go out to all of the people who took the time to make a large portion of this research possible. I would especially like to thank my thesis advisor Dr. Ron Tuttle, whose guidance and critique of my methods kept the research on course. The members of my committee, Drs. Kirk Mathews and Shankar Mall, both took time out of their busy schedules to assist me with this work, for which I am very grateful. A special acknowledgement goes to Capt. Mark Suriano, who spent several hours of his own personal time, passing on his own experience with space nuclear power systems. Finally, I would like to thank my family, friends, and especially the members of the GNE-02M class who helped get me through this project in one piece.

Benjamin R. Kowash

## Table of Contents

Acknowledgements .....	iv
List of Figures .....	vii
List of Tables.....	viii
Abstract .....	ix
I. Introduction.....	1
Background .....	1
Problem Statement .....	3
Motivation .....	4
Scope .....	4
General Approach .....	5
II: Literature Review .....	7
Material Selection .....	7
Description of the Small Ex-Core Heat Pipe Thermionic Reactor (SEHPTR).....	12
Target Term.....	14
Comparison of Radiation Shield Designs .....	15
SP-100 Shield Optimization.....	16
STAR-C Shield Design.....	17
SEHPTR Shield Design.....	17
Summary of Previous Shield Designs.....	18
III: Method of Analysis.....	20
MCNP4C.....	20
Matrix Methods [2:152-153].....	22
“Split_Shield” Code.....	26
Shield Analysis Techniques .....	27
The SEHPTR Source Term.....	28
Shield Spacing and Half Cone Angle Parameters.....	30
Material Thickness For Attenuation Parameter.....	32
Material Thickness for Energy Spectrum Softening Parameter.....	33
Material Thickness For Scattering Parameter.....	35
Number of Shield Sections Parameter.....	37
Shield Geometry Parameter.....	38
Positioning of the Gamma Shield.....	39
Energy Deposition in the Shield.....	40
Split Scatter Shield Design.....	41
IV: Results.....	43

Benchmarking “Split_Shield” .....	43
Methods Used to Troubleshoot the “Split_Shield” Program. ....	48
Split Scatter Shield Parameter Study .....	51
Shield Spacing Parameter.....	51
Material Thickness Parameter. ....	52
Number of Shield Sections Parameter. ....	54
Optimum Shield Geometry. ....	55
Gamma Shield Placement. ....	59
Energy Deposition in the Shields. ....	59
Split Scatter Shield Design.....	59
V: Conclusions .....	63
“Split_Shield” Conclusion .....	63
Radiation Shield Parameters .....	64
Recommendations .....	66
Computer Code Recommendations.....	66
Radiation Shielding Recommendations .....	68
Appendix A: Introductory Tutorial for MCNP-4C .....	71
Tallies.....	71
Variance Reduction. ....	74
Appendix B: SEHPTR Input Deck in MCNP4C .....	76
Appendix C: “Split_Shield” Program .....	79
Appendix D: “MissDiskProbability” Program.....	103
Bibliography.....	106

## List of Figures

Figure 1. Cross Sectional View of a SEHPTR [8:10] .....	14
Figure 2. Baseline Shield Design for SEHPTR [8:78].....	18
Figure 3. Description of Scattering Used in Matrix Methods.....	23
Figure 4. Illustration of the Source Neutron Flux Profile .....	29
Figure 5. Illustration of the Source Photon Flux Profile .....	29
Figure 6. Illustration of Shield Configuration for ‘MissDiskProbability’ Code .....	31
Figure 7. Material Thickness Parameter for Attenuation and Backscatter .....	33
Figure 8. Effect of Material Thickness on the Energy Dependent Neutron Flux .....	35
Figure 9. Depiction of MCNP4C Current Cosine Tally Locations.....	36
Figure 10. Effect of Material Thickness on Scattering Direction .....	37
Figure 11. Effect of Shield Tapering on Particle Scattering .....	39
Figure 12. Angular Distribution of Neutron Flux Between 22.5 and 67.5 Degrees .....	39
Figure 13. Approach to Searching for a Split Shield Optimum.....	42
Figure 14. Difference in Flux Profile Between MCNP4C and “Split_Shield” .....	50
Figure 15. Effect of Shield Spacing and Half Cone Angle on Particle Leakage .....	52
Figure 16. Effect of Shield Splitting on the Neutron Flux .....	55
Figure 17. Neutron and Photon Flux Profiles at the Source Plane.....	56
Figure 18. Location of Source for Particle Leakage at Exactly 500 cm .....	57
Figure 19. Shield Configuration for Preferential Leakage Study.....	58
Figure 20. Design Layout for Splitting the Unit Shield .....	60
Figure 21. Effect of Splitting LiH from Unit Shield and Conserving Mass .....	62
Figure 22. Future Study on Gamma Shield Placement After Splitting LiH .....	65



## **List of Tables**

Table 1. Physical Properties of Candidate Shield Materials [6;7] .....	8
Table 2. Nuclear Properties of Candidate Materials (2200 m/s) [6;7] .....	8
Table 3. Key Design Parameters of SEHPTR[8:12].....	13
Table 4. Optimized Shield Parameters for the SP-100 [10:106].....	16
Table 5. Split_Shield Benchmarking Data for Carbon Shield .....	44
Table 6. Split_Shield Benchmarking Data for Tungsten Shield .....	46
Table 7. Split_Shield Benchmarking Data for Laminated (C-W) Shield .....	47
Table 8. Material Thickness Parameters for Neutron Backscatter and Attenuation .....	53
Table 9. Material Thickness Parameters for Gamma Backscatter and Attenuation.....	53

### **Abstract**

A parameter study was conducted for a space nuclear reactor radiation shield. The focus of this research was to explore alternatives to current radiation shield designs to reduce the mass while maintaining the same shielding performance. MCNP4C was used to determine the parameters necessary to build an optimum shield. A design known as the split scatter shield offered some potential for reductions in shield mass. In theory, less material is required for this type of shield, which uses thin shield sections to scatter radiation away from the dose plane. The parameters for this shield design are the shield geometry, number of shield sections, and material selection.

Split scatter shielding offers a potential for reducing the shield mass by allowing the gamma shield material to be moved closer to the source plane. Further research needs to be conducted on this shielding technique, however, to isolate optimum shield values. Once these optima have been identified, a split shield can be developed and compared to the original shield performance. Finally, an energy deposition study indicates that the split scatter shield will absorb less energy than the unit shield, implying that there may be less thermal stress on a scatter shield.

# PARAMETER STUDY FOR OPTIMIZING THE MASS OF A SPACE NUCLEAR POWER SYSTEM RADIATION SHIELD

## I. Introduction

### Background

Nuclear power for spacecraft applications has been pursued since the earliest days of nuclear reactor research. With a high power density and long operation times, nuclear powered spacecraft offer significant benefits over their solar and chemically powered counterparts. One significant concern when designing such a spacecraft is the shielding of the spacecraft payload from the radiation that comes from the reactor. This radiation shielding problem is further complicated when weight, volume, and mechanical performance constraints are considered.

The traditional method for shielding unmanned space nuclear power systems (SNPS) has been the laminated shadow shield. This shield is placed between the reactor and the payload, creating a shadow in which the payload can hide. Early space reactors like the SNAP-10A operated at such low powers that the shielding of gamma radiation was unimportant [3:9]. As the reactor power increased into the kW<sub>e</sub> range, it became necessary to layer the shields with a low Z material for neutron attenuation and a high Z material for gamma attenuation. Various research studies have concluded that a mass optimized shadow shield will consist of lithium hydride and tungsten layers [8:78; 9; 10:3]. Another effect of the increased power has been an increase in the thermal stresses

within the shield. This additional constraint requires that there must be a trade off between the selection of a material based on its radiation and mechanical properties. Several decades of research into shadow shield optimization has managed to produce a shield that ranges from 20–30% of the total space nuclear power system mass.

Reducing the mass further will require adjustments to the free parameters that are available to the shield designer. These parameters are the material selection, shield geometry, reactor design, reactor and payload location, and the allowable dose limits. The payload of interest will determine the allowable dose limits, so that parameter is effectively fixed. The location of the payload with respect to the reactor will be limited by the method of connecting the two systems. As the separation distance is increased, a mass penalty is imposed for any structure that is required to connect the two systems [9]. Furthermore, there may be volumetric constraints imposed by the launch vehicle to be considered. Although flexible tethers and free flying SNPS have been considered, these pose difficulties of their own because of the need to always keep the reactor and payload in the same relative position to one another for non- $4\pi$  shields. The result is that the separation distance is also effectively fixed to some optimal range, beyond which the mass requirement of the connecting structure exceeds any savings gained by a smaller shield. The selection of materials for SNPS systems has been narrowed down to 8 materials in this research, that meet the requirements for a compact radiation shield. These materials are tungsten, lithium hydride, zirconium hydride, graphite, boron carbide, beryllium, beryllium oxide, and stainless steel. The merits of these materials will be discussed in Chapter II. The design of the reactor will have a significant impact on how the shield is going to be designed. The reactor design will operate under its own

set of constraints, including a mass optimization. This means for the purpose of shield design work, it is necessary to assume that the reactor is optimized and not a free parameter. This leaves the shield geometry and material selection as the only free parameters to work with.

One shielding design that has been examined for space nuclear power systems is the split scatter shield [4]. This design takes a unit shield and divides it up into multiple sections. Regions of vacuum then separate the individual sections so that radiation can reflect off of one shield section and be scattered into space where the probability of backscatter is almost zero. Radiation that is transmitted through the shield will be attenuated and some will be scattered forward into space. When particles reach the next shield section the interaction will occur again. Research conducted by Berga indicates that a split scatter shield can be as much as 4 times as effective as a unit shield because it relies on scattering radiation away from the target rather than attenuation by absorption [4]. Furthermore, Berga predicted that since the absorption of radiation is reduced in the split scatter shield, less energy would be transferred to the material [4:49-50]. This can result in lower shield temperatures and a reduction in the shield thermal stress.

### **Problem Statement**

The goal of this research is to investigate the potential of using a split scatter shield for reducing the shield mass while maintaining the shielding performance of the unit shadow shield. Shield effectiveness is determined by the ability of the shield to match the time integrated neutron flux and gamma dose limits that are outlined in the ‘Target Term’ section of Chapter 2.

## **Motivation**

Although SNPS's have not yet reached their full potential, they still currently offer the best solution to any mission that requires power in the kW<sub>e</sub> to MW<sub>e</sub> range. They are also the best option for powering spacecraft that are going to operate beyond the asteroid belt, where solar power becomes impractical due to spherical divergence of radiation from the sun. Decreasing the mass of the radiation shield, while maintaining the same level of shielding performance will increase the mass available for the payload. Furthermore, if the thermal stresses caused by radiation absorption in the unit shield can be reduced, then materials can be considered that may have been discounted previously in high energy shielding problems.

## **Scope**

This study is limited to a split scatter shield design with a total source-to-dose plane separation distance of 5 meters. Evaluation of the radiation transport was accomplished with a Monte Carlo technique using the computer program MCNP version 4C. This program was operated on a Sun Enterprise 450 workstation, which uses four Ultraspark II processor operating at 400 MHz. The shield is expected to protect the payload for 10-years of continuous operation with a reactor operating at 415 kW<sub>th</sub>. The Small Ex-Core Heat Pipe Thermionic Reactor (SEHPTR) provides the radiation source for this shield design, with a 10-year neutron source term of  $1.06 \times 10^{25}$  neutrons. Material selection for this research is limited to the following 8 materials: lithium hydride, zirconium hydride, carbon, boron carbide, beryllium, beryllium oxide, steel, and tungsten. These materials were selected based on their well-documented and frequent

use in nuclear reactor design. The principal benchmark for shield performance is the SEHPTR radiation shield.

## **General Approach**

This thesis focuses on the application of a split scatter shadow shield as opposed to the traditional unit shadow shield. Four parameters are required to parameterize a split scatter shield and determine its functionality. These parameters are the spacing between shield sections, the individual section thickness, the number of shield sections included, and the placement of the material in the sections. The half cone angle, which defines the radius of each shield section and the size of the dose plane at 5 meters is also a shield design parameter, although it is limited by the selection of a given reactor design. Each of these parameters must be evaluated with respect to the effect that they will have on the performance and the mass of the shield. The perturbation of the shield design parameters as a coupled system can then provide insight on the effectiveness of the split shield concept. A final study will also look at the energy deposited within the split shield sections compared to the unit shield to determine if there may be thermal loading reduction benefits from this design.

The benchmark shield for this research is taken from the Small Ex-Core Heat Pipe Thermionic Reactor (SEHPTR). This concept was designed by EG&G Idaho Inc, and represents one of the most advanced thermionic reactor designs currently available. The shield for the SEHPTR consists of a 10 cm layer of boron carbide, with 2 cm of tungsten located inside the boron carbide 4 cm below the surface. The final layer of the shield is 22 cm of lithium hydride, which is tapered to reduce overall shield mass. An illustration

of the SEHPTR shield is shown in Figure 2. A more detailed description of the SEHPTR is given in Chapter II, under “Description of the Small Ex-Core Heat Pipe Thermionic Reactor (SEHPTR)”.



## **II: Literature Review**

Extensive research has gone into the shielding of SNPS's, which has provided some insight into the techniques and materials that may be useful for developing the split scatter shield. Several subjects are discussed here briefly to provide some background on the tools used in this research, the candidate shielding materials, and previous radiation shield designs.

### **Material Selection**

Extensive research and experience over several decades has resulted in a list of materials that are suitable for shielding in high radiation environments. Because there is no single material that can effectively shield a high power SNPS, it is necessary to combine materials in such a way that their contribution to the shield is maximized. Table 1 is a list of eight materials that were considered for a split scatter shield and their associated physical properties. Table 2 lists the nuclear properties of the materials at thermal energies. Each material possesses certain characteristics that make it suitable for use in a SNPS shield, which must be balanced with certain disadvantages. The remainder of this section discusses the major advantages and disadvantages of the eight materials that are considered for an optimal split scatter shield.

**Table 1. Physical Properties of Candidate Shield Materials [6;7]**

Material	Density [g/cm <sup>3</sup> ]	Atomic Weight [g/mol]	Melting Point [K]
LiH	0.775	7.948	959
ZrH <sub>2.0</sub> wt %	5.40	92.228	900 (Dissociates)
Be	1.85	9.103	1560
BeO	3.025	25.02	2843
Graphite	1.70	12.011	3600 (Sublimates)
B <sub>4</sub> C	2.51	55.251	2450
Steel	7.86	55.847	1536
W	19.30	183.85	3410

**Table 2. Nuclear Properties of Candidate Materials (2200 m/s) [6;7]**

Material	N <sub>A</sub> [atoms/cm <sup>3</sup> ]	σ <sub>absorption</sub> [b]	λ <sub>abs</sub> [cm] <sub>b</sub>	σ <sub>scatter</sub> [b]	λ <sub>scatter</sub> [cm] <sub>b</sub>
LiH	5.87E22	71.33	0.24	39.4	0.43
ZrH <sub>2.0</sub> wt %	3.53E22	0.84	34.13	84	0.34
Be	1.22E23	10	0.82	7.0	1.17
BeO	7.28E22	10	1.37	6.8	2.02
Graphite	8.52E22	3.95	2.97	5.09	2.31
B <sub>4</sub> C	2.74E22	3838	0.01	14.25	2.57
Steel <sub>(a)</sub>	8.48E22	2.53	4.66	11	1.07
W <sub>(a)</sub>	6.32E22	19.2	0.82	5	3.16

(a) Nuclear properties are Maxwellian averaged cross sections (1 MeV)

(b) Mean free path of neutron in material

Lithium hydride (LiH) has long been selected as the best choice for neutron shielding of a SNPS [3:24-30]. The low atomic number of both lithium and hydrogen allows neutrons to be moderated to thermal energies with the minimal number of collisions, where neutron absorption can occur more frequently. Lithium hydride has the lowest density of all of the materials considered, making it the best choice for a mass optimized shield. The primary disadvantage of LiH is that it must be maintained at operating temperatures between 600 and 680 K [3:24-27]. Below 600 K radiolytically induced hydrogen dissociation will cause the volume of the shield to increase as LiH bonds are broken and individual atoms of Li and molecules of H<sub>2</sub> are created [3:27]. This increase in volume increases the stresses throughout the shield and leads to cracking.

Additionally an oxygen impurity in the LiH forms lithium hydroxide (LiOH). At temperatures above 680 K, the LiH and LiOH undergo the following reaction:



This reaction combined with shield punctures by meteorites can lead to hydrogen out gassing, reducing shield performance [10:9]. Maintaining LiH within this temperature range can be difficult since it also has a poor coefficient of thermal conductivity. These thermal constraints dictate where LiH can acceptably be placed in the shield.

Zirconium hydride (ZrH<sub>2</sub>) combines the low atomic weight of hydrogen with the moderate atomic weight of zirconium to make a very effective neutron and moderately effective gamma shield. Furthermore, ZrH<sub>2</sub> does not have the same thermal difficulties that LiH does and is much more stable at higher temperatures [7:326]. The disadvantage to ZrH<sub>2</sub> is that there is no commercial source of the material, which constrains the amount of material and the methods by which it can be processed [7:328].

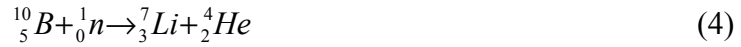
Beryllium (Be) is a lightweight element that is especially effective as a neutron moderator and reflector because of its low atomic number. Beryllium also has a relatively high melting point and maintains its strength at high temperatures [7:276]. Beryllium can have a variety of reactions with both incident neutrons and gamma rays, which can produce additional particles. For incident neutron energies above 1 MeV, beryllium can undergo the reaction  ${}^9\text{Be}(n,2n){}^8\text{Be}$  with a cross-section of 0.5 barns. Incident gamma rays with energies greater than 1.66 MeV can also produce photo-neutrons in beryllium [7:276]. Finally, beryllium produces high-energy secondary gamma rays when it captures neutrons. Approximately 50 gamma rays are produced with

energies ranging from 3-5 MeV and 75 gamma rays with energies from 5-7 MeV for every 100 neutrons that are captured [7:277]. Since the absorption and (n,2n) cross sections are relatively low, the biggest issue when designing shields with beryllium is the production of photo neutrons [7:281]. The material must be placed in a location where either the number of incident photons above 1.66 MeV is negligible, or there is additional shielding beyond the beryllium capable of stopping these secondary neutrons.

Beryllium oxide (BeO, beryllia) has almost the same nuclear properties as beryllium metal, but is a better selection for high temperature shielding applications because of the increased melting point and decreased coefficient of linear thermal expansion [7:278]. The same nuclear considerations must be given to beryllia as beryllium metal when using it in a radiation shield.

Graphite is another excellent material for neutron moderation and reflection, and is only slightly less effective than beryllium. The benefit of graphite, is that it does not undergo any low energy photo-neutron or (n,2n) reactions that increase the neutron population. Since it also has a very high sublimation temperature, it can be placed almost anywhere within the shield and still work effectively. Neutron capture by graphite produces a gamma ray with an average energy of 4.5 MeV [7:283]. The primary disadvantage to using graphite is that its many of its physical properties can change by as much as 2 to 3 times under neutron irradiation [7:282]. The operating temperature of the graphite may help to alleviate some of these problems, since annealing of radiation defects occurs with increasing temperatures [7:282].

Boron carbide ( $B_4C$ ) is a material that takes advantage of carbon to moderate neutrons down to thermal energies, where boron-10 can capture them with its high absorption cross section of 3838 barns [7:337]. The reaction of the  $^{10}B$  is given as:



This reaction also produces a 0.48 MeV gamma ray and 2.31 MeV of kinetic energy [7:337].  $B_4C$  is a good choice as an engineering material because of its high melting point and decent thermal conductivity when properly prepared [7:338]. The disadvantage of using  $B_4C$  is that radiation damage occurs to the material as the boron is burned up in capture reactions. Studies have indicated that at about 10% boron burn-up, some helium release, material cracking, and spalling will occur. After 15% burn-up a swelling of 1% has been observed. Finally, between 16-25% burn-up  $B_4C$  becomes granulated [7:339].

Stainless steel makes a very effective gamma ray shield and has the advantage of possessing good structural properties. Because steel is one of the most commonly used engineering materials, its properties are well known and it is easy to fabricate into any shape. Although steel is effective at slowing neutrons down to thermal energies, it is a source of high-energy gamma rays from neutron capture at resonance energies and inelastic scatter reactions. Over 25 percent of the neutrons captured in steel will result in gamma rays with energies greater than 5 MeV [5:86]. The placement of steel within a shield must therefore be balanced between the ability of the steel to attenuate gamma rays and the production of high-energy gamma rays by neutron capture.

Tungsten makes an excellent gamma shield because of its high density and atomic weight. This material has also long been selected for use in space shielding applications

because it requires the least amount of space for very efficient gamma shielding. Like steel, tungsten also produces high-energy gamma rays from neutron capture at resonance energies and inelastic scattering. For tungsten however, only 6 percent of the neutrons captured result in gamma rays with energies greater than 5 MeV [5:86]. Additionally, the highest energy gamma ray from neutron capture in tungsten is 7.42 MeV while in steel it is 10.16 MeV [5:86].

The production of high-energy gamma rays can be problematic, because it leads to the production of additional gamma rays at lower energies. As the gamma ray energy increases (greater than pair production threshold of 1.02 MeV) so will the probability of pair production reactions. As these high-energy gamma rays are absorbed by pair production an electron and positron will be created each with energy of 0.51 MeV. The electron will then scatter until it is captured, while the positron will annihilate with another electron producing a new gamma ray with energy 1.02 MeV. As the electron and positron travel through the material they will slow down releasing gamma rays in the form of Bremsstrahlung, which will then be Compton scattered or captured by photoelectric absorption. Therefore, although high-energy gamma will be readily absorbed, they can lead to an increase in the number of gamma rays that exist in the region where Compton scattering dominates. It is desirable therefore to have fewer neutron capture reactions that result in high-energy gamma rays.

### **Description of the Small Ex-Core Heat Pipe Thermionic Reactor (SEHPTR)**

The Small Ex-Core Heat Pipe Thermionic Reactor (SEHPTR) was selected as the source term for this study [8]. This SNPS concept was presented in October 1991 by

EG&G Idaho, Inc. A summary of the primary performance parameters for this reactor is listed in Table 3.

**Table 3. Key Design Parameters of SEHPTR[8:12]**

<b>Reactor Parameter</b>	<b>Value</b>
Net Electrical Power [ $\text{kW}_e$ ]	40
Thermal Power [ $\text{kW}_{th}$ ]	415
System Efficiency [%]	10
Core Length [cm]	50
Core Outer Radius [cm]	20
Core Inner Radius [cm]	10
BeO Reflector [cm]	10
Be Reflector Thickness [cm]	7
Heat Pipe Thickness [cm]	2.8
Reactor Subsystem Length [cm]	70

The SEHPTR design was selected for this study because it represents one of the most advanced space reactor systems currently available. The high system efficiency and small core design make it a more desirable option for future missions in space. The SEHPTR is also an attractive system, because of the low mass of the reactor system. The background information on this reactor was very complete making it easier to represent and evaluate in MCNP4C. Figure 1 shows a cross sectional view of the SEHPTR design. The reactor is a hollow cylinder with an inner radius of 10 cm and an outer radius of 20 cm. A control rod path is located at the center of this cylinder and is designed to accommodate a  $\text{B}_4\text{C}$  control rod. Beryllium reflectors at the top and bottom of the core are provided to reflect the axial flux back toward the reactor. Reactivity is controlled by moving beryllium reflectors located on the outside of the core. The reflectors are motor driven and can be rotated to provide the reactor core with an unobstructed window to open space. When the reflectors are in the open position, neutrons are allowed to stream from the reactor into space, and the reactor becomes sub-critical. The reflectors can

likewise be placed in closed or half closed positions to achieve a critical state. The thermionic heat pipe modules are located on both the inside and outside of the core and run the entire length of the reactor. These modules convert the heat from the nuclear reactor into electricity by effectively boiling electrons off of a hot emitter surface ( $\sim 1800$  K) across an inter-electrode gap ( $\leq 0.5$  mm) to a cooler collecting surface ( $\sim 1000$  K) [1:93]. The heat pipes then run out from the reactor and down the outside of the radiation shield to form graphite covered radiating surfaces.

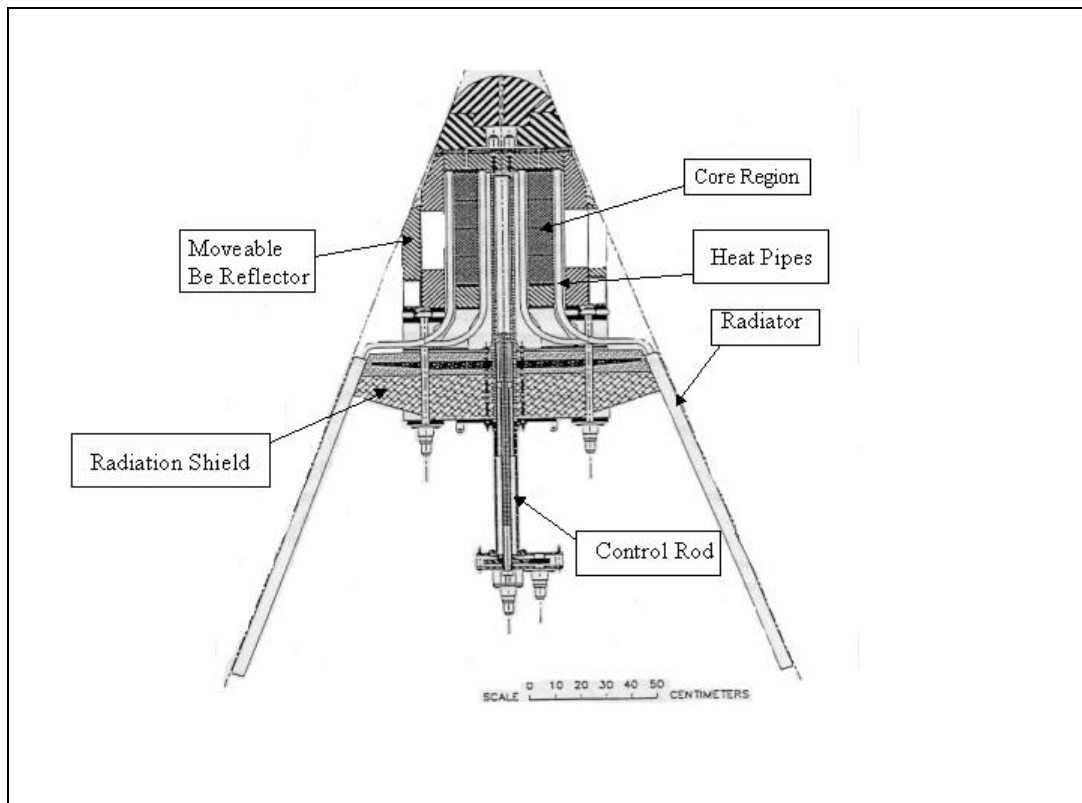


**Figure 1. Cross Sectional View of a SEHPTR [8:10]**

### **Target Term**

The total neutron flux and gamma dose at the target is a function of several variables, some of which are not directly related to the design of the shield. The



separation between the back of the shield and the payload, as well as the size of the payload will in part determine how much radiation is incident upon the module. Furthermore, reactor support structures such as the heat rejection radiators and connecting boom may scatter radiation back towards the payload module. Parameter studies have been performed on the separation distance versus boom mass as well as contributions to the target from scattering off of the radiators [9]. Because the focus of this study is on the effectiveness of a split scatter shadow shield, only the additional scattering back to the dose plane caused by the radiators was considered.

This study assumes an unmanned spacecraft, so the target of concern is the silicon in the spacecraft's computer systems. Several different shield designs have concluded that for an operational reactor lifetime of 10 years, the tolerable neutron fluence is  $10^{15}$  nvt (1 MeV equivalent) and the tolerable gamma dose is  $10^7$  Rad (Si) [8;6;9].

### **Comparison of Radiation Shield Designs**

All radiation shields, regardless of whether they are unit or split, must be capable of meeting certain requirements before they can be considered to effectively shield a SNPS. The primary function is to reduce the reactor-to-payload neutron fluence and gamma dose to acceptable levels. The definition of acceptable limits is determined by the composition and geometry of the payload.

The quality of the neutron and gamma flux must also be considered. Reducing the number of neutrons and gamma rays leaving the back face of the shield is not sufficient. The energy spectrum of the neutron fluence must be softened so that the majority of neutrons leaving the shield are of low energies. Likewise, the energy

spectrum of the gamma flux should be softened so that high-energy pair production and scattering reactions are less likely to occur in the target. The payload must be sufficiently shielded against cosmic radiation, so particles with lower energies that make it through the reactor radiation shield would have a higher probability of being stopped in the payload shield. A brief comparison of the SP-100, STAR-C, and SEHPTR radiation shields is now provided to give some benchmarks to match against the new split scatter shield design.

#### SP-100 Shield Optimization.

Several SNPS studies have focused on designing an optimal radiation shield based on mass, volume, and performance. Lee conducted a shield optimization study for the SP-100, which has an operating power of 2 MW<sub>th</sub> with a 7-year life expectancy [10:20]. Lee's recommendations for a mass and volume optimized shield are listed in Table 4.

**Table 4. Optimized Shield Parameters for the SP-100 [10:106]**

Materials	Mass [kg]	Volume [cm <sup>3</sup> ]
LiH/W	528.39	437402
B <sub>4</sub> C/W	655.35	211176

Lee concluded that the slightly more massive B<sub>4</sub>C/W shield might be the more acceptable shield for higher power reactors, since B<sub>4</sub>C doesn't have the thermal constraints that LiH does, and because it requires about half the volume of the LiH/W shield [10:106]. Lee also concluded that the optimal placement of tungsten within the shield is 40 cm from the core for a LiH shield and 10 cm from the core for a B<sub>4</sub>C shield [10:105].

### STAR-C Shield Design.

The STAR-C is another advanced SNPS design that was designed primarily by General Atomics, and presented on April 9, 1991 at Phillips Laboratory, Kirtland Air Force Base, New Mexico. This reactor was designed to operate at  $340 \text{ kW}_{\text{th}}$  with an efficiency of about 12% to provide  $40 \text{ kW}_e$  of power. The baseline STAR-C shield consists of 21.0 cm of lithium hydride, followed by 0.635 cm of borated stainless steel, and completed with 2.5 cm of tungsten. The mass for the STAR-C shield is 1320 kg. The design requires a 5-meter separation distance from the back of the shield to the payload [9:121]. An additional parameter study concluded that the optimal separation distance between the shield and payload is between 9 and 10 meters. At this distance, the mass of the shield is reduced to 431 kg, with a connecting boom mass of about 250 kg [9:143].

### SEHPTR Shield Design.

As mentioned previously, the SEHPTR design operates at  $415 \text{ kW}_{\text{th}}$  with an efficiency of about 10% to produce  $40 \text{ kW}_e$  of power. The SEHPTR shield consists of 10 cm of  $\text{B}_4\text{C}$ , 2 cm of tungsten, and 22 cm of LiH. A cross-sectional view of the SEHPTR baseline shield, reprinted from the original text, is illustrated in Figure 2 [8:78]. The  $\text{B}_4\text{C}$  is placed closest to the reactor, where shield temperatures will approach 1000 K. The tungsten layer is placed approximately 2.5 cm inside of the  $\text{B}_4\text{C}$  and is tapered towards the edges where the photon flux decreases. The LiH is placed below the  $\text{B}_4\text{C}$ , where the temperature never exceeds 670 K [8:107]. This placement of the LiH also allows for a large radiative surface area for the material to reject heat to space. With this design, the

SEHTPR radiation shield is 800 kg with a shield to payload separation distance of 5 meters [8:6,13].

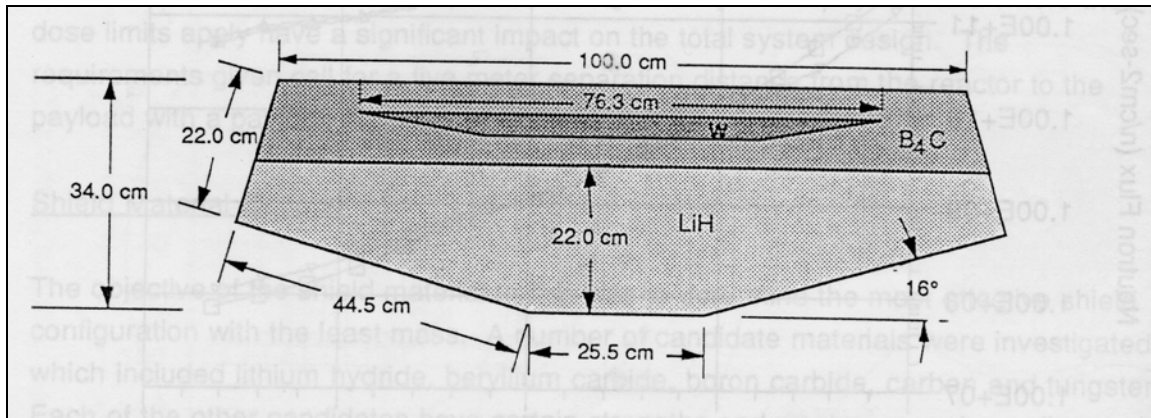


**Figure 2. Baseline Shield Design for SEHPTR [8:78]**

#### Summary of Previous Shield Designs

Previous shield designs indicate that lithium hydride is the material of choice for neutron shielding, while tungsten is used for gamma shielding. Because the split scatter shield will optimize shield performance through radiation scattering, it is important to evaluate additional materials to make sure that there are not better alternatives. In an initial review, it also appears that the split scatter concept will be more effective for neutrons rather than gamma rays. Because the mass of the split shield will increase as it is pushed back, the gamma shield material needs to be as close to the source plane as possible. Additionally, there is a direct relationship between the mass of a material and the gamma ray cross section, which tends to increase the overall cross section for more massive materials. The gamma cross section for most materials has photoelectric effect dominating at low energies, Compton scattering for intermediate energies, and pair production at high energies. It is extremely difficult to control the energies at which gamma rays will interact in the shield, making preferential scattering interactions difficult

to predict and control. Because of these reasons, it is better to keep the gamma shielding material together and use it to attenuate gamma radiation through absorption. Some of the key elements to developing a successful split scatter shield are reducing the overall mass required for the gamma shield by moving it closer to the source plane and enhancing neutron scatter by splitting the neutron shielding material.

### **III: Method of Analysis**

Two methods were considered for the evaluation of the split scatter shield. The first method uses the Monte Carlo code MCNP4C directly, with optimized importance functions and locations of particle splits to decrease the computer evaluation time. The second technique is the matrix method, which is similar to the method of successive scatters to calculate the effectiveness of the split scatter shield. This technique was applied in an effort to speed up the split shield experiments, and used material shielding information taken from MCNP4C runs.

Seven experiments were conducted for the split scatter shield to study key parameters such as material selection, shield spacing, material thickness, and shield geometry. The first two experiments used a similar technique to study the parameters for material thickness for attenuation and material thickness for scattering. The third experiment uses a simple Monte Carlo technique to look at the relationship between shield spacing and the half cone angle to study the loss of particles as they stream through vacuum between shield sections. The fourth and fifth experiments were designed to explore the effect of the number of shield sections and the geometry on shield performance. The final two experiments were designed to test the entire scatter shield when assembled. These experiments included studies on the proper positioning of the gamma shield to minimize  $(n,\gamma)$  reactions and energy deposition in the shields.

#### **MCNP4C**

The primary analytical tool used to perform the shielding analysis was the Monte Carlo N-Particle transport code, version 4C (MCNP4C). This code, obtained from the

RSICC computer code collection, uses a Monte Carlo technique to provide an estimate of the neutron and photon transport through a given selection of materials and geometries. An explanation of the Monte Carlo technique can be found in a variety of radiation transport texts, including the text by Lewis and Miller [11] or in the reference documentation that comes with MCNP4C [17]. A tutorial included in Appendix A describes the features of MCNP4C that were used in this research.

A sample input deck has been included in Appendix B of this report to demonstrate how the problems are set up for the code. This input deck models the Small Ex-Core Heat Pipe Thermionic Reactor (SEHPTR) and a short explanation is given after each section to describe how to set up a model in MCNP4C. Chapters four and five of the MCNP4C documentation provides further examples of MCNP4C input and output and can be referenced for additional help in understanding the code [17:4\_1,5\_1].

MCNP4C was selected for this thesis because it offers a lot of flexibility in shield design. Complex geometries can be created in three dimensions and then visually plotted using the MCNP4C plot routine [17:B\_1]. This feature allows the user to detect any flaws in the geometry of the problem and correct them before spending time running a problem that is not properly defined. MCNP4C is capable of running neutron, photon, electron, neutron-photon, and neutron-photon-electron transport problems. The last two types of problems account for interactions such as photo-neutron production, Bremsstrahlung, and photons created from neutron capture to name a few. The variety of tallies that MCNP4C can provide is another feature that makes this program robust. Particle distributions can be reported in a variety of ways, to include the current, partial current, flux, flux at a point detector, or energy deposition in a material.

The primary disadvantage to using a Monte Carlo technique is that it is computationally expensive and contains inherent stochastic error [13]. Monte Carlo techniques are computationally expensive because the precision of the result is directly related to the number of particles that are sampled. It can be shown that the precision of a tally changes as  $1/\sqrt{n}$ , where  $n$  is the number of particles that are contributing to a tally [13]. The use of appropriate variance reduction techniques will help to increase the precision while reducing the variance for smaller particle sampling batches. The stochastic error can be quantified through the application of batch sampling. This technique involves running the same experiment multiple times but with a different set of random numbers. When the results are compared against one another, the designer can determine how much of the error is associated with statistical noise in the problem [13].

### **Matrix Methods [2:152-153]**

Since the calculations for MCNP4C are computationally expensive, the matrix methods approach was considered to perform cheap calculations on the split scatter shield [13]. This method is similar to the method of successive scatters, by using an attenuation estimator to calculate the bulk transport of radiation through the shield. The distribution of particles can then be determined at user-defined interfaces. For this technique, the shield is broken into a set of regions that characterize different materials. Particles are started at the source plane and travel through the first material region. Upon reaching the next material, some of the particles are transmitted forward, while some are reflected back toward the source. These reflected particles are then transported back to the source,



reflected, and again transported back across material 1 to contribute to the total particle distribution at the material interface. Figure 3 illustrates this process for two materials.

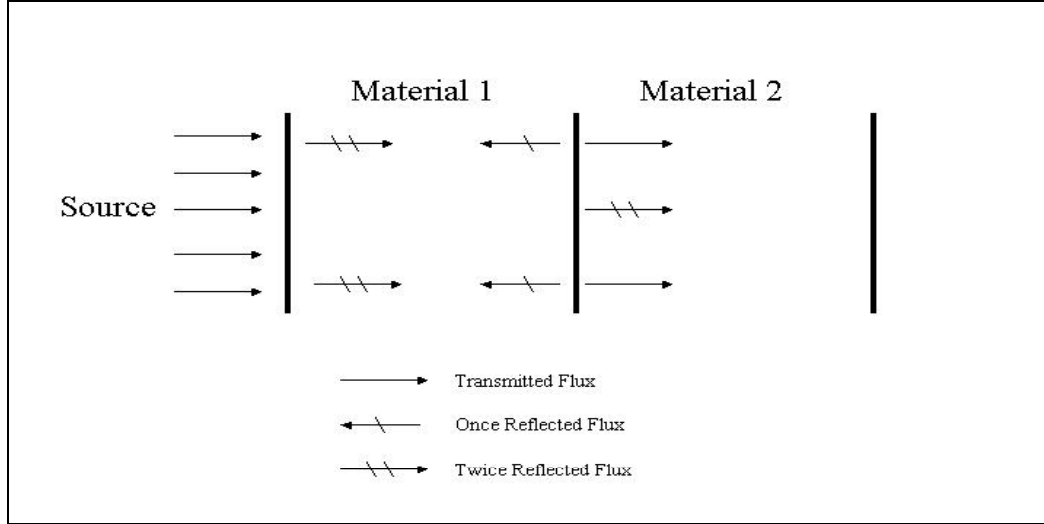


**Figure 3. Description of Scattering Used in Matrix Methods**

Only twice reflected particles are considered for split scatter shield applications, because only initial and twice scattered contributions to the particle distribution are significant in the results.

The matrix methods technique is applied by solving a set of equations that each describes an individual piece of the split scatter shield. Equations 5 and 6 describe the particle distribution at the right edge of a material region, while Equation 7 describes the source term for the split shield problem.

$$J_n^F = J_{n-1}^F \cdot T_n^F + J_{n+1}^B \cdot T_{n+1}^B \cdot R_n^F \quad (5)$$

where

- $J_n^F \equiv$  # of particles traveling forward at the right side of region n
- $J_{n-1}^F \equiv$  # of particles traveling forward from the right side of region (n-1)
- $J_{n+1}^B \equiv$  # of particles traveling backward from right side of region (n+1)
- $T_n^F \equiv$  Forward transmission attenuation coefficient of region n
- $T_{n+1}^B \equiv$  Backward transmission attenuation coefficient of region (n+1)
- $R_n^F \equiv$  Reflection coefficient off of right face of region n

$$J_n^B = J_{n+1}^B \cdot T_{n+1}^B + J_{n-1}^F \cdot T_n^F \cdot R_{n+1}^B \quad (6)$$

where

- $J_n^B \equiv \#$  of particles traveling backward at right side of region n
- $J_{n+1}^B \equiv \#$  of particles traveling backward from the right side of region (n+1)
- $J_{n-1}^F \equiv \#$  of particles traveling forward from the right side of region (n-1)
- $T_{n+1}^B \equiv$  Backward transmission attenuation coefficient of region (n+1)
- $T_n^F \equiv$  Forward transmission attenuation coefficient of region n
- $R_{n+1}^B \equiv$  Reflection coefficient off of left face of region (n+1)

$$J_0^F = J_{SRC} + J_n^B \cdot T_n^B \cdot R_0^F \quad (7)$$

where

- $J_0^F \equiv \#$  of particles traveling forward from the source
- $J_{SRC} \equiv \#$  of source particles
- $J_n^B \equiv \#$  of particles traveling backward from the right side of region n
- $T_n^B \equiv$  Backward transmission attenuation coefficient of region n
- $R_0^F \equiv$  Reflection coefficient off of the source plane

Equations 5 through 7 can be combined for a set number of regions to create a system of equations that describes the distribution of particles at each of the region interfaces.

Equations 8 through 11 are used to solve the forward distribution of particles at the region interfaces and are based on the distribution of particles going backward at the region interfaces and from the source.

$$J_0^F = J_{SRC} + J_1^B \cdot T_1^B \cdot R_0^F \quad (8)$$

$$J_1^F = J_{SRC} \cdot T_1^F + J_1^B \cdot T_1^B \cdot R_0^F \cdot T_1^F + J_2^B \cdot T_2^B \cdot R_1^F \quad (9)$$

$$J_2^F = J_{SRC} \cdot T_1^F \cdot T_2^F + J_1^B \cdot T_1^B \cdot R_0^F \cdot T_1^F \cdot T_2^F + J_2^B \cdot T_2^B \cdot R_1^F \quad (10)$$

$$J_n^F = J_{SRC} \cdot \prod_{i=1}^n T_i^F + J_1^B \cdot T_1^B \cdot R_0^F \cdot \prod_{i=1}^n T_i^F + J_2^B \cdot T_2^B \cdot R_1^F \cdot \prod_{i=2}^n T_i^F + \dots + J_n^B \cdot T_n^B \cdot T_n^F \cdot R_{n-1}^F \quad (11)$$

These equations can be solved simultaneously with a linear algebra equation of the form shown in equation 12.

$$\vec{J}_F = \overline{\overline{A}}_F \cdot \vec{J}_B + \vec{T}_F \cdot J_{SRC} \quad (12)$$

where

- $J_F \equiv$  Vector of particle distributions in the forward direction
- $J_B \equiv$  Vector of particle distributions in the backward direction
- $J_{SRC} \equiv$  Source term (Scalar)
- $A_F \equiv$  Matrix of transmission and reflection coefficients
- $T_F \equiv$  Vector of transmission coefficients

Equation 12 can be solved, if the backward particle distribution is known as well as the transmission and reflection coefficients for all of the regions. The backward particle distribution can be determined by rearranging equations 5 through 7 to create equations 13 through 16.

$$J_0^B = J_0^F \cdot T_1^F \cdot T_1^B \cdot R_2^B + J_1^F \cdot T_2^F \cdot R_3^B \cdot T_1^B \cdot T_2^B + \dots + J_n^F \cdot T_{n+1}^F \cdot R_{n+2}^B \cdot \prod_{i=1}^{n+1} T_i^B \quad (13)$$

$$J_1^B = J_0^F \cdot T_1^F \cdot R_2^B + J_1^F \cdot T_2^F \cdot T_2^B \cdot R_3^B + \dots + J_n^F \cdot T_{n+1}^F \cdot R_{n+2}^B \cdot \prod_{i=2}^{n+1} T_i^B \quad (14)$$

$$J_2^B = J_1^F \cdot T_2^F \cdot R_3^B + J_2^F \cdot T_3^F \cdot T_3^B \cdot R_4^B + \dots + J_n^F \cdot T_{n+1}^F \cdot R_{n+2}^B \cdot \prod_{i=3}^n T_i^B \quad (15)$$

$$J_n^B = J_{n-1}^F \cdot T_n^F \cdot R_{n+1}^B + J_n^F \cdot T_{n+1}^F \cdot T_{n+1}^B \cdot R_{n+2}^B \quad (16)$$

These equations can also be solved simultaneously with a linear algebra equation of the form shown in equation 17.

$$\vec{J}_B = \overline{\overline{A}}_B \cdot \vec{J}_F \quad (17)$$

Now there are solutions for the forward and backward particle distributions at the region interfaces. The FORTRAN-90 program “Split\_Shield” was developed to create the operator matrices and then used to solve for the particle distributions at the interfaces using an iterative technique.

#### “Split\_Shield” Code.

A copy of the “Split\_Shield” source code is located in Appendix B. The first step of “Split\_Shield” is building the attenuation operator matrices for both the forward and backward transmission of particles. The values for the forward and backward transmission and reflection coefficients are determined by running MCNP4C for the eight different materials. For each material (including vacuum), a series of input decks was created to demonstrate how the particle distribution changes with an increase in material thickness. This is the same procedure that is discussed later in this report to perform the analysis for the optimum material thickness for an attenuator. The particle distribution data from the MCNP4C runs are placed into data files for each material, which are then used to create the  $A_F$  and  $A_B$  matrices based on equations 8 through 11 for the forward matrix and 13 through 16 for the backward matrix.

The program first reads the shield parameters from an input file. The input shield parameters include the shield name, the number of shield sections, and the thickness of material in each region. For each region, the program opens the specified material data file and an interpolation routine is performed on the data to determine the transmission and reflection coefficients for a specified material thickness. Next the program starts

filling individual arrays with the forward and backward values of the transmission and reflection coefficients. This results in four arrays that are the same size as the number of regions in the problem plus 1. These arrays are the forward transmission array, the backward transmission array, the forward reflection array, and the backward reflection array. The next routine takes these arrays and combines different elements of them to create a matrix with values that represent the coefficients in equations 8 through 11 (forward coefficient matrix) and 13 through 16 (backward coefficient matrix).

Multiplying the source term by the appropriate values from the forward transmission array creates the source vector. Finally, the program calculates the forward and reverse particle distribution vectors using an iterative process. This calculates the relative error between the particle distribution for the current and previous iteration and outputs results when the difference in distributions meets a convergence criterion. The last portion of the program calculates the mass and volume of the shield and then prints the entire set of shield results to an output file.

### **Shield Analysis Techniques**

For the initial split scatter shield study, the geometry for all shields was limited to a frustum (truncated cone) that has the same dimensions as the cone used to bound the SEHPTR design (vertex at 137 cm, half cone angle of 21 degrees). The top of this frustum coincides with the bottom of the SEHPTR at 0 cm. At this location, the radius of the frustum is 52.7 cm. Several experiments were designed to determine the four parameters needed to characterize a mass optimized split scatter shield.

### The SEHPTR Source Term.

The distribution of neutrons and photons that cross from the reactor into the radiation shield was determined by running MCNP4C with a k-eigenvalue calculation and utilizing a series of ring detectors on the bottom plane of the reactor. Each detector tally was split into 15 energy groups for neutrons and 9 energy groups for photons. The energy dependent neutron and photon flux profiles leaving the bottom of the reactor into the shield are shown in Figures 4 and 5 respectively. These Figures indicate that around 20 cm, there is a drop in both the photon and neutron flux, which coincides with the outer edge of the reactor core.

The source term is represented in shielding problems without the presence of the reactor by using the MCNP4C Surface Source Write card [17:3\_65-66]. The SSW card allows the user to specify a plane at which the particle distribution is required. MCNP4C will then track every particle crossing this plane and record the particle direction and energy in an output file. A Surface Source Read card can then be used for all subsequent shielding problems to source these stored particles into the problem [17:3\_66-69]. This allows the user to run multiple shield designs using SEHPTR data, without having to run the k-eigenvalue problem repeatedly. Care must be taken when using these features to include any materials that might reflect particles back to the reactor and affect the reactivity. Since the original SEHPTR design placed the radiation shield 20 cm below the bottom of the reactor, it is not necessary to include the shield in the k-eigenvalue calculations [8:10].

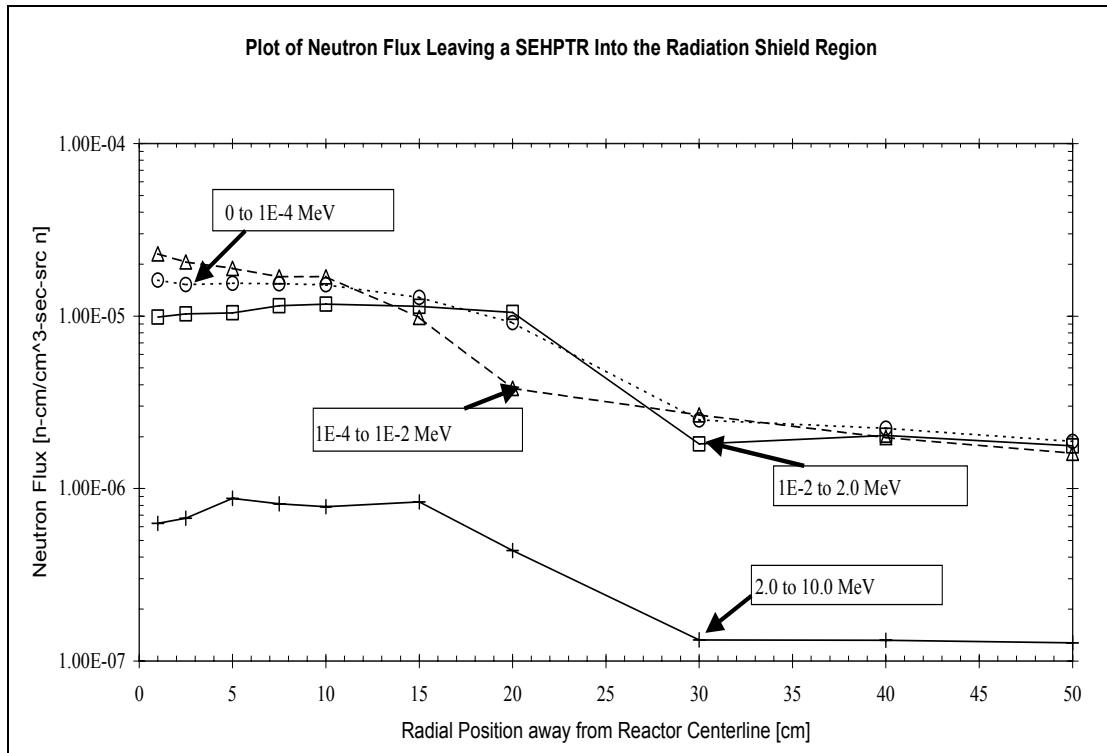


**Figure 4. Illustration of the Source Neutron Flux Profile**

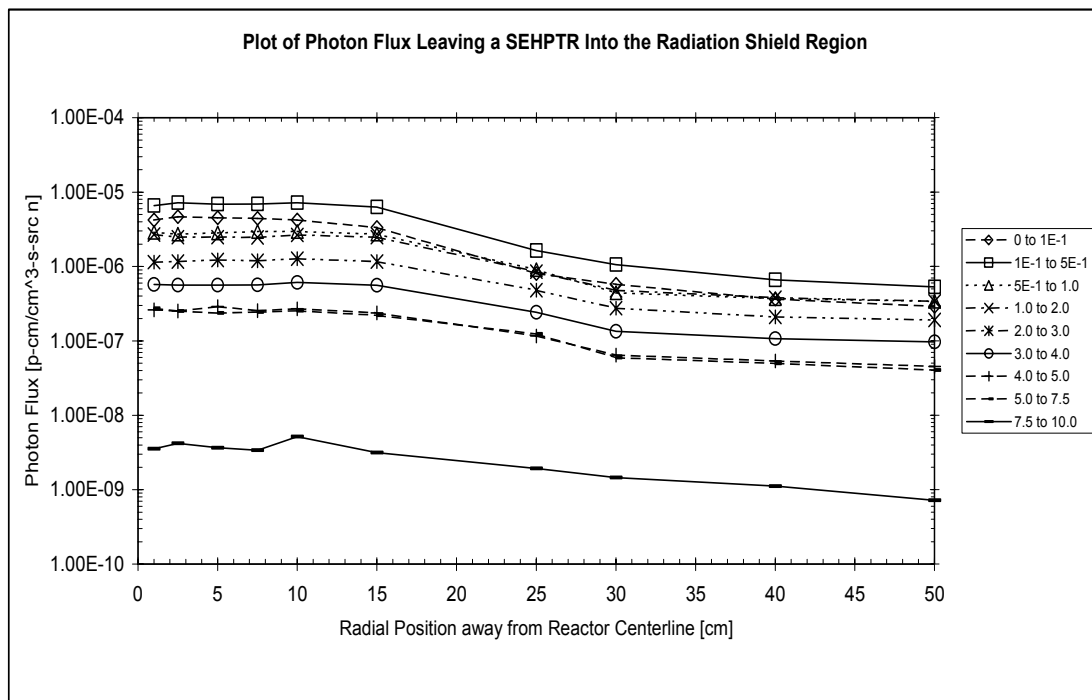


**Figure 5. Illustration of the Source Photon Flux Profile**

All MCNP4C tallies are reported “per source particle”, because the distribution estimates consist of fractions of particles that contribute to the tally. It is necessary therefore, to determine the total number of source neutrons in the SEHPTR for a 10-year system lifetime. The total number of source neutrons was estimated by dividing the thermal power of the reactor (410 kW<sub>e</sub>) by the average energy released per fission (193.7 MeV/fission). This number was then multiplied by the average number of neutrons released per fast fission in U-235 (~2.5 n/fission), to provide the total number of neutrons that are produced in the reactor per second. The total number of neutrons that are then produced given a 10-year operating cycle is  $1.06 \times 10^{25}$  neutrons.

#### Shield Spacing and Half Cone Angle Parameters.

The shield spacing and half cone angle parameters are extremely important to the success of a split scatter shield. The proper spacing of the shields and the angle of the shield shadow will influence how many particles can leak from the system before reaching the next shield section. These parameters were explored using a simple Monte Carlo code developed by Mathews that calculates the probability of particles missing the target shield in a two section split shield design [14]. This code can be found in Appendix D. The program allows the user to input the half cone angle of the system, the location of the first and second shield sections, the number of particles to sample, and the number of batches to run.

The program functions by drawing three random numbers that determines the radial and angular position of the particle on a source disk, and the cosine of the angle at which the particle is leaving the disk. This information will show where the particle



starts on the source disk, and the direction it is heading will indicate where the particle is located when it has reached the target disk. If the location of the particle lies outside the space of the target disk after following the set trajectory, then it will have missed and a tally is accumulated. Figure 6 illustrates how this problem is set up and the variables that define particle location and direction.  $R_1$  and  $R_2$  are the radii of each of the respective disks. The starting radius of the particles is determined by multiplying the radius of the source disk by a random number from 0 to 1. Next the angular location of the particle on the source disk is calculated by multiplying  $2\pi$  with a random number from 0 to 1. This provides the value for  $\omega$ . Finally, the direction the particle travels is determined by selecting a random number between 0 and 1, which is the cosine of  $\theta$ .

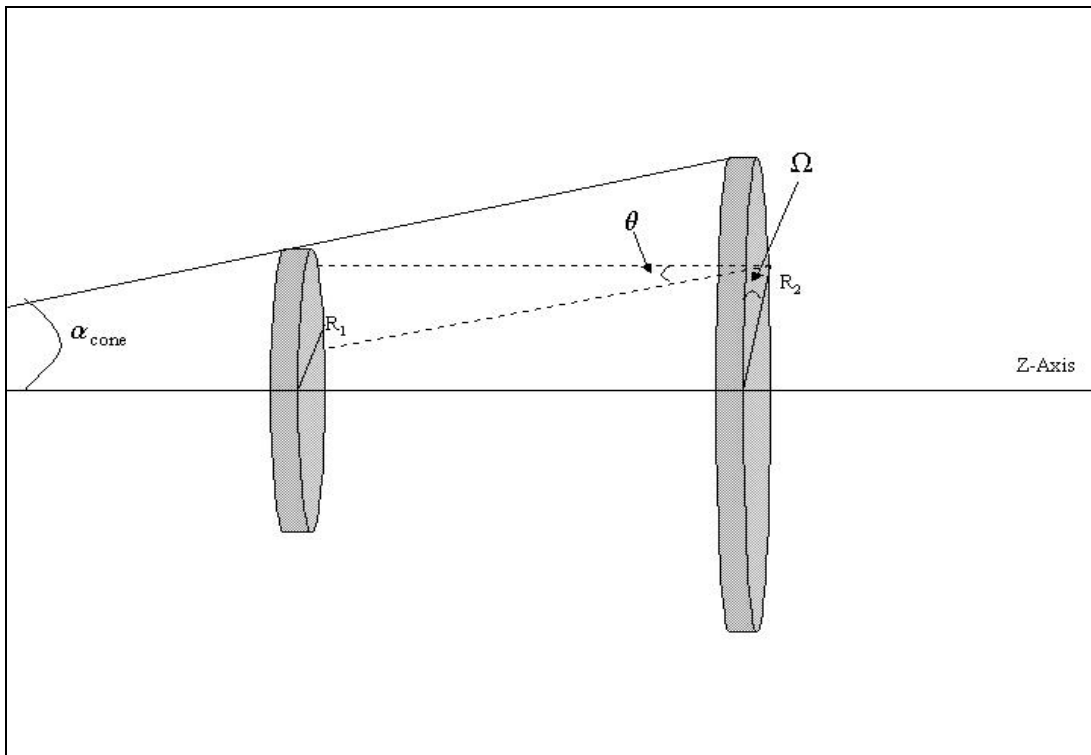


**Figure 6. Illustration of Shield Configuration for ‘MissDiskProbability’ Code**

This program makes it possible to study the effects that the shield spacing and half cone angle ( $\alpha_{\text{cone}}$ ) have on the leakage of particles from the system. For

simplification isotropic scattering was assumed for particles leaving the source disk. A final note is that the code allows either disk 1 or disk 2 to be the source disk. This allows the user to study particles that stream forward from the first disk, as well as the particles that are back scattered after hitting the second disk.

#### Material Thickness For Attenuation Parameter.

The technique for determining the material attenuation thickness parameter relies on MCNP4C to estimate the particle flux and current after passing through a given thickness of material. Particles are tracked through a material of increasing thickness and tallies are taken to determine how many particles travel through and are backscattered by the slab. The transmission and backscatter parameters for a given material are then illustrated by plotting the tallies versus material thickness. Figure 7 illustrates this process using LiH as the shield material. Using this plot allows the designer to select a material and thickness to meet a shield dose limit requirement. For split scatter shield applications, the backscatter parameter is more important since primary particle loss is by scatter away from the system. Particles that are scattered from the front face of a shield will be directed back toward a shield with a smaller radius. The result is that there is a better chance for the particles to escape from the system. Based on Figure 7, split shields using lithium hydride should focus on selecting a thickness that is less than about 7 cm. Beyond 7 cm, there is no significant increase in backscatter performance with an increase in shield mass. This technique was applied to the eight candidate materials listed in Chapter II, to allow for comparison between them regarding their radiation attenuation performance versus mass. Because backscatter is the primary parameter in attenuation

performance for split shields, the material comparison will be based on the thickness at which 85% of the total material backscatter is achieved. The 85% reduction thickness is used because of the diminishing returns from reflection that are seen as the thickness increases. It also provides a standard set point from which to evaluate the performance of the individual materials in an unbiased manner.

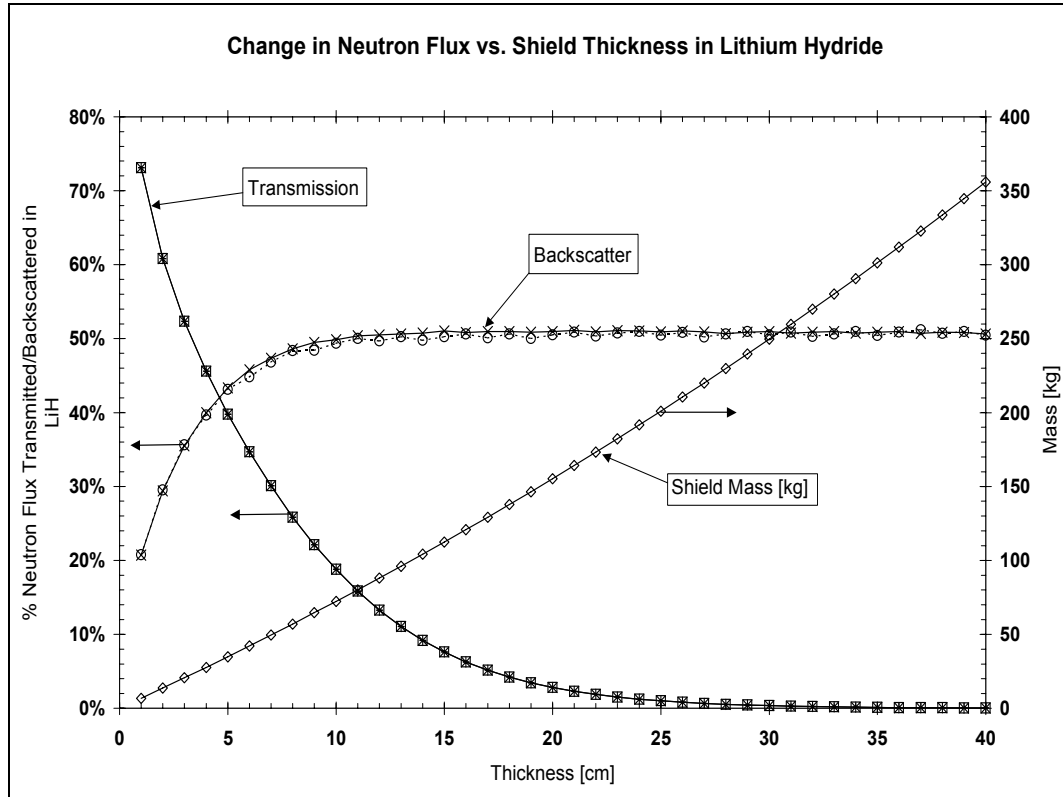


**Figure 7. Material Thickness Parameter for Attenuation and Backscatter**

#### Material Thickness for Energy Spectrum Softening Parameter.

The change in the total flux or current is not the only condition that must be satisfied when determining the effectiveness of a shielding material. The ability of the material to soften (reduce the average energy) the energy spectrum of the particle distribution must also be taken into account. For this shielding application, a material cannot be considered effective if it is transparent to high-energy particles. MCNP4C

allows the user to break any tally into a number of energy bins. The tallies used in determining the material thickness all included energy binning into three coarse energy groups for both neutrons and photons. The energy groups for neutrons are set up to track particles that are in the fast (1.0 to 10.0 MeV), resonance (0.01 to 1.0 MeV), and sub-resonance (0 to 0.01 MeV) ranges. Photon energy groups were set up to track photons with energies in the pair production, Compton scattering, and photoelectric effect ranges. The energy groups are designed to be fairly coarse to allow for an easy comparison between different materials. Once the energy dependence is determined for each material, it is plotted to demonstrate which materials are most effective at softening the particle flux. Figure 8 uses LiH to demonstrate how the energy dependence of the flux changes with increasing thickness.

From this plot, it is seen that the higher energy neutrons are quickly attenuated, and scattered into the lowest energy group. This is why the curve for the thermal neutrons initially grows, before decaying away at around 10 cm. Although there is a net increase in the low energy group neutron flux by about an order of magnitude at 5 cm, there is also a corresponding drop by a half order of magnitude in the higher energy group fluxes. This same procedure was used to generate neutron and photon flux energy softening plots for all materials in this study.

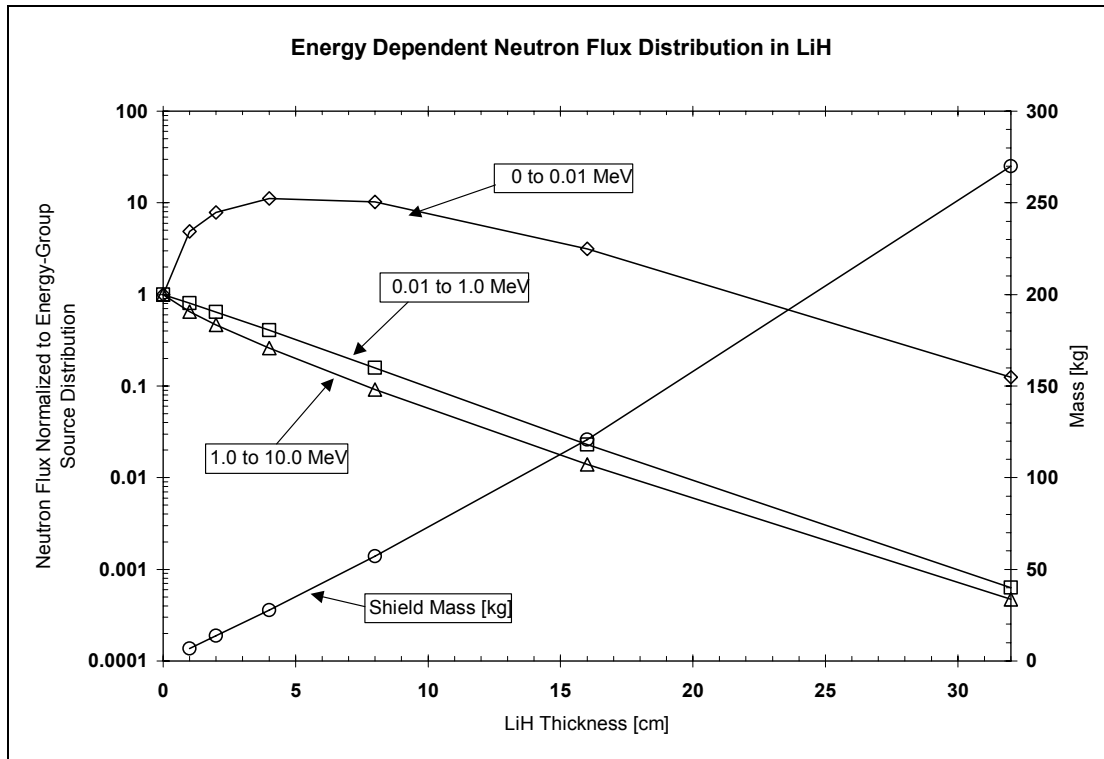


**Figure 8. Effect of Material Thickness on the Energy Dependent Neutron Flux**

#### Material Thickness For Scattering Parameter.

The optimal material thickness for radiation scattering is not necessarily equal to the optimal material thickness for radiation absorption. For this experiment a MCNP4C current tally is used with the cosine tally modifier to determine how the thickness of a material affects the direction that particles will scatter. The reference vector for this tally is the axis that runs through the length of the shield and points in the direction of the particle flow (z-vector). Figure 9 illustrates the reference vector and the location of the different direction cosine bins.

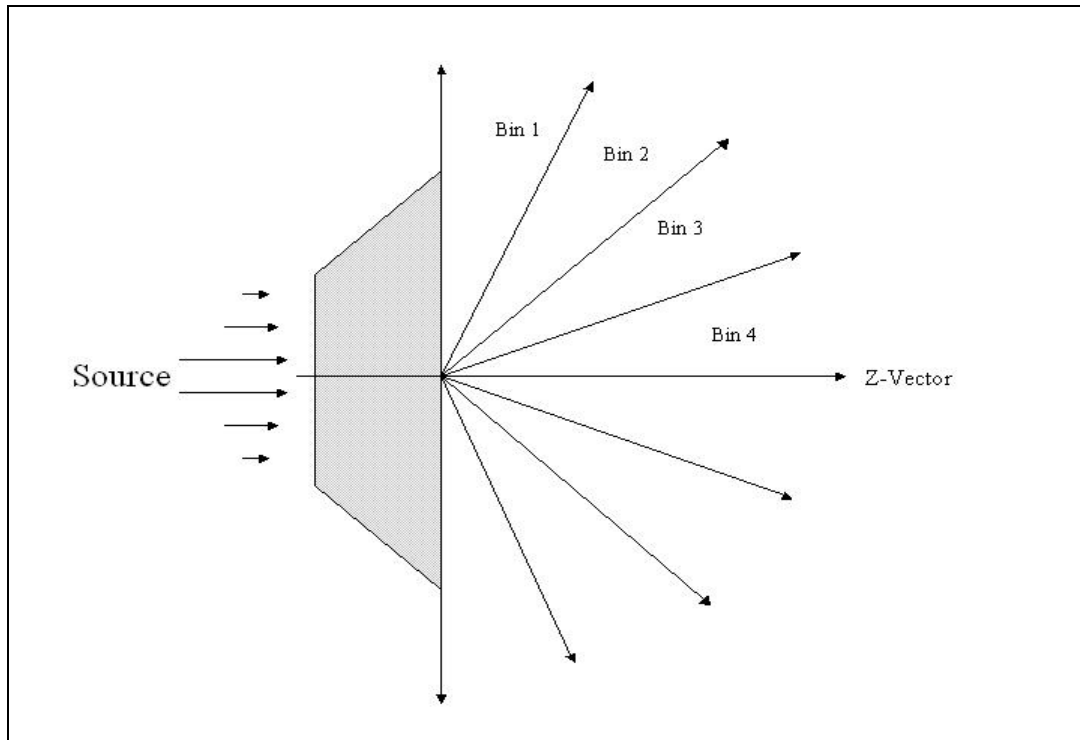


**Figure 9. Depiction of MCNP4C Current Cosine Tally Locations**

Four equally spaced cosine bins were created each with an angle of 22.5 degrees. The optimum scattering thickness is illustrated by plotting the current tallies along with the mass of the shield section. LiH is again used in Figure 10 to illustrate how increasing the material thickness influences the direction that particles will be scattered. A word of caution is required, because selecting equally spaced angular bins will produce unequally spaced  $\cos(\theta)$  values, which in turn means that the solid angle bins will be unequally spaced. Because of this feature, Figure 10 can be somewhat misleading. The outer two angle bins will actually have smaller solid angles while the middle bins are approximately twice as large as the outer bins. Therefore, the actual angular current distribution should be fairly flat across each shield sections. This does not change the fact that the materials are still ineffective at changing the direction that particles scatter.

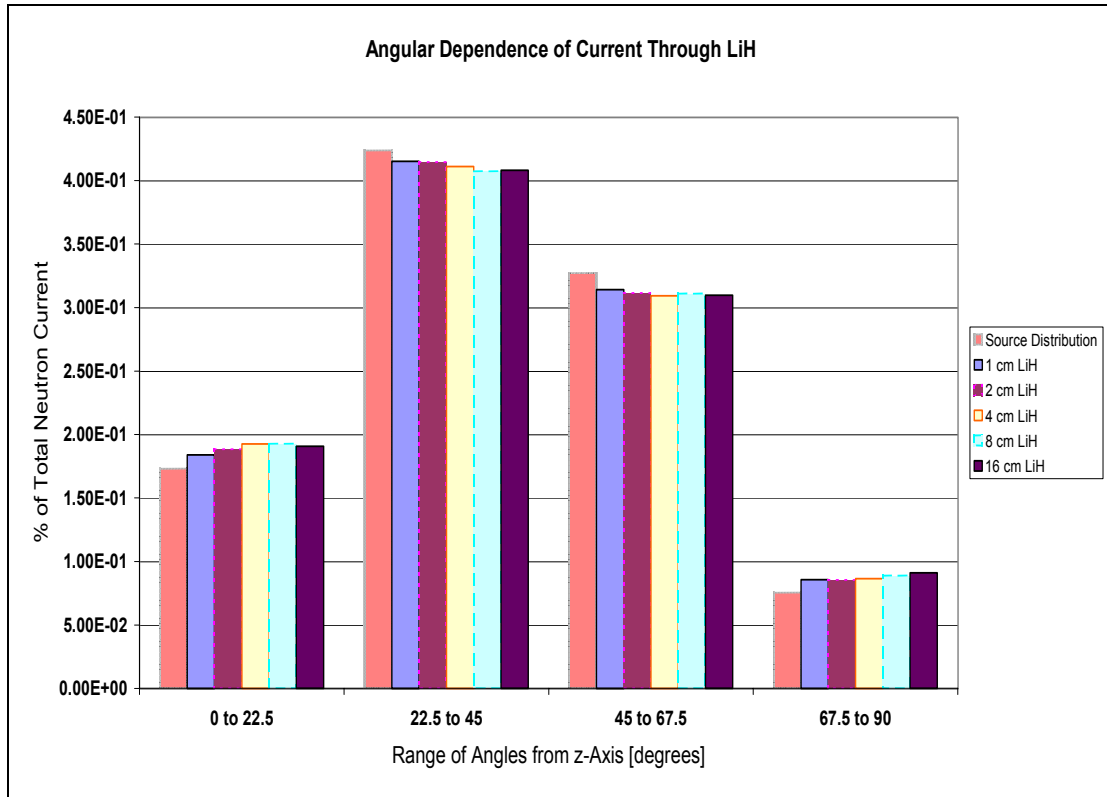


**Figure 10. Effect of Material Thickness on Scattering Direction**

Increasing the LiH thickness reduces the scattering into the central angles and increases scattering toward the centerline and outer edges. Therefore, it is not advantageous from a scattering perspective to increase the thickness of the LiH further.

#### Number of Shield Sections Parameter.

For this experiment, the unit shield was split into a two-section, three-section, and four-section shield respectively, with each section of equal thickness. The total length of the shield is fixed at 500 cm, which accounts for the shield thickness and 233.5 cm of vacuum on each side. Each time the shield is split, the vacuum and shield sections are expanded evenly between the source and dose planes. A flux tally is then placed on the dose plane so that the particle distribution from different shield configurations can be plotted and the effect of shield splitting evaluated. A coarse energy spectrum of the

neutron flux is also tallied to determine whether certain energy particles are scattered from the shield sections more effectively.

#### Shield Geometry Parameter.

Because the purpose of the split scatter shield is to scatter radiation out of the shielded solid angle, it might not be necessary to always cover the entire shield shadow. Consider a particle that has been scattered off of a shield section and is heading in a direction that will remove it from the shielded solid angle. If a material is placed in the path of this particle before it reaches escape, then there is a probability that the particle might be scattered back toward the dose plane [13]. Figure 11 provides an illustration of this scattering process.

The geometry parameter focuses on the proper tapering and sizing of the shield sections to allow particles to escape that have a high escape probability. This analysis was strongly influenced by the results obtained in the material scattering study. One way to illustrate the amount of particles that will leak is to go to the edge of the source plane and map out the space that is covered by particles traveling between 22.5 and 67.5 degrees. This technique is illustrated in Figure 12, which shows a region some distance past the source plane, where the total flux should be reduced.



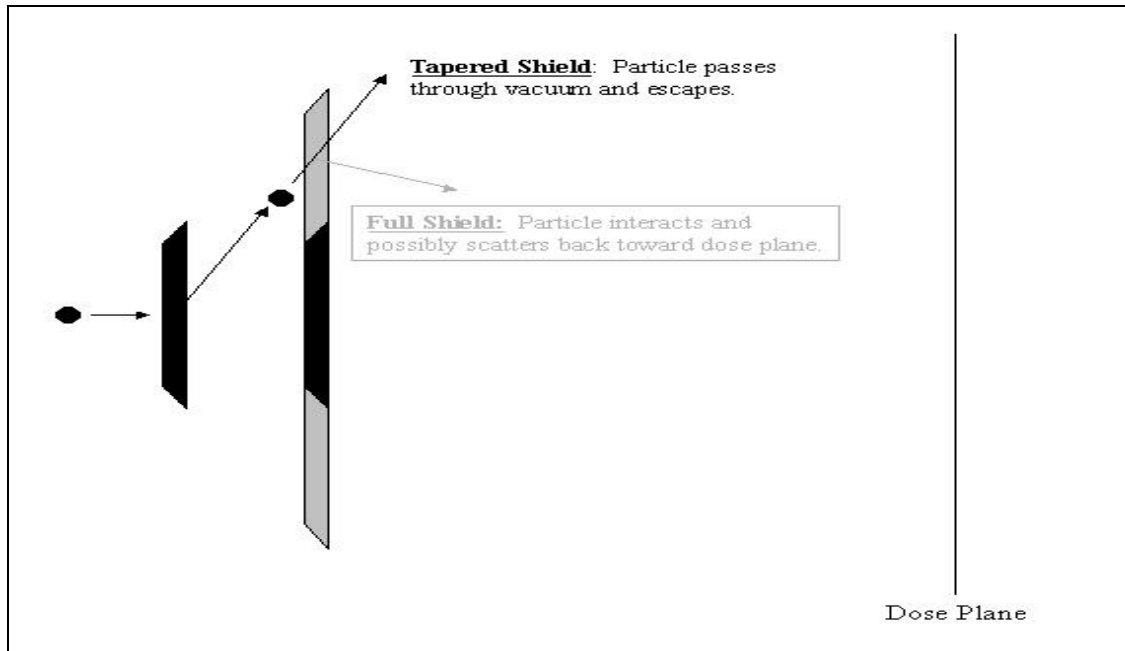


**Figure 11. Effect of Shield Tapering on Particle Scattering**

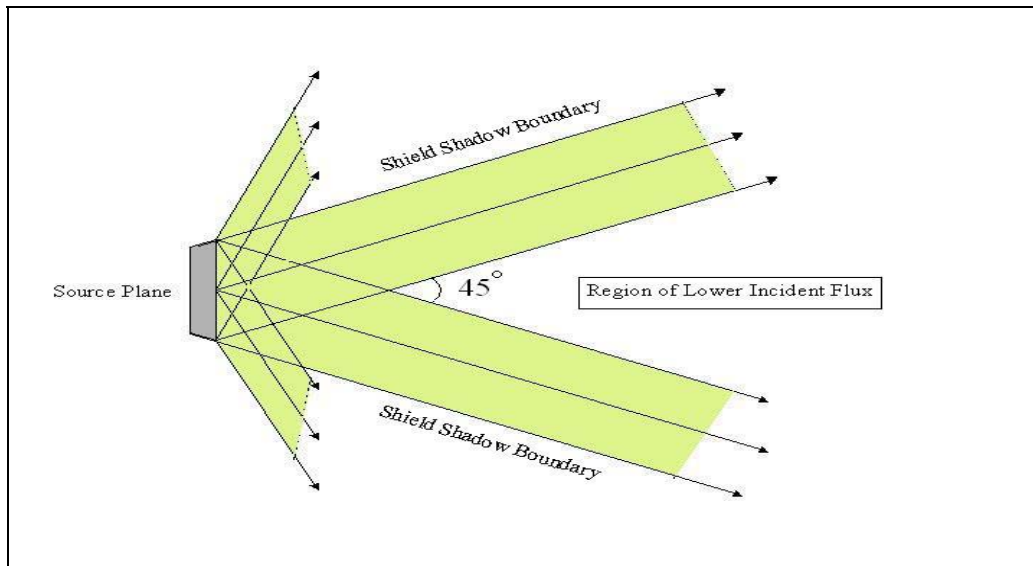


**Figure 12. Angular Distribution of Neutron Flux Between 22.5 and 67.5 Degrees**

### Positioning of the Gamma Shield.

One issue for gamma shielding that was mentioned in the materials section of the literature review, is the capture of neutrons by the gamma shield material [6]. These captures, along with inelastic neutron scattering off materials like steel or tungsten will

result in an increase in the gamma ray distribution in the shield. Therefore, the placement of the gamma shielding material within the shield is important for optimizing performance as well as for mass considerations [10]. The shield cannot be placed directly adjacent to the reactor, because the resultant gamma ray hardening will require additional shielding at another point in the shield. As the gamma ray shielding material is moved further from the reactor, the mass will increase because the divergence of the flux will require a larger shielded area. Analyzing several configurations of the unit shield and measuring the gamma ray dose at the dose plane determined the optimal placement of the gamma shielding material. The type of shield analyzed should not adversely affect the results of this test, because the key factor for gamma shield flux hardening is the energy of the neutrons. The neutron flux energy spectrum will need to be softened by a certain amount of material regardless of the shield that is used. Therefore, the results from this test can be taken from the unit shield and applied to the split scatter shield.

#### Energy Deposition in the Shield.

Berga predicted in his thesis, that the amount of energy deposited in a split scatter shield would be reduced, because the shield relies on scattering radiation rather than absorbing it [4:49-50]. The total energy deposited within any shield is a combination of many sources. Among these are gamma heating, neutron capture, neutron scattering, heat transferred from the radiators, and heat transferred from the reactor. Although some of these processes are beyond the scope of this research, an estimate of the energy deposited in the shield by scattering, gamma heating, and neutron capture can be determined by using an energy deposition tally in MCNP4C [16:3\_74]. This tally will report the

average energy deposited in a given cell in units of MeV per gram. To determine whether the split scatter shield is advantageous from a thermal viewpoint, the unit shield is analyzed with MCNP4C using the energy deposition tally. A split scatter shield is then evaluated and the values are compared to the unit shield to determine whether there is a significant reduction in the energy transferred to the shield.

#### Split Scatter Shield Design.

The process of determining an individual parameter cannot be completed without direct coupling to the other parameters in the split shield. These parameters are evaluated individually to provide insight for the proper coupling of the system to achieve an optimized shield. The split scatter shield design process can progress forward by looking at the shield and cone angle spacing study to provide initial input into the system. This will provide an estimate of the particles that can be lost through leakage alone. The next step is to select materials that will maximize the reflection of particles back toward the source plane with a minimal amount of mass. The selection of the materials must then be balanced with the shield spacing to ensure that the particles that are reflected are given an adequate chance to leak before reaching the next shield section. Furthermore, the performance of the shield must be balanced with the increased mass of the shield as split sections are moved further from the source plane and are required to increase in radius to shield the entire shadow.

A small experiment was performed to determine whether there is an optimum split shield configuration. In this experiment, the unit SEHPTR shield was used, except that portions of the lithium hydride shield were split off and moved closer to the payload.

The change in the neutron fluence and photon dose were then measured and plotted to demonstrate the effectiveness of splitting some material from the original shield and moving it backward. This experiment looked at two different cases. The first case removed a quarter of the lithium hydride material and moved it closer to the payload. For comparison, the new split shield section was reduced in thickness so that the overall mass of the unit shield was conserved at 850 kg. A diagram of this shield configuration is shown in Figure 13.

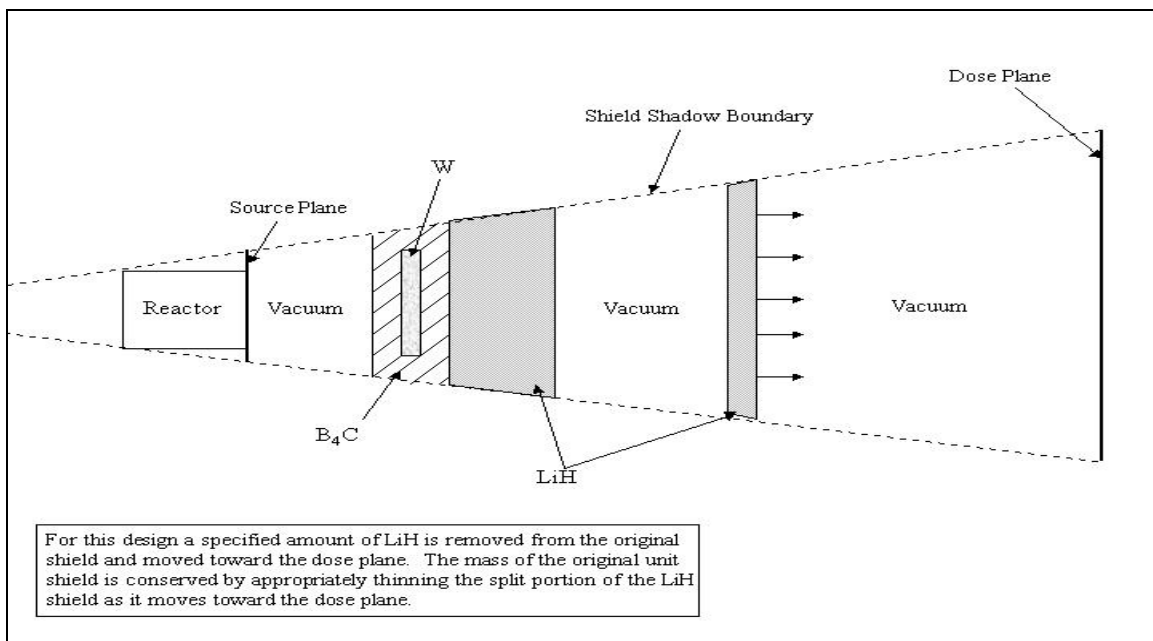


**Figure 13. Approach to Searching for a Split Shield Optimum**

## **IV: Results**

The evaluation of the split scatter shield provided some challenges that were not foreseen when the research was first started. The benchmarking efforts for “Split\_Shield” indicated that it would not accurately predict the neutron and photon flux values making it unusable for the remainder of the study. Regardless, this research did produce a set of shield design parameters that are applicable for a variety of space shielding applications and were useful in evaluating the split scatter shield.

### **Benchmarking “Split\_Shield”**

Benchmarking for “Split\_Shield” was accomplished by comparing results from MCNP4C with “Split\_Shield”. All of the results shown in this benchmarking section are given for the most recent version of the “Split\_Shield” code. Therefore, all of the corrections that are discussed in the next section regarding code troubleshooting have been implemented.

Three separate benchmarking tests were selected to evaluate “Split\_Shield”. The first benchmarking test was used to determine the ability of “Split\_Shield” to replicate the neutron flux as reported in MCNP4C. This test evaluated a split shield that consists of 80 cm of vacuum and 20 cm of carbon. For each new shield evaluation, the carbon is divided into an increasingly larger number of shield sections. The unit shield is 40 cm of vacuum, 20 cm of carbon, and 40 cm of vacuum. The most split shield is 13.33 cm of vacuum followed by 4 cm of carbon, repeated for 5 shield sections. The total length of the shield however, is always maintained at 100 cm.

Table 5 lists the dimensions for all of the shields, as well as the neutron and photon flux distributions from both MCNP4C and “Split\_Shield”. This data shows that “Split\_Shield” overestimates both the neutron and photon flux for the unit shield. The neutron flux matches the MCNP4C results somewhat closely for two, three, and four section split shields. For shields with more than three sections however, the “Split\_Shield” neutron flux begins to increase greater than the MCNP benchmark.

**Table 5. Split\_Shield Benchmarking Data for Carbon Shield**

# Shield Sections	Vacuum Width [cm]	Carbon Width [cm]	Split_Shield n Flux [n/cm <sup>2</sup> -sec-src n]	MCNP n Flux [n/cm <sup>2</sup> -sec-src n]
1 - Unit	40	20	8.450E-6	6.707E-6 +/-1.31E-7
2	26.7	10	5.690E-6	5.510E-6 +/- 1.12E-7
3	20	6.7	4.850E-6	5.228E-6 +/- 1.11E-7
4	16	5	4.860E-6	5.165E-6 +/- 1.12E-7
5	13.3	4	5.160E-6	5.131E-6 +/- 1.01E-7
# Shield Sections	Vacuum Width [cm]	Carbon Width [cm]	Split_Shield $\gamma$ Flux [ $\gamma$ /cm <sup>2</sup> -sec-src $\gamma$ ]	MCNP $\gamma$ Flux [ $\gamma$ /cm <sup>2</sup> -sec-src $\gamma$ ]
1 - Unit	40	20	1.260E-5	9.540E-6 +/- 1.48E-7
2	26.7	10	1.410E-5	9.774E-6 +/- 1.55E-7
3	20	6.7	1.780E-5	9.761E-6 +/- 1.62E-7
4	16	5	4.820E-5	9.815E-6 +/-1.61E-7
5	13.3	4	Diverged	9.839E-6 +/-1.59E-7

The MCNP4C results indicate an initial decrease in the neutron flux with shield splitting, and then a leveling out for shields that are split more than three times. The

“Split\_Shield” results for photon flux drastically depart from the MCNP results after two shield sections, and always over predict the values. The MCNP4C data indicates that the photon flux should remain fairly constant for all shields, no matter the amount of splitting.

The second benchmarking test, evaluated the effectiveness of “Split\_Shield” for gamma shielding applications. This test was identical in style to the first test, except that now tungsten was used as the shielding material. The overall dimensions of the unit shield were 46 cm of vacuum and 4 cm of tungsten, with the total shield width fixed at 50 cm. The process for splitting the shields was the same as the one used for the tests with carbon.

Table 6 lists the dimensions for the tungsten shields, and the results from “Split\_Shield” and “MCNP4C”. “Split\_Shield” gave results indicating a decrease in the neutron flux with shield splitting, while MCNP4C shows that the neutron flux is relatively unaffected by shield splitting. The photon flux from “Split\_Shield” decreases until the splitting exceeds three shields, at which point the flux levels off. MCNP4C indicates that the photon flux should also be unaffected by the splitting of the shields.

The final benchmarking test evaluated the ability of “Split\_Shield” to accurately predict the neutron and photon flux distribution for laminated shields with different materials. This test evaluated a shield composed of 80 cm vacuum, 18.5 cm carbon, and 1.5 cm tungsten, with the total shield width always fixed at 100 cm. The splitting procedure from the first two tests was again used to create four separate shield cases.

**Table 6. Split\_Shield Benchmarking Data for Tungsten Shield**

# Shield Sections	Vacuum Width [cm]	Tungsten Width [cm]	Split_Shield n Flux [n/cm <sup>2</sup> -sec-src n]	MCNP n Flux [n/cm <sup>2</sup> -sec-src n]
1 – Unit	23	4	2.76E-5	2.89E-5 +/- 3.04E-7
2	15.33	2	2.40E-5	2.85E-5 +/- 2.98E-7
3	11.5	1.33	2.09E-5	2.87E-5 +/- 3.50E-7
4	9.20	1	2.06E-5	2.84E-5 +/- 3.45E-7
5	7.67	0.8	1.90E-5	2.85E-5 +/- 3.44E-7
# Shield Sections	Vacuum Width [cm]	Tungsten Width [cm]	Split_Shield $\gamma$ Flux [ $\gamma$ /cm <sup>2</sup> -sec-src $\gamma$ ]	MCNP $\gamma$ Flux [ $\gamma$ /cm <sup>2</sup> -sec-src $\gamma$ ]
1 – Unit	23	4	1.59E-6	1.88E-6 +/- 7.58E-8
2	15.33	2	1.14E-6	1.90E-6 +/- 7.24E-8
3	11.5	1.33	8.95E-7	2.10E-6 +/- 8.38E-8
4	9.20	1	9.34E-7	1.93E-6 +/- 7.57E-8
5	7.67	0.8	8.65E-7	1.93E-6 +/- 7.21E-8

Table 7 provides a list of the shield dimensions and performance values from both “Split\_Shield” and MCNP4C. For the unit and two-section shield, “Split\_Shield” comes fairly close to matching the neutron flux values given by MCNP4C. The last two shields however, diverge using “Split\_Shield”, while MCNP4C shows a continuous gradual decrease in neutron flux. The photon flux values from “Split\_Shield” do not show a general trend, but instead go up for two shield sections, drop below the unit shield flux for three sections, and then increase slightly for four sections. MCNP4C however,



indicates that the photon flux should remain relatively unchanged, regardless of the shield splitting.

**Table 7. Split\_Shield Benchmarking Data for Laminated (C-W) Shield**

# Shield Sections	Vacuum Width [cm]	Carbon Width [cm]	Tungsten Width [cm]	Split_Shield n Flux [n/cm <sup>2</sup> -sec-src n]	MCNP n Flux [n/cm <sup>2</sup> -sec-src n]
1	40	18.5	1.5	5.39E-6	5.57E-6 +/- 1.26E-7
2	26.7	9.25	0.75	5.15E-6	5.02E-6 +/- 9.73E-8
3	20	6.17	0.5	7.76E-6	4.77E-6 +/- 1.03E-7
4	16	4.63	0.375	1.24E-5	4.70E-6 +/- 9.75E-8
# Shield Sections	Vacuum Width [cm]	Carbon Width [cm]	Tungsten Width [cm]	Split_Shield $\gamma$ Flux [ $\gamma$ /cm <sup>2</sup> -sec-src $\gamma$ ]	MCNP $\gamma$ Flux [ $\gamma$ /cm <sup>2</sup> -sec-src $\gamma$ ]
1	40	18.5	1.5	2.34E-6	2.09E-6 +/- 6.30E-8
2	26.7	9.25	0.75	3.93E-6	2.14E-6 +/- 5.77E-8
3	20	6.17	0.5	1.37E-6	2.18E-6 +/- 6.43E-8
4	16	4.63	0.375	1.80E-6	2.19E-6 +/- 6.19E-8

The three experiments used to benchmark “Split\_Shield” indicate that the program is not effective at predicting the neutron or photon flux in a split scatter shield. The behavior of the neutron flux in the first and third tests indicate that there may be a numerical instability in the program logic, causing the results to diverge. The error in the results increases as more shields sections are evaluated, which also indicates that maybe there is some error in each shield section material.

### Methods Used to Troubleshoot the “Split\_Shield” Program.

Another series of tests were performed in an attempt to fix “Split\_Shield”, or at least bring it into better agreement with MCNP4C. The first possible source of error was in the source term distribution. At the time of code development, the SEHPTR source term was not complete, so an estimation of the source term had to be substituted for MCNP4C evaluations. The material data tables that were created for “Split\_Shield” used an exponential distribution of the source from the centerline of the shield out to the edge. This results in the highest flux at the center of the shield with little or no flux out at the shield’s edge. From the SEHPTR source term however, it is shown that the source decreases more like a cosine function from the shield centerline to the edge. For benchmarking purposes however, the choice of distribution shouldn’t matter as long as it is consistently used in both MCNP4C and “Split\_Shield. The greater problem with the distribution is that “Split\_Shield” doesn’t account for changes to the flux profile as additional shielding sections are used.

All of the material data tables in “Split\_Shield” are created using MCNP4C calculations on separate shields with increasing thickness. Therefore, the source distribution for the 1 cm shield is the same as the distribution for all other shields. An MCNP4C calculation was performed to evaluate the shape of the flux after passing through a single shield section. The result indicates that the flux profile exiting a shield section is flattened across the shield and the energy distribution is softened. Since “Split\_Shield” always uses the source distribution for every shield section, this will lead to an overestimation of the shield flux and energy profile when compared to MCNP4C results.

Another factor that “Split\_Shield” is insensitive to is the direction particles are heading after they pass through a shield section. When particles exit a shield section in “Split\_Shield” they are headed in a variety of directions. At this point “Split\_Shield” goes to the next shield section, where the starting source distribution is again applied. This doesn’t take into account the particles that were going to leave the problem after interacting in the first shield, or particles that were scattered back toward the dose plane. The only information that is carried from shield section to shield section is the total fraction of particles that crossed the material boundary. As the split shield gets longer, the shield sections will get larger in diameter. This means that there is a higher probability that particles will remain in the shield, rather than leak out the boundaries. “Split\_Shield” will not recognize this however, since the individual shield sections always start with a radius of 52.7 cm and increase based on the length of the section. MCNP4C does not suffer from this problem, because all particles are continuously tracked until they leak from the problem, are absorbed, or killed by Russian roulette. This effect causes the particle flux reported by “Split\_Shield” to be lower than MCNP4C, with the difference increasing as more shield sections are used. A method to determine the difference between the MCNP4C flux and the “Split\_Shield” flux is to run particles through a material and then take tallies at increasing distances from the shield, as shown in Figure 14.

The results from Figure 14 imply that the “Split\_Shield” values could be brought into agreement with MCNP4C by multiplication with an appropriate exponential factor. Fitting exponential curves to both sets of data and comparing the difference provided the multiplication factor required. The same technique was applied for the backward

transmission of particles to find a backward multiplication factor. The “Split\_Shield” program was then modified with these factors and the benchmark tests performed again.

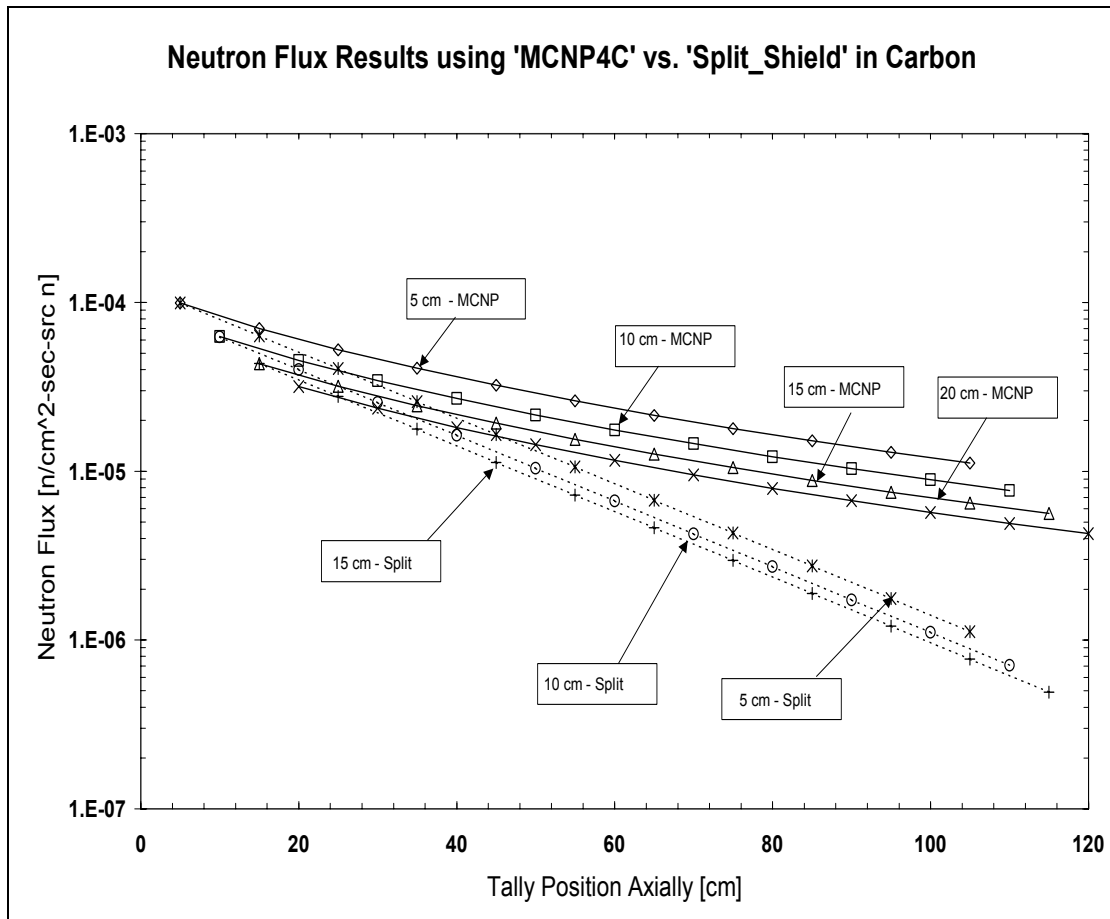


**Figure 14. Difference in Flux Profile Between MCNP4C and “Split\_Shield”**

One final issue considered, was the effect of error propagation from the material data files into the “Split\_Shield” results. A certain amount of stochastic error is associated with MCNP4C tallies, which was recorded when the material data files were created. Each time a mathematical operation is performed on numbers that contain uncertainty, the uncertainty in the solution is increased. Therefore, as the number of mathematical operations increase, so does the uncertainty. Shield problems with long convergence times increase the number of operations required, which can lead to more

error and possibly a divergence in the results. Steps were taken to implement an error handling routine into “Split\_Shield”. Due to time constraints however, the effect of error on the results was not fully explored and the error handling routine was not verified. Ultimately, “Split\_Shield” had to be set aside so that research into the optimum shielding parameters could be pursued further. Therefore, all of the split scatter shield experiments were conducted using MCNP4C.

### **Split Scatter Shield Parameter Study**

#### Shield Spacing Parameter.

The relationship between the shield spacing, half cone angle and the loss of particles was studied by plotting the probability of particles missing a shield given a shield separation distance. Such a plot is shown in Figure 15. This plot shows that the probability of a particle hitting the target shield from either direction decreases faster initially and then begins to fall off at a constant rate as the shield separation distance is increased. Furthermore, if the required shadow shield angle is reduced the leakage is increased for a given shield separation distance. For a 21-degree half cone angle, about half of the particles miss the target shield for a spacing of just 20 cm. A designer may choose to design a shield that has many split shield sections with short separation distances. This has the effect of losing half the particles from forward leakage from shield to shield. If the shield material is effective at reflecting radiation, it may be possible to quickly remove a large quantity of particles from the system.

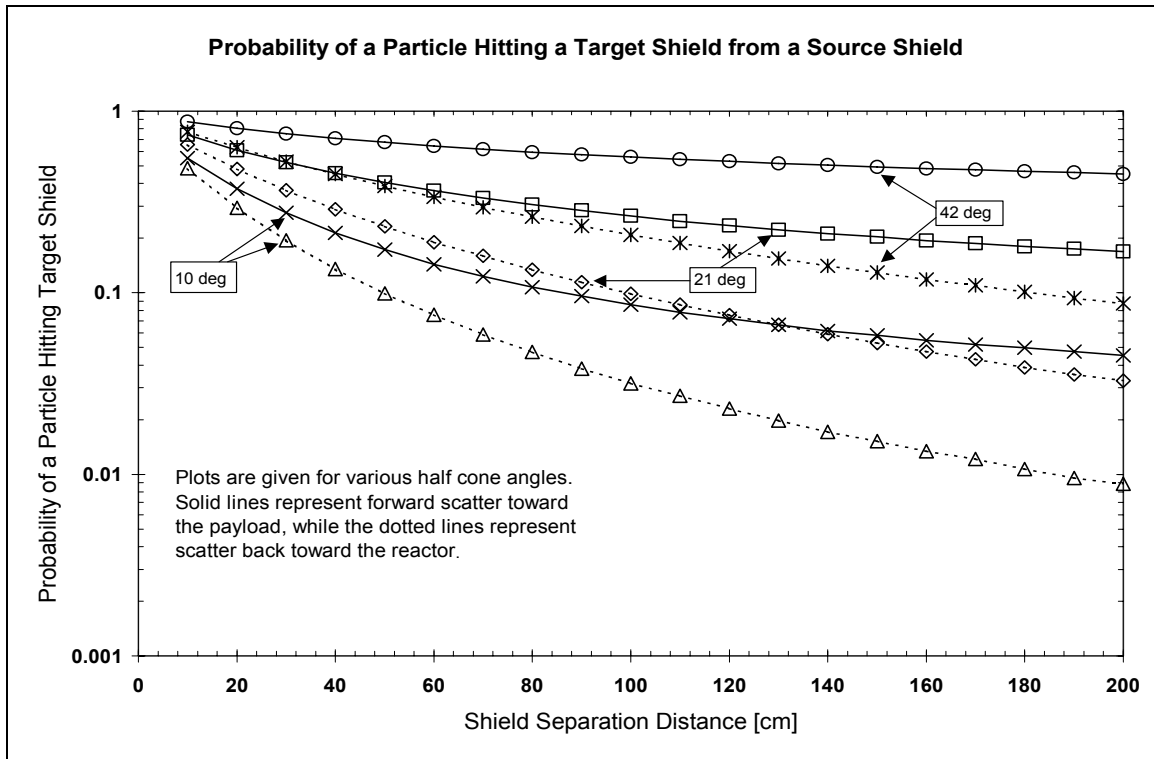


**Figure 15. Effect of Shield Spacing and Half Cone Angle on Particle Leakage**

#### Material Thickness Parameter.

The material thickness study provided insight into the best selection of materials for the use in the split scatter shield. Table 8 lists the attenuation thickness values at which 85% of the maximum neutron backscatter possible for each material is achieved. The percent flux reduction shows how much a material was able to reduce the neutron flux at this thickness.

Table 8 indicates that beryllium is the best material for backscattering neutrons, although the 85% backscatter thickness is at 10 cm. The backscatter for 35 kg of beryllium, which is equal to the 85% backscatter mass of lithium hydride, is only 38.2%. From a mass standpoint, the best material for this shielding application for the materials listed in Table 8 is LiH.

**Table 8. Material Thickness Parameters for Neutron Backscatter and Attenuation**

Material	Maximum % Back Scatter	85 % Back Scatter [cm]	% Flux Transmitted	Mass of Shield at Source Plane [kg]
LiH	51	5	60.2	35
ZrH <sub>2</sub>	53	4	60.0	192
Be	80	10	76.1	172
C	72	12	76.4	203
B <sub>4</sub> C	56	4	62.2	89
Steel	69	9	67.3	651
W	55	3.2	55.2	545

Table 9 shows how each of the materials performs for backscattering and attenuating gamma rays. The layout of the table is the same as Table 8, except that the values are for gamma ray shielding.

**Table 9. Material Thickness Parameters for Gamma Backscatter and Attenuation**

Material	Maximum % Back Scatter	85 % Back Scatter [cm]	% Flux Transmitted	Mass of Shield at Source Plane [kg]
LiH	31	19	35.3	147
ZrH <sub>2</sub>	19	1.5	59.2	71
Be	40	12	38.7	209
C	37	9	44.3	149
B <sub>4</sub> C	39	7	46.7	159
Steel	25	1	64.7	68
W	12	0.3	56.6	50

Table 9 indicates that from a mass standpoint, steel or ZrH<sub>2</sub> may be the best materials for shielding gamma rays in a split shield environment. With such low backscatter values however, it appears that splitting the gamma shield will not be as effective as for neutron shielding. The splitting of the gamma shield is investigated further in the section on the shield splitting, and will be discussed at that time.

The particle scattering parameter studied using plots similar to Figure 10, did not appear to change significantly for an increase in shielding thickness. In fact, increasing the shield thickness flattened the angular profile of the current for both particle types.

The particles scattering toward the center of the shield tended to increase with the addition of material, while the particles that were scattering into the region from 45 to 90 degrees decreased. Overall, the total change in the particle direction was not significant. The largest scattering angle for the neutron source was between 22.5 and 45 degrees, which accounts for 42.4% of the total angular distribution. When 16 cm of LiH is used as a shield, the scattering into this angle range is reduced to 40.8% of the total angular distribution. The experiments conducted for photons indicate the same general trends. The overall indication from the attenuation and scattering parameter studies is that for split shield applications, the shield sections should be kept relatively thin when compared to the layers in the unit shield. It also appears based on the scattering study (Figure 10), that these materials will not be particularly effective at changing the direction that particles are scattered as they pass through a shield section.

#### Number of Shield Sections Parameter.

The results of this experiment indicate that splitting the radiation shield does produce an overall reduction in the neutron flux. Figure 16 shows the change in flux at the dose plane as the number of split shields is increased. Splitting the shield into two sections reduces the 0.1 MeV neutron flux by approximately 44%, with an increase in shield mass of 6%. This increase in mass comes from moving the second shield section closer to the dose plane, which will increase the required shadow radius. The effect of shield splitting on the gamma dose is nearly identical to the neutron flux, with the total dose reduced by approximately 43% for two shield sections.



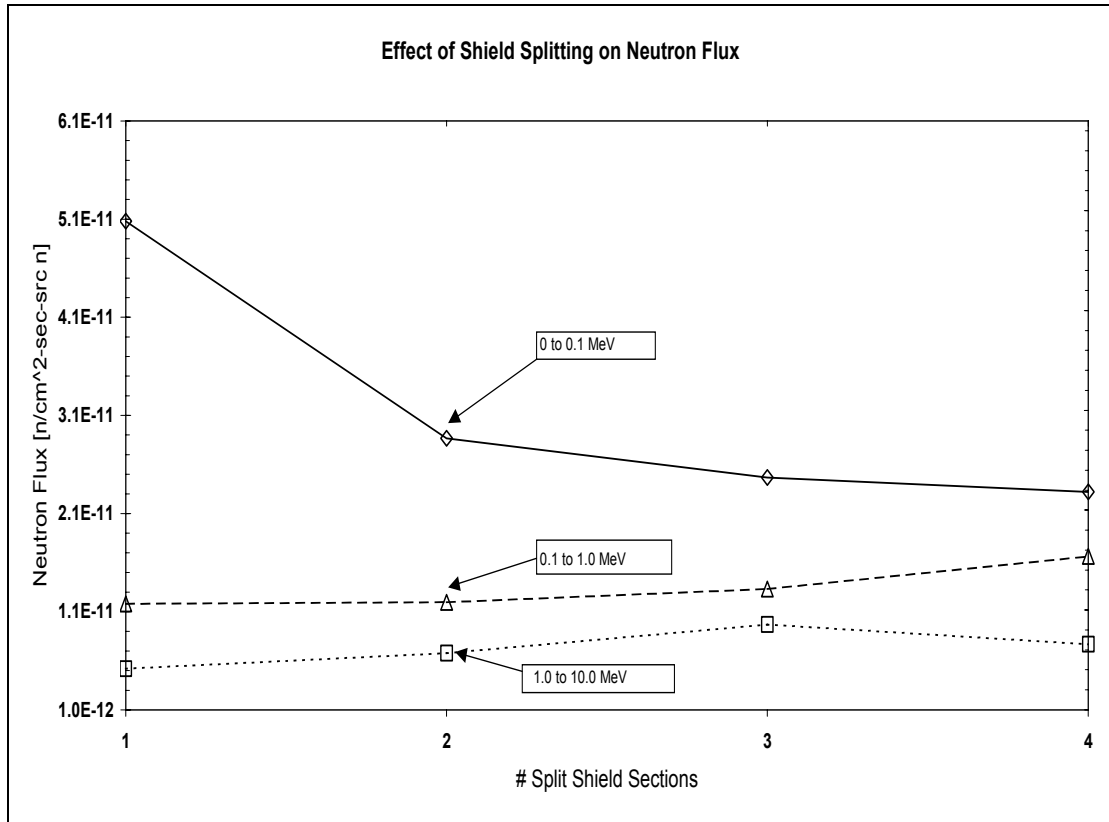


**Figure 16. Effect of Shield Splitting on the Neutron Flux**

#### Optimum Shield Geometry.

For a SEHPTR design, the distribution of particles (similar for both neutrons and gamma rays) along the face of the source plane is highest between 0 and 30 cm, which accounts for 90% of all particles leaving the source. Figure 17 shows the distribution of source particles as a function of distance from the shield centerline.

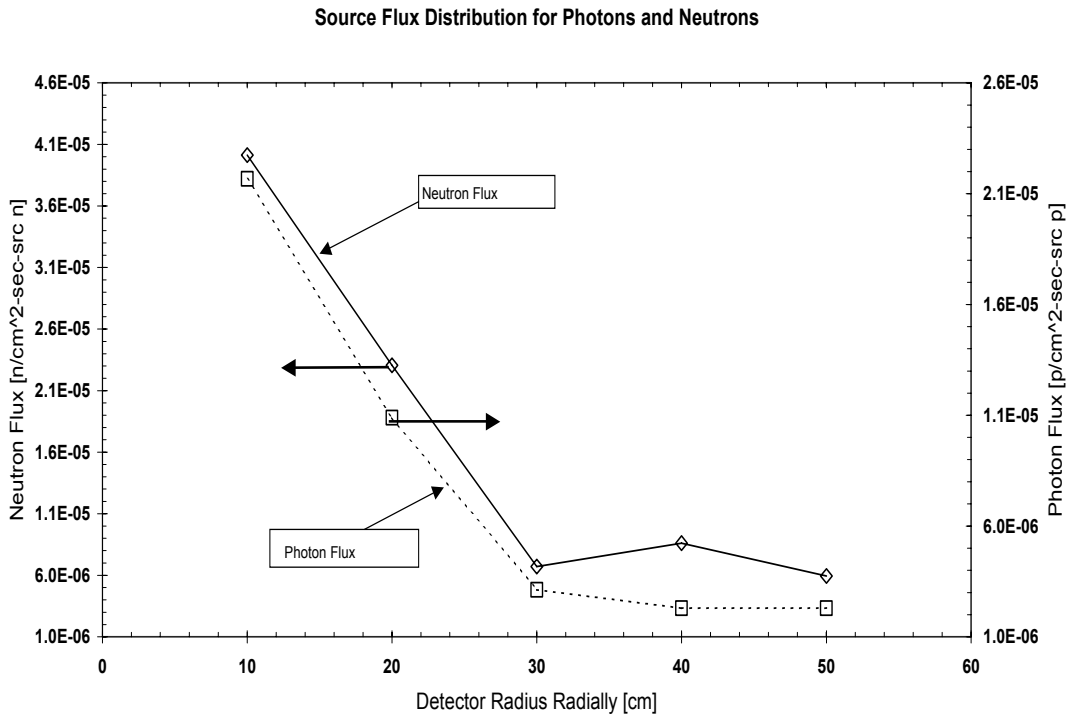


**Figure 17. Neutron and Photon Flux Profiles at the Source Plane**

The unit shadow shield designed originally for the SEHPTR has a shadow angle of 21 degrees [8:10]. This means that separating the source plane by 3475 cm from the dose plane without shielding, will remove all but the 15% of the total flux that is streaming forward between 0 and 22.5 degrees. Since the shadow angle between the source and dose plane is 21 degrees, most of this forward flux will not diverge out of the shadow radius. This means that even the best geometric configuration will require shielding for 15% of the total flux.

The final observation regarding the shielding geometry is also related to the 21-degree source-to-dose plane shadow angle. There exists a location somewhere on the source plane where particles streaming into the angle greater than 22.5 degrees will leak from the shadow angle of 21 degrees at exactly the source-to-dose plane separation

distance of 500 cm. This location is found by determining the radius of the dose plane at 500 cm, which is 242 cm. The radius that is swept out by the 22.5-degree angle at 500 cm is calculated to be 207 cm. Subtracting the dose plane radius by this swept out radius sets the boundary on the source plane for particles that will not leak from the shadow at 500 cm. This source plane radius is calculated to be 35 cm. This process is shown in Figure 18.

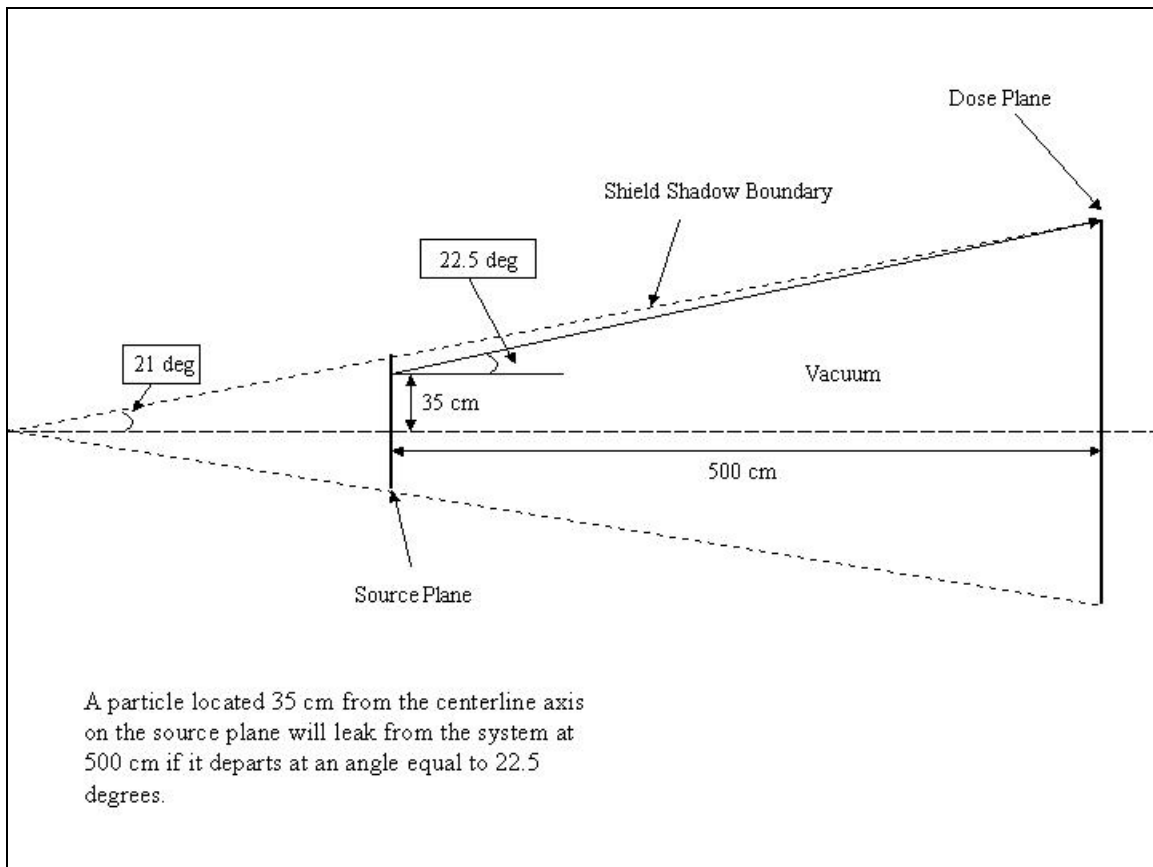


**Figure 18. Location of Source for Particle Leakage at Exactly 500 cm**

Intuitively it would seem that the shield radius would only have to extend far enough to absorb the particles that will not leak before the dose plane is reached. This is not the case however, because the small fraction of particles that are streaming forward at the edges of the source planes will not be attenuated and greatly increase the tally at the

dose plane. A test was conducted to demonstrate this effect, by taking the unit shield and removing the material around the edge so that the front face of the shield only saw the forward scattered particles from the 35 cm radius source plane. Assuming a 50 cm source plane, this left a 15 cm radius that saw limited or no shielding at all for forward sourced particles. A series of ring detectors was then placed along the dose plane to determine the radius that was still within the acceptable limits. This shield configuration can be seen in Figure 19.

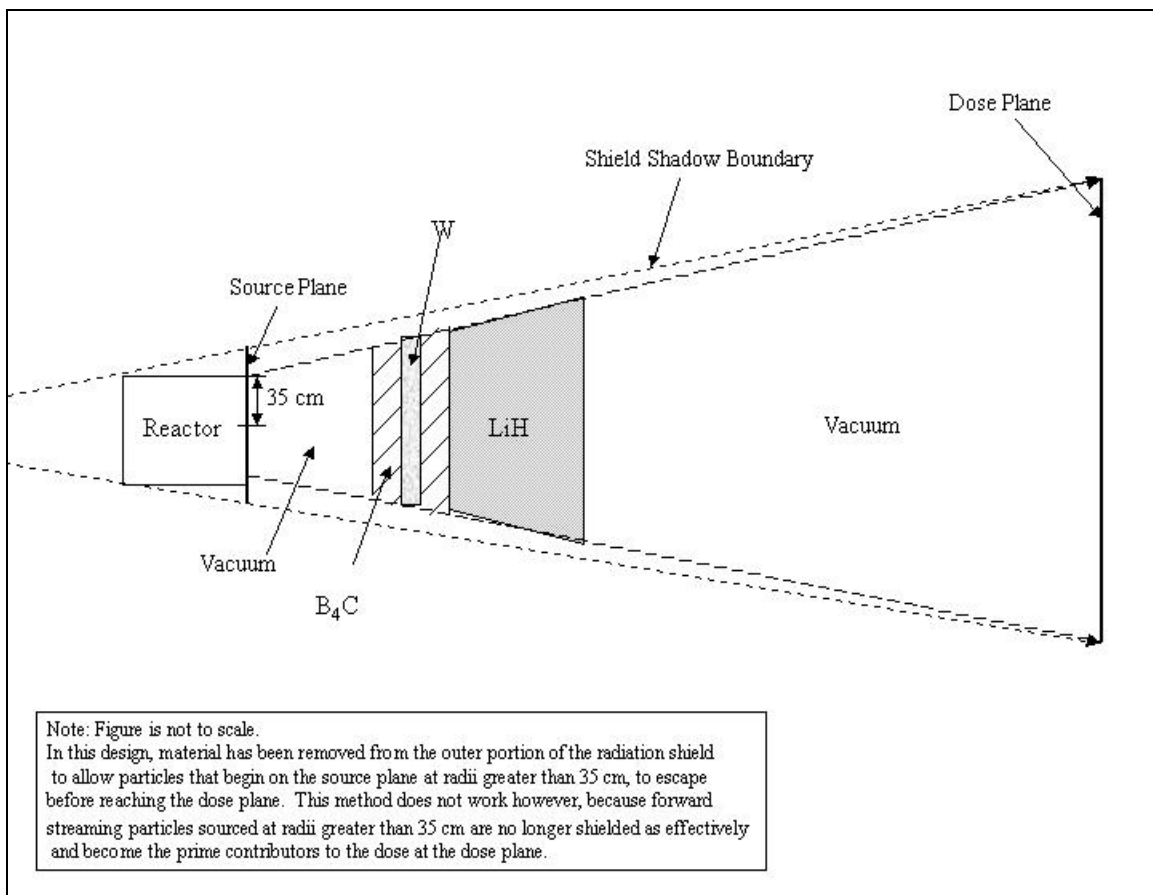


**Figure 19. Shield Configuration for Preferential Leakage Study**

For a unit shield, the dose plane radius is 484 cm, but the removal of shield material to allow for leakage reduced this radius to approximately 100 cm. This would indicate that not only are the forward source particles an issue, but also particles that are

sourced in at an angle and have less material to travel through before reaching the dose plane. So, to effectively shield the dose plane, at least the first shield section must cover the entire shadow angle.

#### Gamma Shield Placement.

The gamma shielding material used for this parameter study was tungsten. Placing the gamma shield behind 4 cm of neutron moderating material proved to be the optimal configuration for the tungsten. At this location, the photon dose was reduced by a factor of two when compared to the gamma shield material placed on the surface of the shield. The difference in mass between the two locations was only 20 kg. Again this result correlates with the design parameters used for the SEHPTR shield, which used 2 cm of tungsten placed 4 cm below the shield surface.

#### Energy Deposition in the Shields.

The total energy delivered to a two-section split scatter shield was 12% less than the energy delivered to the unit shield. This result implies that some of the B<sub>4</sub>C used in the shield due to thermal constraints might be exchanged for LiH, which is about half as massive for approximately the same neutron backscatter and attenuation performance.

#### Split Scatter Shield Design.

A split scatter shield was constructed using some of the design parameters listed in this section and then compared to the unit shield. This design split the SEHPTR unit shield evenly into two pieces and separated them by 50 cm. The source-to-shield separation distance was maintained at 20 cm, for the sake of comparison. An illustration of this shield design is shown in Figure 20.

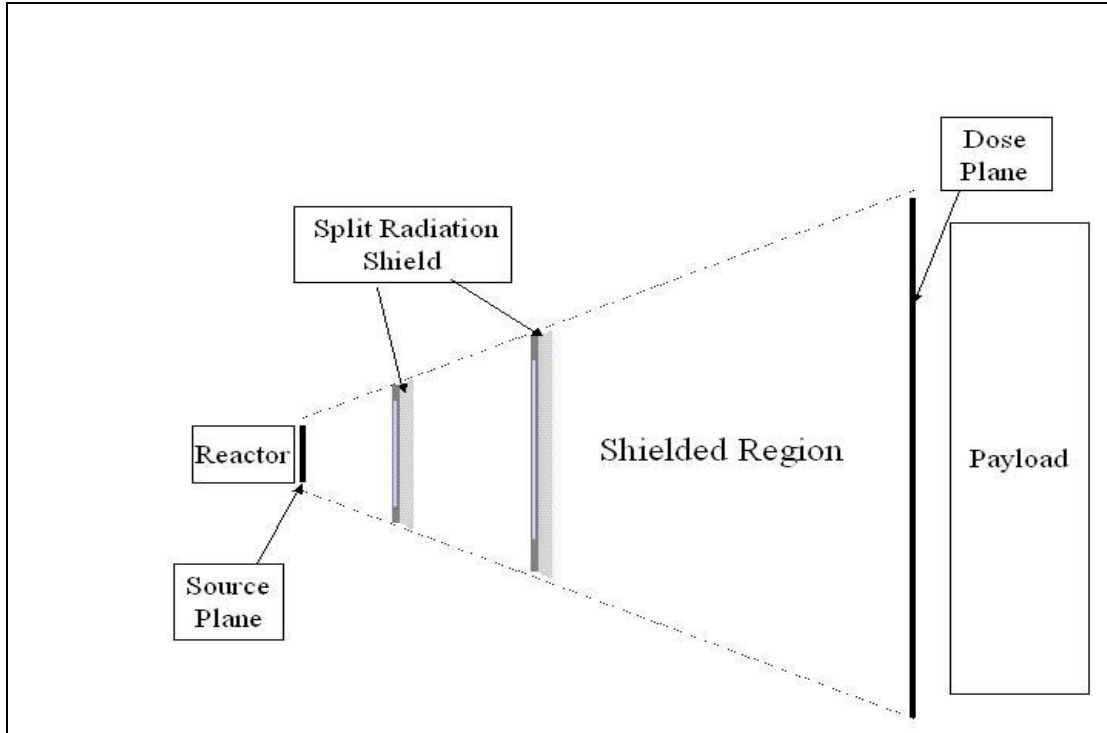


**Figure 20. Design Layout for Splitting the Unit Shield**

Although the split shield was able to meet the limits required at the dose plane, there was a 25% increase in the mass of the shield. This increase in mass comes from the requirement that the entire shadow angle must be shielded, and is given by the following equation:

$$\frac{d_{mass}}{dh} = 2\pi \cdot t \cdot h \cdot \tan^2(\theta) \quad (18)$$

where:

$t \equiv$  Shield Thickness [cm]

$h \equiv$  Distance from Source Plane to Front Face of Shield Section [cm]

$\theta \equiv$  Half Cone Angle of Shield Shadow

Equation 18 indicates that an increase in source-plane to shield-face distance will be accompanied by a direct increase in the mass. Splitting the shield into two sections

pushes the second shield section 87 cm from the source plane. At this distance, the front face radius of the second shield is 86 cm.

The next experiment focused on keeping the gamma shield material together, rather than splitting it into sections. Because the gamma shield material has such a large impact on the shield mass, keeping it together and placing it as close to the source plane as possible should reduce the mass. Furthermore, the shield splitting parameter study as well as data from benchmarking ‘Split\_Shield’ indicated that the dose reduction from splitting the gamma shield was negligible. Instead, the  $B_4C$  and W layers were maintained in the same position as the unit shield, while a portion of the LiH was split from the shield and pushed backward. This shield configuration can be seen in Figure 13, and the procedure is listed in Chapter III under the heading ‘Split Scatter Shield Design’. The results of this study are shown in Figure 21.

This plot shows that the neutron shielding effectiveness is reduced when half of the LiH shield is split from the unit shield and moved toward the dose plane. When only a quarter of the LiH is split however, the neutron fluence remains relatively constant while the gamma ray dose is reduced by 14% at a 50 cm shield separation distance. This reduction in the gamma dose now offers a degree of freedom in the placement of the gamma shield. The gamma shield can be moved closer to the source plane, until the original gamma dose is achieved.

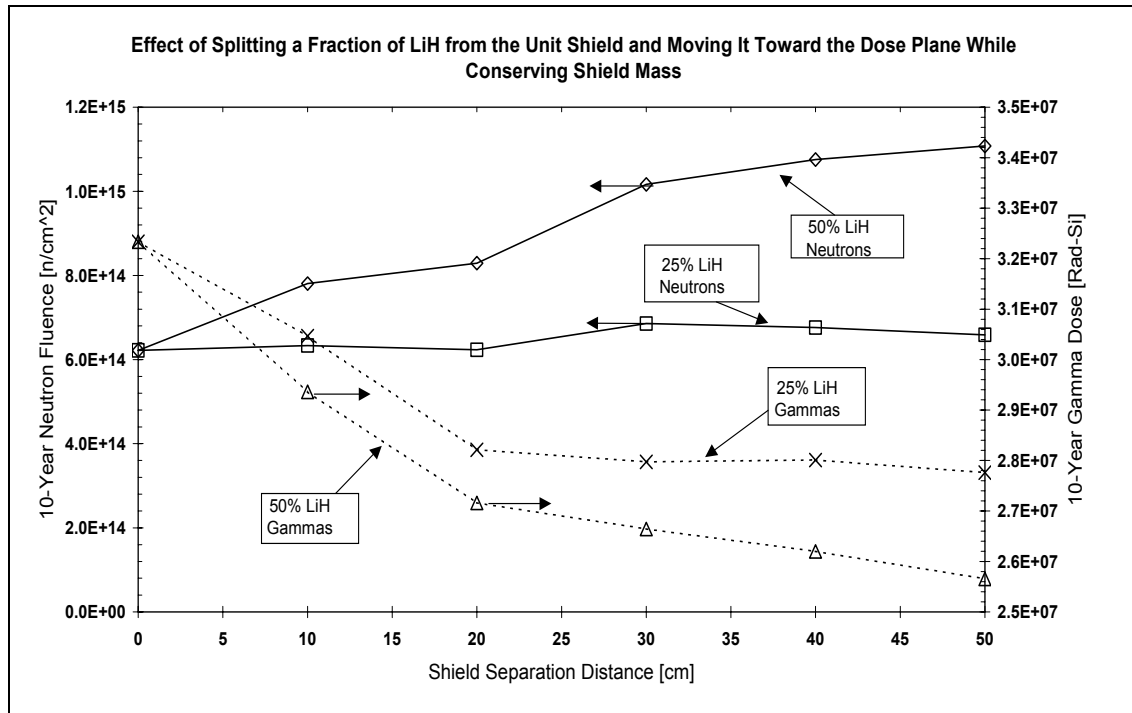


**Figure 21. Effect of Splitting LiH from Unit Shield and Conserving Mass**

An additional plot is required for this study, that will show whether the neutron fluence will decrease for shields that are less than a quarter of the LiH shield. The next step in this study is to split multiple layers of LiH from the unit shield and study the effect of moving them closer to the dose plane while conserving mass. This study indicates that it should be possible to reduce the mass of the radiation shield by moving the gamma shield closer to the source plane, while splitting the neutron shield. The neutron shield sections are then moved closer to dose plane, but no mass penalty is imposed because they are thinned to conserve mass.



## **V: Conclusions**

### **“Split\_Shield” Conclusion**

Although “Split\_Shield” ultimately did not work, its development was important in the creation of the material data files and for understanding some of the basic difficulties in designing radiation shields. MCNP4C is a very robust code, and provides the user with many capabilities, but the relatively long times required to operate the code and construct the input decks limited the total amount of research that could be conducted. In the future, MCNP4C should still be used to model the final three-dimensional shield, but a code needs to either be developed or used off the shelf (FEMP-2D, TWODANT), that will decrease the analysis time. A discrete ordinates technique would only require two-dimension analysis due to the shield symmetry. These techniques introduce some difficulties of their own, but developed correctly would significantly speed up the analysis.

The use of simple algorithms to explore shield design parameters is also highly suggested. The parametric study using the code developed by Mathews (Appendix D) was only applied very late into the study. This program uses a very simple Monte Carlo technique, but the results provided a large degree of insight into developing a successful split scatter shield. The code in Appendix D could be further modified to include material cross sections to study first flight escape probabilities for a two-shield system. Further modifications could explore the problem when a third shield is added to the problem. Simplifying the problem and custom designing algorithms to analyze the

problem would have provided more insight into the problem, without the complexity required when using a large program like MCNP4C.

### **Radiation Shield Parameters**

Although the parameters in this study are tailored for the SEHPTR, many of the values and the techniques that were characterized can be applied to a variety of SNPS shield design problems. The parameters studied include the shield spacing for split scatter shields, material selection, geometry, and gamma shield placement. Additionally, the energy deposition in the split scatter shield was examined and compared to the unit shield.

Several important insights were gained from this study that can be beneficial for future research. The first and most important aspect is that this shield design problem is inherently coupled, and any attempts to optimize the system as a compilation of uncoupled parameters will lead to poor results. The independently studied parameters in this research are used to provide a staging ground for designing a coupled shield.

For the materials studied, LiH is the best option for a reduced mass neutron shielding material. The amount of backscatter achieved with minimal mass was unmatched by any of the other seven candidate materials. The best selection for gamma-shielding material is slightly less obvious as steel,  $ZrH_2$ , and tungsten all have desirable properties as shields. Because scattering of the gamma rays is more difficult to control, it seems likely that the best option for the gamma shield is to keep it lumped as a single material. This is also important, because the mass of the gamma shield will ultimately

contribute to a large portion of the overall shield mass. If the gamma shield is lumped, it can be placed as close to the source plane as possible.

The results from splitting part of the LiH from the shield and moving it backward while conserving mass indicate that the gamma dose will decrease as the split shield section is moved closer to the dose plane. A new step in the design would be to fix the split LiH shield at some distance from the primary shield. Then the gamma shield could be moved closer to the reactor face until the gamma dose climbed back up to the original unit shield values. A diagram of this procedure is shown in Figure 22.

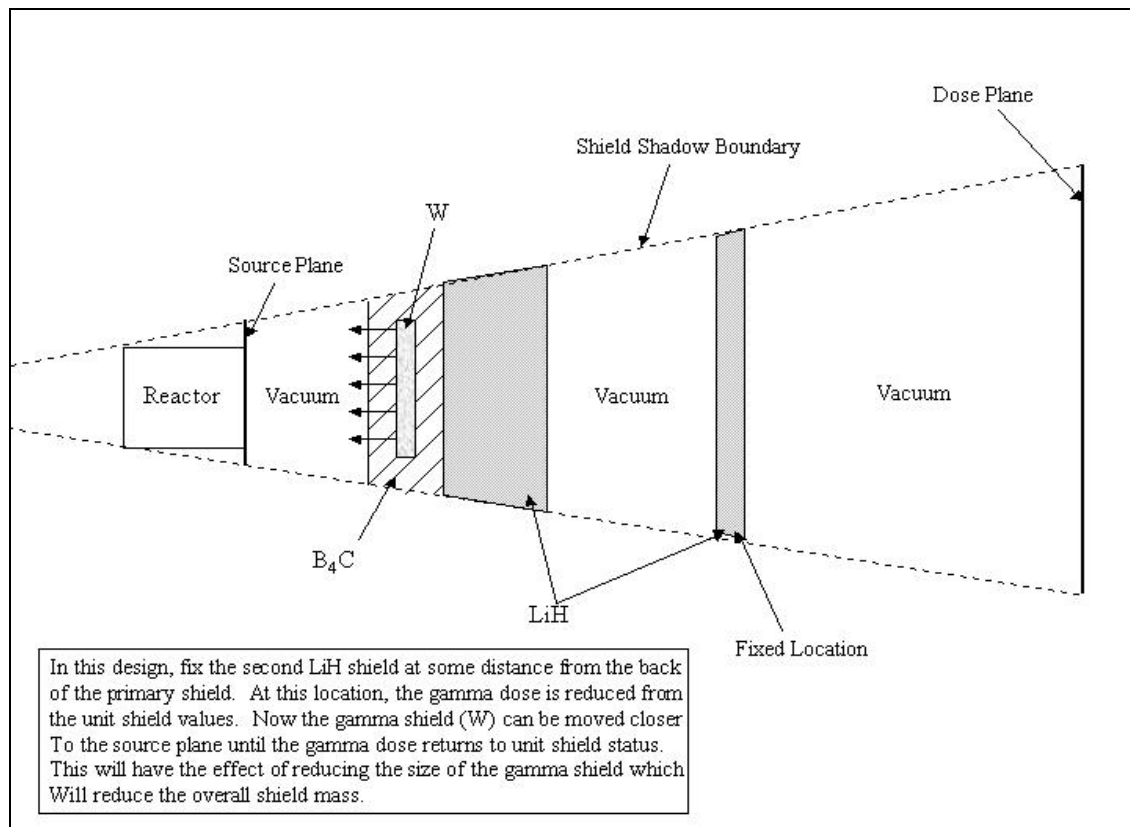


**Figure 22. Future Study on Gamma Shield Placement After Splitting LiH**

Although this research did not produce a mass optimized split scatter shield, the parameter studies on the shield spacing and half cone angle, material attenuation thickness, particle scattering, and geometry have all provided evidence that this shield

may be practical for reducing the overall shield mass while maintaining the performance of the unit shield. The final study that involved splitting off a portion of the LiH shield demonstrated that the neutron fluence remains relatively constant when a quarter of the shield material is split and moved closer to the dose plane. Furthermore, the gamma dose was shown to decrease when both a quarter of the LiH was split and moved as well as when half of the LiH was split and moved. As a result, it seems that there is an optimized solution for the split scatter shield and future research should be conducted to determine where the optima exist.

## **Recommendations**

### Computer Code Recommendations

The acquisition or development of a computer code that will speed up the shield analysis time is desirable for future research on the split scatter shield. Additional debugging work on “Split\_Shield” is desirable, because the program offers a wide range of possibilities related to the capabilities of MCNP4C. One function that needs to be replaced in the program is the method for calculating the particle loss when streaming across a vacuum. The simple Monte Carlo code provided in Appendix D could be implemented into the code to provide these simple calculations. Provided that the code can be fixed, the next step would be to incorporate multi-energy group transmission and reflection coefficients into the material data files. Material data files could be created using other tallies as well, including the particle angular distribution.

One feature of MCNP4C that was tested, but not applied is the concept of weight windows [17:2\_137-141]. Weight windows are similar to the importance values for

individual cells, except that they provide a window on the limits for splitting and roulette, rather than a cutoff value. One advantage to using weight windows, is that MCNP4C has a built in weight window generator, which most of the time can generate the weight windows automatically [17:3\_43-44]. This works by first running the problem with a guess for the importance values. MCNP4C then builds an importance function as the problem runs and from that determines what the windows for each cell should be. An improved importance function would reduce the variance of the results, with fewer particles. This technique is one way that the effectiveness of MCNP4C could be improved in shielding calculations.

Finally, work should be taken toward developing simple algorithms that can provide insight into key shield design parameters. These algorithms do not need to be extremely complex, but should be useful for indicating trends that will help in understanding how a split scatter shield functions. Ultimately the limited results in this research were due to a combination of MCNP run times as well as time lost trying to decouple and solve a system that is inherently coupled. Each shield configuration required anywhere from 30 to 90 minutes to build a MCNP input deck. The deck build time was directly related to the complexity of the shield design and the amount of geometry splitting required to attain satisfactory results. Once the deck was built, MCNP took on average 30 to 60 minutes per shield running on two computer systems. The first is a Sun Enterprise 450, running 4 processors at 400 MHz each. Each of the processors is a 4 Ultraspark II, with 4 megabytes of Ecache per processor. For this research all problems were run linearly assigning one process per processor. The total memory for this system was 2 gigabytes. The second machine was an Ultra Spark 10 operating at 440

MHz. The processor is an UltraPark2i, with 2 megabytes of Ecache. The total memory available for this system was 1 gigabyte.

### Radiation Shielding Recommendations

There were several tests that were not performed, or only examined briefly that could use further inspection. The first set of tests further investigates the heat deposition in the split scatter shield. For high power reactors, the split scatter shield may be advantageous since it will absorb less energy. A more detailed examination of the heat deposition is required, along with a detailed analysis of the thermal transport of the energy. Another study of interest is the effect of the radiators on the shield performance. This should be considered for split scatter shield applications since it could be an issue with particles that normally should leak but don't, because they get scattered from the heat pipes. It may also be worthwhile to rerun the angular distribution tests, except with a refined set of angles. This would better characterize where the particles are traveling and possibly new ways to optimize the geometry.

A search for split shield optima should be undertaken as well to determine whether or not this design is viable for replacing the unit shield. A study should be conducted, where the LiH in the unit shield is split multiple times and each section is moved back a given distance while conserving the mass of the unit shield by thinning the split sections. The data from the material attenuation study and the shield spacing study may be helpful in this portion of the design to give ballpark figures on the amount of shielding required. It is known for example that the 10-year neutron fluence must be reduced by about 10 orders of magnitude to meet the dose limits for the payload. The

technique used for examining the effect of shield separation distance on particle loss can be used to select appropriate shield spacing. The material attenuation data given from plots similar to Figure 7 can then be used to select a material thickness that will maximize neutron reflection from shield to shield. Combining this data allows the designer to estimate the reduction in neutron fluence attained from crossing a region of vacuum and interacting in the shield material. The process is then repeated for the next shield section, carrying on the particles that managed to survive from the last set of interactions. This method makes it possible to get a quick estimate for how many shield sections may be necessary and whether they will fit the size and mass constraints imposed by the designer.

Split scatter shielding offers the potential for reducing the radiation shield mass, and several optima appear to exist for such a design. This research has provided a staging ground from which future studies can be conducted. Once all of the shield parameters have been coupled and studied, it will then be possible to design a shield and determine whether or not it can be used as an alternative to the unit shield.

Finally, it should be noted that this research focused only on the radiation shielding properties of the system. Mechanical performance and stability were not examined, and are a topic for future research as well. A wide range of materials was avoided in this study that may be advantageous for enhanced scattering. Specifically the organic shield materials such as polymers are candidate materials because of their high hydrogen content. If split scatter shielding can reduce the energy deposited in each shield section, materials such as these may become applicable. A more detailed study of

this unique shield design is therefore necessary to study the entire system in its coupled form.



## **Appendix A: Introductory Tutorial for MCNP-4C**

This appendix is included to provide a short explanation of the MCNP4C features used in this research so that discussion is understandable throughout the document. A full description of MCNP4C's capabilities can be found in the reference documentation that comes with the code [16].

### Tallies.

Tallies are used by MCNP4C to allow a user to specify a point, ring, area, or volume that particles are passing through and provide an estimate of how they are distributed. The type of particle distribution is specified by the user and is in the form of values like current, flux, or energy deposition. A variety of tallies and ways to modify them are described in the reference documentation [16:2\_76-99].

Three tally modifiers of particular importance in this research are the energy and angular distribution modifiers and the tally multiplication modifier. The energy modifier specifies how a given tally is to be divided into energy bins [16:3\_83]. If no modifier is present, then all particles of all energies contribute to the tally. If for example, two energy groups are needed, then the user inputs a cutoff value which separates the high and low energy particles. All particles below this cutoff will contribute to the tally from zero to the cutoff energy, while all particles with energy above the cutoff will be discarded. As more groups are added, the cutoff values bound the energy bins of interest.

The angular distribution modifier specifies how the particles at a tally are distributed by angle. This modifier works in the same manner as the energy tally, with

the angle specified in terms of  $\mu$  ( $\mu = \cos(\theta)$ ) [16:3\_85]. If for example, two equal angular bins are desired, then the user specifies a modifier at zero. All particles that scatter into the angle between  $-1$  and  $0$  will be placed into one bin, and all particles that scatter into the angle between  $0$  and  $1$  will be placed into the other bin. The angular distribution modifier can only be used with the current tally, since it is the only tally that is angle dependent. Both the energy and angle tally modifiers were used throughout this study to understand how the particles are distributed after they interact with different shield sections.

The tally multiplier is a modifier that was used to convert a photon flux into a photon dose in silicon [16:3\_87]. This conversion is achieved by using the tally multiplier card to convert the photon flux to a photon-heating tally in silicon (units of MeV/g). The conversion is then done by the following equation:

$$Dose = \frac{T_P C N_A \eta \times 10^{-24}}{A} \quad (1)$$

where

$T_P \equiv$  Photon Heating Tally [MeV/g]

$C \equiv$  Normalization Constant =  $(1.602 \times 10^{-6} \text{ ergs/MeV}) / (100 \text{ ergs/g})$

Note:  $1 \text{ rad} = 100 \text{ ergs/g}$

$N_A \equiv$  Avagadro's Number [atoms / mol] =  $6.02 \times 10^{23}$

$\eta \equiv$  Number of Atoms per Molecule (=1 for Silicon)

$A \equiv$  Atomic Weight [g / mol] (=28 for Silicon)

The use of the photon dose is more practical in shielding calculations since damage to the payload is more understandable in terms of the energy absorbed, rather than the flux of photons incident on the system. Because neutrons will primarily cause damage through

lattice dislocations by scattering and transmutations by neutron capture, the time integrated neutron flux is a better estimator for neutron damage.

For this research, ring detectors and surface tallies were used to provide information about the current, flux, and dose at different locations within the shield and from the source. Surface tallies represent the distribution of particles at a surface located in the shield. A ring detector is a form of the point detector that can be used in situations where the geometry is symmetric about the coordinate axis [16:2\_88-91]. Contributions to a point detector tally in MCNP4C are determined at the source and every time a particle has a collision [16:2\_85-87]. When a particle interacts in MCNP4C, a new direction is sampled that is influenced by the cross section of the atom or electron that the particle interacted with. For a point detector, the program determines the probability of the particle scattering toward the detector rather than in the sampled direction. This new weighted pseudo-particle is then transported to the detector without interaction and its contribution to the flux detector tally is given by:

$$\Phi(\vec{r}, E, t, \mu) = \frac{Wp(\mu)e^{-\lambda}}{2\pi R^2} \quad (2)$$

where

- W  $\equiv$  particle weight
- p( $\mu$ )  $\equiv$  probability of scatter toward the detector from current position
- $\lambda \equiv$  total number of mean free paths integrated over the trajectory  
from the source or collision point to the detector
- R  $\equiv$  distance from the source or collision point to the detector

The Wp( $\mu$ ) term dictates the weight of the particle that is leaving the source or collision point, and the direction from which it leaves that point. The  $e^{-\lambda}$  term is how much the pseudo-particle is attenuated between the source or collision point and the

detector and the  $1/(2\pi R^2)$  term is the divergence of the particle as it travels to the detector. The actual source or collision particle continues along its random walk until it reaches another collision where another pseudo-particle is created and transported to the detector. A ring detector operates in much the same way, except that particles are transported to the nearest point on a symmetrical ring. A more detailed description of detector and tallies in MCNP4C can be found in the software documentation [16:2\_76-99].

### Variance Reduction.

Since Monte Carlo tallies are nothing more than the mean occurrence of a given process (i.e. flux, current) in a sample, the precision of a result will increase with the number of particles sampled. The tradeoff is that more computer time is required to achieve better statistics on a tally. Variance reduction techniques are methods used to increase the probability that a particle contribute to the tally, without biasing the statistics. MCNP4C offers a variety of these techniques to help reduce the computer time required while increasing the precision of the results [16:3\_32]. In this research the methods of geometric- and energy-splitting with Russian roulette were used.

For thick shielding problems, there is a high probability that many of the particles will be absorbed or scattered out of the shield before they reach the tally. If the materials have high absorption cross-sections, then it is possible that out of millions of sampled particles, only a few might contribute to the tally statistics. This problem is alleviated using the method of geometric splitting with Russian roulette [16:2\_133-135]. With this technique, the problem is divided up into zones that are each assigned a relative

importance. When a particle crosses from a region of low importance into a region of high importance, it is split into several equally weighted particles, whose total weight is equal to the weight of the original particle. Each of these particles is then tracked in MCNP4C individually like the original particle. When a particle travels from a region of high importance to a region of lower importance, the Russian roulette game is played. Russian roulette takes the ratio of the high and low importance values and then draws a random number between 0 and 1. If the ratio of the importance values is greater than this number, the particle is allowed to continue on with a weight that is diminished by the importance ratio. If the number is less than the importance ratio, then the particle is killed and no longer tracked. The method of geometric splitting with Russian roulette ensures that there are always a large number of particles that will contribute to the tally. Furthermore, particles that are headed into regions less important to the tally are less likely to be tracked, which reduces computer-processing time. Energy splitting with Russian roulette uses the same technique as geometry splitting, except the particles are split based on their transition from one energy group to another [16:2\_135-136].

## Appendix B: SEHPTR Input Deck in MCNP4C

```

Fiss_src -- Models SEHPTR for use as source term
1      1  -16.4935  -1 2 15 -16 $Fuel Region 1
2      2  -14.0342  -2 3 15 -16 $Fuel Region 2
3      3  -13.8300  -3 4 15 -16 $Fuel Region 3
4      4  -13.6580  -4 5 15 -16 $Fuel Region 4
5      5  -13.5092  -5 6 15 -16 $Fuel Region 5
6      6  -13.3754  -6 7 15 -16 $Fuel Region 6
7      7  -13.2638  -7 8 15 -16 $Fuel Region 7
8      8  -13.1631  -8 9 15 -16 $Fuel Region 8
9      9  -13.0712  -9 10 15 -16 $Fuel Region 9
10     10  -15.5800 -10 11 15 -16 $Fuel Region 10
11     11  -9.9450  -11 12 15 -16 $Heat Pipe Ring Inside
12     11  -9.9450  -13 1 14 -16 $Heat Pipe Ring Outside
13     12  -3.0229  -1 14 -15 $BeO Reflector Bottom
14     12  -3.0229  -13 16 -17 $BeO Reflector Top
15     12  -3.0229  -18 13 24 -17 -25 $BeO Reflector Upper Side
16     12  -3.0229  -18 13 14 -19 $BeO Reflector Lower Side
17     12  -3.0229  -18 13 19 -24 20 -22 $BeO Relector Middle
18     12  -3.0229  -18 13 19 -24 21 -23 $ " "
19     12  -3.0229  -18 13 19 -24 -20 22 $ " "
20     12  -3.0229  -18 13 19 -24 -21 23 $ " "
21     0      -18 13 19 -24 -21 22 $Windows in BeO
22     0      -18 13 19 -24 20 23 $ " "
23     0      -18 13 19 -24 21 -22 $ " "
24     0      -18 13 19 -24 -20 -23 $ " "
25     13  -1.8475  18 -26 27 -25 -29 30 $Outer Be Reflectors
26     13  -1.8475  18 -26 27 -25 28 31
27     13  -1.8475  18 -26 27 -25 29 -30
28     13  -1.8475  18 -26 27 -25 -28 -31
29     0      18 -26 -25 27 28 -30 $Void Between Be
30     0      18 -26 -25 27 29 -31
31     0      18 -26 -25 27 -28 30
32     0      18 -26 -25 27 -29 31
33     0      -32 15 -16 $Control rod path
34     0      14 -25 26 $Void region
35     0      14 -27 18 -26 $Void region
36     12  -3.0229  15 -16 32 -12 $Inner core BeO reflector
37     0      -14:17:25 $Boundary of problem

c Surface Definitions for reactor [cm]
1      cz 20 $Fuel Region
2      cz 19 $ " "
3      cz 18 $ " "
4      cz 17 $ " "
5      cz 16 $ " "
6      cz 15 $ " "
7      cz 14 $ " "
8      cz 13 $ " "
9      cz 12 $ " "
10     cz 11 $ " "
11     cz 10 $ " "

```

```

12    cz 7.2 $Heat Pipe Location inside
13    cz 22.8 $Heat Pipe Location outside
14    pz 0 $ Bottom plane of reactor and dose plane
15    pz 10 $Bounds top surface of bottom BeO reflector
16    pz 60 $Bounds bottom surface of top BeO reflector
17    pz 70 $ Top plane of reactor
18    cz 32.8 $Outer surface of BeO Reflectors
19    pz 17 $Bounds top surface of bottom-side BeO reflectors
20    py 0
21    1 py 0 $Describes planes that form BeO regions
22    p 1 1 0 0 $ " "
23    1 p 1 1 0 0 $ " "
24    pz 47 $Bounds bottom surface of top-side BeO reflectors
25    kz 150 0.121 $Cone that bounds outer surface of reactor
26    cz 39.8 $Outer surface of Be Reflectors
27    pz 14 $Bounds bottom surface of Be reflectors
28    p 0.087 1 0 0 $Describes planes that form Be regions
29    1 p 0.087 1 0 0 $ " "
30    p 0.839 1 0 0 $ " "
31    1 p 0.839 1 0 0 $ " "
32    cz 3.2 $Inner BeO reflector boundary

c Cylindrical Fission Source
mode n p
c $This line defines the location of the source and the distribution
sdef Pos=0 0 35 Erg=D1 Rad=D2 Ext=D3 Axs=0 0 1 Par=1
SP1 -3 0.988 2.349 $Specifies sampling from the Maxwell Spectrum
SI2 10 20 $Gives the sampling radii boundaries
SI3 25 $Half height of the cylinder
SSW -14 $Writes particles heading below surface 14 to file
C $This function tells MCNP4C to run the k-eigenvalue calculation
KCODE IKZ=200 KCT=600
C $These next lines define the importance vales for the cells
imp:N 3 5 5.2 5.4 5.6 5.8 6 6.2 6.4 3.5 2 2 8 1 1 &
      7.5 4 4 4 4 4 4 4 4 3 3 3 3 3 3 3 3 7 &
      7 3 0
imp:P 4 6 6.5 7 7.5 8 8.5 9 9.5 6 4 4 12 3.5 2 9 &
      2 2 2 2 2 2 2 2 1 1 1 1 1 1 1 1 5 4 4 5 0
c Define material and region importance
c Material is defined by Atomic Number//Atomic Weight and wt% in cell
M1 92235 0.0929 92238 0.0029 74000 0.7126 8016 0.1916
M2 92235 0.1735 92238 0.0054 74000 0.4634 8016 0.3578
M3 92235 0.1802 92238 0.0056 74000 0.4428 8016 0.3715
M4 92235 0.1858 92238 0.0057 74000 0.4254 8016 0.3831
M5 92235 0.1907 92238 0.0059 74000 0.4103 8016 0.3931
M6 92235 0.1950 92238 0.0060 74000 0.3968 8016 0.4021
M7 92235 0.1987 92238 0.0061 74000 0.3856 8016 0.4096
M8 92235 0.2020 92238 0.0062 74000 0.3754 8016 0.4164
M9 92235 0.2050 92238 0.0063 74000 0.3661 8016 0.4226
M10 92235 0.1229 92238 0.0038 74000 0.6199 8016 0.2534
M11 74000 0.5787 42000 0.3629 11023 0.0306 3007 0.0279
M12 4009 0.5000 8016 0.5000
M13 4009 1.0000
c
*tr1 0 0 0 90 180 90 0 90 90 90 90 0

```

```

WWG 5 5 0 0 $Calls the weight window generator
c
c Tally definitions
c These define ring detector tallies.
f5z:n 0.15 1.0 0.1  0.15 2.5 0.1  0.15 5.0 0.1  0.15 7.5 0.1 &
      0.15 10.0 0.1  0.15 15.0 0.1  0.15 20.0 0.1  0.15 30.0 0.1 &
      0.15 40.0 0  0.15 50.0 0
c
f55z:p 0.15 1.0 0.1  0.15 2.5 0.1  0.15 5.0 0.1  0.15 7.5 0.1 &
      0.15 10.0 0.1  0.15 15.0 0.1  0.15 25.0 0.1  0.15 30.0 0.1 &
      0.15 40.0 0  0.15 50.0 0
c
C $These define the energy splitting bins
e5 1E-5  5E-5  1E-4  5E-4  1E-3  5E-3  1E-2  5E-2  1E-1  1.0  2.0 &
   3.0  4.0  5.0  10.0
c
e55 1E-1  5E-1  1.0  2.0  3.0  4.0  5.0  7.5  10.0

```



## Appendix C: “Split\_Shield” Program

This appendix contains the source code for the FORTRAN-90 program “Split\_Shield”. Program comments are preceded by an exclamation mark and are in italics.

### Program Shield\_Design

```
!*****
!  
!  
! Title: Shield Design  
! By: Ben Kowash  
! Date: 30 Oct 01  
!  
! Purpose: This code will speed up the design optimization process for  
! developing a radiation shield. The problem solved is one in which a  
! source is separated from a target by vacuum and a set of  
! shields. The intent, is for the shields to scatter radiation away  
! from the dose plane out into space.  
! Transport through the shield materials is handled by the MCNP-4C code.  
!  
!  
!  
!*****  
Use GlobalData  
Use Initialize  
Use Matrix_Build  
Use Eval_Shield  
  
Implicit None  
  
Call InitializeData  
Call Transmit_Matrix  
Call Reflect_Matrix  
Call Solution_Matrix  
Call Flux_Calculation  
Call Shield_Properties  
Call Results  
  
End Program Shield_Design
```

## Module GlobalData

Implicit None

```
Real(8), Allocatable, Dimension(:, :) :: J_fwdN !Neutron current right
Real(8), Allocatable, Dimension(:, :) :: J_revN !Neutron current left
Real(8), Allocatable, Dimension(:, :) :: J_fwdP !Photon current right
Real(8), Allocatable, Dimension(:, :) :: J_revP !Photon current left
Real(8), Allocatable, Dimension(:) :: reg_density !Zone Density [g/cm^3]
Real(8), Allocatable, Dimension(:, :) :: reg_dim !Zone width [cm]
Real(8), Allocatable, Dimension(:) :: volume !Shield volume [cm^3]
Real(8), Allocatable, Dimension(:) :: mass !Shield mass [kg]
Character(Len=8), Allocatable, Dimension(:) :: reg_name !Zone name
```

*!Arrays that hold the transmission values & their errors*

```
Real(8), Allocatable, Dimension(:, :) :: T_fwdN
Real(8), Allocatable, Dimension(:, :) :: T_revN
Real(8), Allocatable, Dimension(:, :) :: T_fwdP
Real(8), Allocatable, Dimension(:, :) :: T_revP
```

*!Arrays that hold the reflection values and their errors*

```
Real(8), Allocatable, Dimension(:, :) :: R_fwdN
Real(8), Allocatable, Dimension(:, :) :: R_revN
Real(8), Allocatable, Dimension(:, :) :: R_fwdP
Real(8), Allocatable, Dimension(:, :) :: R_revP
```

*!Arrays that hold the solution coefficients matrix*

```
Real(8), Allocatable, Dimension(:, :) :: sol_fwdN
Real(8), Allocatable, Dimension(:, :) :: sol_revN
Real(8), Allocatable, Dimension(:, :) :: sol_fwdP
Real(8), Allocatable, Dimension(:, :) :: sol_revP
```

*!Arrays that hold the error matrix*

```
Real(8), Allocatable, Dimension(:, :) :: err_fwdN
Real(8), Allocatable, Dimension(:, :) :: err_revN
Real(8), Allocatable, Dimension(:, :) :: err_fwdP
Real(8), Allocatable, Dimension(:, :) :: err_revP
```

*!Arrays that hold the source vector and error*

```
Real(8), Allocatable, Dimension(:, :) :: src_fwdN
Real(8), Allocatable, Dimension(:, :) :: srcErr_fwdN
Real(8), Allocatable, Dimension(:, :) :: src_fwdP
Real(8), Allocatable, Dimension(:, :) :: srcErr_fwdP
```

```
Character(Len=12) :: shield_name
```

```
Real(8) :: src_neutron !Number of source neutrons
```

```
Real(8) :: src_photon !Number of source photons
```

```
Real(8), Parameter :: Pi=3.14579
```

```
Real(8), Parameter :: src_norm = 2.28259E-04 !Source Flux
```

```
Real(8), Allocatable, Dimension(:, :) :: src_normRev
```

```
Integer :: zones !Number of zones in problem
```

**End Module GlobalData**

## Module Initialize

Use GlobalData

Implicit None

Contains

```
!*****
!  
!  
!*****
Subroutine InitializeData

!*****
!  
! Title: InititalizeData
! By: Ben Kowash
! Data: 11 Nov 01
!  
! Description: This subroutine reads namelist information for an
!               input file called "shield_input.txt". This file
!               contains information on the number of zones in
!               the shield, and what the zones are made up of.
!  
!  
!  
!  
!*****
Implicit None

Character(Len=12) :: name
Integer :: num_region !Number of regions in problem
Real(8) :: Nsource, Psource !Source n and p flux [n-cm/cm^3-sec]
Integer :: i
Real(8) :: width !Width of given region

!NameList Declaration

NameList/Shield/name, num_region, Nsource, Psource

NameList/Material/name, width

!Open file and get input
Open(Unit=10, File="Shield_Input.txt")
Read(10,NML = Shield)

shield_name = name
zones = num_region
src_neutron = Nsource
src_photon = Psource

!Check arrays for prior allocation and then allocate

If (Allocated(reg_name)) Deallocate(reg_name)
Allocate(reg_name(0:zones))
```

```

    If (Allocated(reg_density)) Deallocate(reg_density)
    Allocate(reg_density(0:zones))

    If (Allocated(reg_dim)) Deallocate(reg_dim)
    Allocate(reg_dim(1,0:zones))

!Allocate Transmission arrays
    If (Allocated(T_fwdN)) Deallocate(T_fwdN)
    Allocate(T_fwdN(0:zones,2))

    If (Allocated(T_revN)) Deallocate(T_revN)
    Allocate(T_revN(0:zones,2))

    If (Allocated(T_fwdP)) Deallocate(T_fwdP)
    Allocate(T_fwdP(0:zones,2))

    If (Allocated(T_revP)) Deallocate(T_revP)
    Allocate(T_revP(0:zones,2))

!Allocate Reflection arrays
    If (Allocated(R_fwdN)) Deallocate(R_fwdN)
    Allocate(R_fwdN(0:zones,2))

    If (Allocated(R_revN)) Deallocate(R_revN)
    Allocate(R_revN(0:zones,2))

    If (Allocated(R_fwdP)) Deallocate(R_fwdP)
    Allocate(R_fwdP(0:zones,2))

    If (Allocated(R_revP)) Deallocate(R_revP)
    Allocate(R_revP(0:zones,2))

!Allocate source arrays
    If (Allocated(src_fwdN)) Deallocate(src_fwdN)
    Allocate(src_fwdN(1,0:zones))

    If (Allocated(srcErr_fwdN)) Deallocate(srcErr_fwdN)
    Allocate(srcErr_fwdN(1,0:zones))

    If (Allocated(src_fwdP)) Deallocate(src_fwdP)
    Allocate(src_fwdP(1,0:zones))

    If (Allocated(srcErr_fwdP)) Deallocate(srcErr_fwdP)
    Allocate(srcErr_fwdP(1,0:zones))

!Allocate solution arrays
    If (Allocated(sol_fwdN)) Deallocate(sol_fwdN)
    Allocate(sol_fwdN(0:zones,0:zones))

    If (Allocated(sol_revN)) Deallocate(sol_revN)
    Allocate(sol_revN(0:zones,0:zones))

    If (Allocated(sol_fwdP)) Deallocate(sol_fwdP)
    Allocate(sol_fwdP(0:zones,0:zones))

```

```

    If (Allocated(sol_revP)) Deallocate(sol_revP)
    Allocate(sol_revP(0:zones,0:zones))

!Allocate error arrays

    If (Allocated(err_fwdN)) Deallocate(err_fwdN)
    Allocate(err_fwdN(0:zones,0:zones))

    If (Allocated(err_revN)) Deallocate(err_revN)
    Allocate(err_revN(0:zones,0:zones))

    If (Allocated(err_fwdP)) Deallocate(err_fwdP)
    Allocate(err_fwdP(0:zones,0:zones))

    If (Allocated(err_revP)) Deallocate(err_revP)
    Allocate(err_revP(0:zones,0:zones))

    If (Allocated(src_normRev)) Deallocate(src_normRev)
    Allocate(src_normRev(1,0:zones))

    Do i=0, zones

        Read(10,NML = Material)

        reg_name(i) = name
        reg_dim(1,i) = width

    End Do

    Close(10)

!Set up the reverse source normalization matrix with the proper values
!The values from the material data files is in the form of either the
!flux or current. This value is normalized by the flux or current that
!comes from the source plane. The result of this, is that the shields
!are represented by the percentage that they can reduce the flux or
!current by. Once the particle distribution is determined, the values
!are un-normalized to give the correct values.

    Do i=0, zones

        If (reg_dim(1,i) == 0.0d0) then
            src_normRev(1,i) = src_norm
        Else
            src_normRev(1,i) = src_norm * (sqrt(0.148) * 137.0d0)&
                ** 2.0d0 / (sqrt(0.148) * &
                (137.0d0 + reg_dim(1,i))) ** 2.0d0
        End If

    End Do

    End Subroutine InitializeData

End Module Initialize

```

## Module Matrix\_Build

Use GlobalData

Implicit None

Contains

```
!*****  
!  
!*****
```

Subroutine Transmit\_Matrix

```
!*****  
!  
! Name: Transmit_Matrix  
! By: Ben Kowash  
! Date: 11 Nov 01  
!  
! Description: This subroutine constructs a matrix, which contains  
!               the transmission information of particles through a  
!               given region. The transmission matrix contains  
!               both the transmission through vacuum and material.  
!  
! v 0.1 - Builds transmission matrix for 1 Energy group only  
! v 0.2 - Adds arrays which take into account error of estimators  
!         and creates error matrices.  
!  
!  
!*****
```

Implicit None

```
Integer :: i  
Real(8) :: x, x_low, x_hi !Location in region [cm]  
Real(8) :: t_low, t_hi !Transmission values for hi and low  
Real(8) :: err_low, err_hi !Error values on transmission  
Character(Len=20) :: infile  
Character(Len=1) :: mode !Tracks photons or neutrons
```

Do i=0, zones

    If (reg\_name(i) == "Source") then

```
        T_fwdN(i,1) = 0.0d0  
        T_fwdN(i,2) = 0.0d0  
        T_fwdP(i,1) = 0.0d0  
        T_fwdP(i,2) = 0.0d0  
        T_revN(i,1) = 0.0d0  
        T_revN(i,2) = 0.0d0  
        T_revP(i,1) = 0.0d0  
        T_revP(i,2) = 0.0d0
```

    Else

```
        !Determine the value for the forward transmission  
        infile = TRIM(reg_name(i)) // "f.dat"
```

```

Open(Unit = 10, File = Trim(infile), Action = 'Read')

Read(10,100) reg_density(i)
100 Format(/, T11, F6.2)
Read(10,120) mode
120 Format(T6,A1,/)

Do
    !Find the bounding values of x
    Do
        Read(10,*) x
        If (reg_dim(1,i) < x) then
            Backspace(10)
            Backspace(10)
            Read(10,200) x_low, t_low, err_low
            200 Format(F5.2,T15,ES11.5,T30,F6.4)
            Read(10,300) x_hi,t_hi,err_hi,
            300 Format(F5.2,T15,ES11.5,T30,F6.4)
            Exit
        End If
    End Do

    !Use an interpolation function to find the transmission
    !value
    If (mode == "n") then
        T_fwdN(i,1) = Interpolate(x_low,x_hi,t_low, &
            t_hi,reg_dim(1,i))/ src_norm
        T_fwdN(i,2) = Interpolate(x_low,x_hi,err_low, &
            err_hi,reg_dim(1,i))

    Else If (mode == "p") then
        T_fwdP(i,1) = Interpolate(x_low,x_hi,t_low, &
            t_hi, reg_dim(1,i)) / src_norm
        T_fwdP(i,2) = Interpolate(x_low,x_hi,err_low, &
            err_hi, reg_dim(1,i))

    End If

    If (reg_name(i) == "Vac") then

        T_fwdP(i,1) = T_fwdN(i,1)
        T_fwdP(i,2) = T_fwdN(i,2)

    End If

    If (mode /= "p" .and. reg_name(i) /= "Vac") then
        Do
            Read(10,320) mode
            320 Format(T6,A1)
            If (mode == "p") then
                Read(10,330)
                330 Format(/)
                Exit
            End If
        End If
    End If

```

```

        End Do
    Else
        Exit
    End If

End Do

Close(10)

!Determine the value for the reverse transmission
infile = TRIM(reg_name(i)) // "r.dat"

Open(Unit = 20, File = Trim(infile), Action = 'Read')

Read(20,400)
400 Format(//)
Read(20,420) mode
420 Format(T6,A1,//)

Do
    !Find the low value of x
    Do
        Read(20,*) x
        If (reg_dim(1,i) < x) then
            Backspace(20)
            Backspace(20)
            Read(20,500) x_low, t_low, err_low
            500 Format(F5.2,T15,ES11.5,T30,F6.4)
            Read(20,600) x_hi, t_hi, err_hi
            600 Format(F5.2,T15,ES11.5,T30,F6.4)
            Exit
        End If
    End Do

    !Use an interpolation function to find the transmission
    !value
    If (mode == "n") then
        T_revN(i,1) = Interpolate(x_low,x_hi,t_low, &
                                t_hi,reg_dim(1,i)) / &
                                src_normRev(1,i)
        T_revN(i,2) = Interpolate(x_low,x_hi,err_low, &
                                err_hi, reg_dim(1,i))

    Else If (mode == "p") then
        T_revP(i,1) = Interpolate(x_low,x_hi, &
                                t_low,t_hi,reg_dim(1,i)) / &
                                src_normRev(1,i)
        T_fwdP(i,2) = Interpolate(x_low,x_hi, &
                                err_low,err_hi,reg_dim(1,i))
    End If

    If (reg_name(i) == "Vac") then
        T_revP(i,1) = T_revN(i,1)
        T_revP(i,2) = T_revN(i,2)
    End If

```



```

        End If

        If (mode /= "p" .and. reg_name(i) /= "Vac") then
            Do
                Read(20,620) mode
                620 Format(T6,A1)
                If (mode == "p") then
                    Read(20,630)
                    630 Format(/)
                    Exit
                End If
            End Do
        Else
            Exit
        End If

    End Do

    Close(20)

End If

End Do

End Subroutine Transmit_Matrix

!*****
!  

!*****
Subroutine Reflect_Matrix

!*****
!  

! Name: Reflect_Matrix
! By: Ben Kowash
! Date: 11 Nov 01
!  

! Description: This subroutine constructs a matrix which contains the
!               reflection information of particles off a given region.
!  

! v 0.1 - Builds reflection matrix for 1 Energy group only
! v 0.2 - Adds arrays which take into account error of estimators
!         and creates error matrices.
!  

!*****
Implicit None

Integer :: i
Real(8) :: x, x_low, x_hi !Location in region [cm]
Real(8) :: r_low, r_hi !Transmission values for hi and low
Real(8) :: err_low, err_hi !Error values on transmission
Character(Len=12) :: infile
Character(Len=1) :: mode !Tracks photons or neutrons

```

```

Do i=0, zones

    If (reg_name(i) == "Vac") then
        ! There is no reflection from a vacuum so these are set to 0.
        R_fwdN(i,1) = 0.0d0
        R_fwdN(i,2) = 0.0d0
        R_fwdP(i,1) = 0.0d0
        R_fwdP(i,2) = 0.0d0
        R_revN(i,1) = 0.0d0
        R_revN(i,2) = 0.0d0
        R_revP(i,1) = 0.0d0
        R_revP(i,2) = 0.0d0

    Else If (reg_name(i) == "Source") then

        R_fwdN(i,1) = 0.0d0
        R_fwdN(i,2) = 0.0d0
        R_fwdP(i,1) = 0.0d0
        R_fwdP(i,2) = 0.0d0
        R_revN(i,1) = 0.6818 !Neutron reflection off source
        R_revN(i,2) = 0.0022 !Neutron reflection error
        R_revP(i,1) = 0.3241 !Photon reflection off source
        R_revP(i,2) = 0.0021 !Photon reflection error

    Else

        !Determine the value for the forward transmission
        infile = TRIM(reg_name(i)) // "f.dat"

        Open(Unit = 10, File = Trim(infile), Action = 'Read')

        Read(10,100) reg_density(i)
        100 Format(/,T11, F6.2)
        Read(10,120) mode
        120 Format(T6,A1,/)

        Do
            !Find the low value of x
            Do
                Read(10,*) x
                If (reg_dim(1,i) < x) then
                    Backspace(10)
                    Backspace(10)
                    Read(10,200) x_low, r_low, err_low
                    200 Format(F5.2,T45,ES11.5,T60,F6.4)
                    Read(10,300) x_hi, r_hi, err_hi
                    300 Format(F5.2,T45,ES11.5,T60,F6.4)
                    Exit
                End If
            End Do

            !Use an interpolation function to find the transmission value
            If (mode == "n") then
                R_fwdN(i,1) = Interpolate(x_low,x_hi,r_low, &
                    r_hi,reg_dim(1,i)) / src_norm
            End If
        End Do
    End If
End Do

```

```

        R_fwdN(i,2) = Interpolate(x_low,x_hi,err_low, &
                                err_hi, reg_dim(1,i))

    Else If (mode == "p") then
        R_fwdP(i,1) = Interpolate(x_low,x_hi,r_low, &
                                r_hi,reg_dim(1,i)) / src_norm
        R_fwdP(i,2) = Interpolate(x_low,x_hi,err_low, &
                                err_hi,reg_dim(1,i))

    End If

    If (mode /= "p" .and. reg_name(i) /= "Vac") then
        Do
            Read(10,320) mode
            320 Format(T6,A1)
            If (mode == "p") then
                Read(10,330)
                330 Format(/)
                Exit
            End If
        End Do
    Else
        Exit
    End If

End Do

Close(10)

!Determine the value for the reverse transmission
infile = TRIM(reg_name(i)) // "r.dat"

Open(Unit = 20, File = Trim(infile), Action = 'Read')

Read(20,400)
400 Format(/)
Read(20,420) mode
420 Format(T6,A1,/)

Do
    !Find the low value of x
    Do
        Read(20,*) x
        If (reg_dim(1,i) < x) then
            Backspace(20)
            Backspace(20)
            Read(20,500) x_low, r_low, err_low
            500 Format(F5.2,T45,ES11.5,T60,F6.4)
            Read(20,600) x_hi, r_hi, err_hi
            600 Format(F5.2,T45,ES11.5,T60,F6.4)
            Exit
        End If
    End Do
End Do

```

```

!Use an interpolation function to find the transmission
!value
    If (mode == "n") then
        R_revN(i,1) = Interpolate(x_low,x_hi,r_low, &
                                   r_hi,reg_dim(1,i)) / &
                                   src_normRev(1,i)
        R_revN(i,2) = Interpolate(x_low,x_hi,err_low, &
                                   err_hi,reg_dim(1,i))

    Else If (mode == "p") then
        R_revP(i,1) = Interpolate(x_low,x_hi,r_low, &
                                   r_hi,reg_dim(1,i)) / &
                                   src_normRev(1,i)
        R_revP(i,2) = Interpolate(x_low,x_hi,err_low, &
                                   err_hi, reg_dim(1,i))

    End If

    If (mode /= "p" .and. reg_name(i) /= "Vac") then
    Do
        Read(20,620) mode
        620 Format(T6,A1)
        If (mode == "p") then
            Read(20,630)
            630 Format(/)
            Exit
        End If
    End Do
Else
    Exit
End If

End Do

Close(20)

End If

End Do

End Subroutine Reflect_Matrix

! *****
!
! *****

```

# Subroutine Shield\_Matrix

```

!*****
!
! Name: Shield_Matrix
! By: Ben Kowash
! Date: 11 Nov 01
!
! Description: This subroutine takes the reflection and transmission
!              matrices that have been created, and combines them
!              to form the shield matrix to the shielding problem
!              of interest.
!
! v 0.1 - Builds the total shield matrix for 1 Energy group only
!
!*****
Implicit None

Integer :: i, j

sol_fwdN = 0.0d0
sol_revN = 0.0d0
sol_fwdP = 0.0d0
sol_revP = 0.0d0

err_fwdN = 0.0d0
err_revN = 0.0d0
err_fwdP = 0.0d0
err_revP = 0.0d0

!Calculate the forward solution matrix
Do i=1, zones

    Do j=0,zones

        If ((i-j)==1) then
            sol_fwdN(i,j) = T_revN(i,1) * R_revN(i-1,1)
            If (sol_fwdN(i,j) == 0.0d0) then
                err_fwdN(i,j) = 0.0d0
            Else
                err_fwdN(i,j) = sqrt(T_revN(i,2) ** 2.0d0 + &
                                     R_revN(i-1,2) ** 2.0d0)
            End If

            sol_fwdP(i,j) = T_revP(i,1) * R_revP(i-1,1)
            If (sol_fwdP(i,j) == 0.0d0) then
                err_fwdP(i,j) = 0.0d0
            Else
                err_fwdP(i,j) = sqrt(T_revP(i,2) ** 2.0d0 + &
                                     R_revP(i-1,2) ** 2.0d0)
            End If

        Else If ((i-j) < 1) then

            sol_fwdN(i,j) = sol_fwdN(i,j-1) * T_fwdN(i,1)

```

```

    If (sol_fwdN(i,j) == 0.0d0) then
        err_fwdN(i,j) = 0.0d0
    Else
        err_fwdN(i,j) = sqrt(err_fwdN(i,j-1)**2.0d0 + &
            T_fwdN(j,2) ** 2.0d0)
    End If

    sol_fwdP(i,j) = sol_fwdP(i,j-1) * T_fwdP(i,1)
    If (sol_fwdP(i,j) == 0.0d0) then
        err_fwdP(i,j) = 0.0d0
    Else
        err_fwdP(i,j) = sqrt(err_fwdP(i,j-1)**2.0d0 + &
            T_fwdP(j,2) ** 2.0d0)
    End If

End If

End Do

End Do

!Calculate the reverse solution matrix
Do i=0, zones

    Do j=zones, 0, -1

        If ((i-j)==-1) then
            If (i < (zones - 1)) then
                sol_revN(i,j) = T_fwdN(i+1,1) * R_fwdN(i+2,1)
                If (sol_revN(i,j) == 0.0d0) then
                    err_revN(i,j) = 0.0d0
                Else
                    err_revN(i,j) = sqrt(T_fwdN(i+1,2) &
                        **2.0d0 + R_fwdN(i+1,2) &
                        **2.0d0)
                End If

                sol_revP(i,j) = T_fwdP(i+1,1) * R_fwdP(i+2,1)
                If (sol_revP(i,j) == 0.0d0) then
                    err_revN(i,j) = 0.0d0
                Else
                    err_revP(i,j) = sqrt(T_fwdP(i+1,2)**2.0d0 + &
                        R_fwdP(i+2,2) ** 2.0d0)
                End If

            End If

        Else If ((i-j) >= 0) then
            If (i /= zones) then
                sol_revN(i,j) = sol_revN(i,j+1) * T_revN(i+1,1)
                If (sol_revN(i,j) == 0.0d0) then
                    err_revN(i,j) = 0.0d0
                Else
                    err_revN(i,j) = sqrt(err_revN(i,j+1) &
                        **2.0d0 + T_revN(j+1,2) &

```

```

**2.0d0)
End If

sol_revP(i,j) = sol_revP(i,j+1) * T_revP(i+1,1)
If (sol_revP(i,j) == 0.0d0) then
    err_revP(i,j) = 0.0d0
Else
    err_revP(i,j) = sqrt(err_revP(i,j+1) &
        **2.0d0 + T_revP(j+1,2) &
        **2.0d0)
End If

End If

End If

End Do

End Do

Src_fwdN = 0.0d0
SrcErr_fwdN = 0.0d0
Src_fwdP = 0.0d0
SrcErr_fwdP = 0.0d0

!Build the source matrix that specifies the initial boundary conditions
Do i=0, zones

    If (i == 0) then
        Src_fwdN(1,i) = src_neutron
        Src_fwdP(1,i) = src_photon

    Else
        Src_fwdN(1,i) = Src_fwdN(1,i-1) * T_fwdN(i,1)
        SrcErr_fwdN(1,i) = sqrt(SrcErr_fwdN(1,i-1) ** 2.0d0 + &
            T_fwdN(i,2) ** 2.0d0)

        Src_fwdP(1,i) = Src_fwdP(1,i-1) * T_fwdP(i,1)
        SrcErr_fwdP(1,i) = sqrt(SrcErr_fwdP(1,i-1) ** 2.0d0 + &
            T_fwdP(i,2) ** 2.0d0)

    End If

End Do

End Subroutine Shield_Matrix

! *****
!
! *****

```

```

Real Function Interpolate(x_low, x_hi, y_low, y_hi, x_value)

!*****
! Name: Interpolate
! By: Ben Kowash
! Date: 11 Nov 01
!
! Description: This function interpolates between two known values using
!              three known corresponding points.
!
! v 0.1 - Implements a linear interpolation method
! v 0.2 - Converts the y-values, which are logarithmic in nature
!         so that the linear interpolation scheme will be more accurate.
!
!*****
Implicit None

Real(8), Intent(IN) :: x_low, x_hi, x_value
Real(8), Intent(IN) :: y_low, y_hi

If (x_low == x_value) then
    Interpolate = y_low
Else
    Interpolate = exp(ln(y_hi)+((ln(y_hi)-ln(y_low))/ &
        (x_hi-x_low))*(x_value-x_hi))
End If

End Function Interpolate

!*****
!
!*****
End Module Matrix_Build

```



# MODULE EVAL\_SHIELD

USE GLOBALDATA

IMPLICIT NONE

CONTAINS

```
! *****
!  
! *****
SUBROUTINE FLUX_CALCULATION
```

```
! *****
!  TITLE:  FLUX_CALCULATION
!  BY:    BEN KOWASH
!  DATE:  10 NOV 01
!  
!  DESCRIPTION:  THIS SUBROUTINE CALCULATES THE LEFT- AND RIGHTWARD
!                FLOWING CURRENT AT THE BOUNDARIES BETWEEN MATERIALS.  THE
!                SOLUTION MATRIX COMBINED WITH THE SOURCE VECTOR IS USED
!                TO CALCULATE THE RIGHT FLOWING CURRENT FIRST.
!                THIS RIGHTWARD CURRENT IS THEN USED IN A SECOND
!                CALCULATION TO CALCULATE THE LEFTWARD CURRENT.
!                THIS PROCESS IS CONTINUED ITERATIVELY UNTIL THE
!                VALUES OF THE FLUX CONVERGE WITHIN SOME TOLERANCE.
!  
!  
!  V0.1 - CALCULATES THE FLUXES FOR 1 ENERGY GROUP ONLY
!  
! *****
IMPLICIT NONE
```

```
REAL(8), ALLOCATABLE, DIMENSION(:, :) :: J_OLDNF !PREV ITERATION VALUE
REAL(8), ALLOCATABLE, DIMENSION(:, :) :: J_OLDNR !PREV ITERATION VALUE
REAL(8), ALLOCATABLE, DIMENSION(:, :) :: J_OLDPF !PREV ITERATION VALUE
REAL(8), ALLOCATABLE, DIMENSION(:, :) :: J_OLDPR !PREV ITERATION VALUE
REAL(8), ALLOCATABLE, DIMENSION(:, :) :: J_ERRNF !N CURRENT ERR FWD
REAL(8), ALLOCATABLE, DIMENSION(:, :) :: J_ERRNR !N CURRENT ERR BKWD
REAL(8), ALLOCATABLE, DIMENSION(:, :) :: J_ERRPF !P CURRENT ERR FWD
REAL(8), ALLOCATABLE, DIMENSION(:, :) :: J_ERRPR !P CURRENT ERR BKWD  
  
REAL(8), PARAMETER :: TOLERANCE = 1E-6 !CONVERGENCE TOL. FOR CURRENT
REAL(8) :: ERRMAX_FWD, ERRMAX_REV !ERROR IN TOLERANCE CALCULATIONS
REAL(8) :: TEMP_ERR !USED TO CALCULATE TOTAL ERROR ON MATRICES
INTEGER :: I, J
INTEGER :: ITER !COUNTS ITERATIONS TO CONVERGENCE
LOGICAL :: CONVERGED
REAL(8) :: X
```

*!DEALLOCATE TRANSMISSION AND REFLECTION ARRAYS, WHICH AREN'T NEEDED*

*!DEALLOCATE TRANSMISSION ARRAYS*

DEALLOCATE(T\_FWDN)  
DEALLOCATE(T\_REVN)  
DEALLOCATE(T\_FWDP)  
DEALLOCATE(T\_REVP)

*!ALLOCATE REFLECTION ARRAYS*

DEALLOCATE(R\_FWDN)  
DEALLOCATE(R\_REVN)  
DEALLOCATE(R\_FWDP)  
DEALLOCATE(R\_REVP)

*!CHECK ALLOCATION ON FLUX ARRAYS AND THEN ALLOCATE*

IF (ALLOCATED(J\_FWDN)) DEALLOCATE(J\_FWDN)  
ALLOCATE(J\_FWDN(1,0:ZONES))

IF (ALLOCATED(J\_FWDP)) DEALLOCATE(J\_FWDP)  
ALLOCATE(J\_FWDP(1,0:ZONES))

IF (ALLOCATED(J\_REVN)) DEALLOCATE(J\_REVN)  
ALLOCATE(J\_REVN(1,0:ZONES))

IF (ALLOCATED(J\_REVP)) DEALLOCATE(J\_REVP)  
ALLOCATE(J\_REVP(1,0:ZONES))

IF (ALLOCATED(J\_OLDNF)) DEALLOCATE(J\_OLDNF)  
ALLOCATE(J\_OLDNF(1,0:ZONES))

IF (ALLOCATED(J\_OLDPF)) DEALLOCATE(J\_OLDPF)  
ALLOCATE(J\_OLDPF(1,0:ZONES))

IF (ALLOCATED(J\_OLDNR)) DEALLOCATE(J\_OLDNR)  
ALLOCATE(J\_OLDNR(1,0:ZONES))

IF (ALLOCATED(J\_OLDPR)) DEALLOCATE(J\_OLDPR)  
ALLOCATE(J\_OLDPR(1,0:ZONES))

IF (ALLOCATED(J\_ERRNF)) DEALLOCATE(J\_ERRNF)  
ALLOCATE(J\_ERRNF(1,0:ZONES))

IF (ALLOCATED(J\_ERRNR)) DEALLOCATE(J\_ERRNR)  
ALLOCATE(J\_ERRNR(1,0:ZONES))

IF (ALLOCATED(J\_ERRPF)) DEALLOCATE(J\_ERRPF)  
ALLOCATE(J\_ERRPF(1,0:ZONES))

IF (ALLOCATED(J\_ERRPR)) DEALLOCATE(J\_ERRPR)  
ALLOCATE(J\_ERRPR(1,0:ZONES))

*!BEGIN ITERATION PROCESS TO CONVERGE ON SOLUTION*

J\_OLDNF = 0.0  
J\_OLDPF = 0.0

```

J_OLDNR = 0.0
J_OLDPR = 0.0
J_FWDN = 0
J_REVN = 0
J_FWDP = 0
J_REVP = 0

J_ERRNF = SRCERR_FWDN
J_ERRNR = 0.0
J_ERRPF = SRCERR_FWDP
J_ERRPR = 0.0

ITER = 0

!CALCULATE THE NEUTRON CURRENT
DO
    !CALCULATE RIGHT DIRECTIONAL NEUTRON FLUX
    J_FWDN = MATMUL(J_REVN, SOL_FWDN) + SRC_FWDN

    X = 0
    !THIS LOOP CORRECTS THE CURRENT VECTOR WITH THE
    !EXPONENTIAL FACTOR THAT WAS FOUND WHEN COMPARING
    !"SPLIT_SHIELD" RESULTS WITH MCNP4C.

    DO I=0, ZONES
        J_FWDN(1,I) = J_FWDN(1,I) * EXP(0.0235 * X) / 1.11
        X = X + REG_DIM(1,I)
    END DO

    !CALCULATE THE ERROR FOR THE CALCULATIONS FORWARD
    DO I=0, ZONES
        IF (J_REVN(1,I) /= 0.0D0) THEN
            TEMP_ERR = SQRT(J_ERRNR(1,I) ** 2.0D0 + &
                SRCERR_FWDN(1,I) ** 2.0D0)
        ELSE
            TEMP_ERR = SQRT((SRCERR_FWDN(1,I) / &
                SRC_FWDN(1,I)) ** 2.0D0)
        END IF

        DO J=0, ZONES
            TEMP_ERR = SQRT(TEMP_ERR ** 2.0D0 + ERR_FWDN(I,J) ** 2.0D0)
        END DO

        IF (J_REVN(1,I) /= 0.0D0) THEN
            J_ERRNF(1,I) = SQRT(TEMP_ERR ** 2.0D0 + &
                J_ERRNR(1,I) ** 2.0D0)
        ELSE
            J_ERRNF(1,I) = SQRT((TEMP_ERR / J_FWDN(1,I)) ** 2.0D0)
        END IF
    END DO

    !CALCULATE LEFT DIRECTIONAL NEUTRON CURRENT
    J_REVN = MATMUL(J_FWDN, SOL_REVN)

```

```

X = 0
DO I=0, ZONES
    J_REVN(1,I) = J_REVN(1,I)
    X = X + REG_DIM(1,I)
END DO

!CALCULATE THE ERROR FOR THE CALCULATIONS BACKWARD
DO I=0, ZONES
    TEMP_ERR = SQRT(J_ERRNF(1,I) ** 2.0D0)
    DO J=0, ZONES
        TEMP_ERR = SQRT(TEMP_ERR ** 2.0D0 + ERR_REVN(I,J) ** 2.0D0)
    END DO

    IF (J_REVN(1,I) /= 0.0D0) THEN
        J_ERRNR(1,I) = SQRT(TEMP_ERR ** 2.0D0 + &
            J_ERRNF(1,I) ** 2.0D0)
    ELSE
        J_ERRNR(1,I) = SQRT(J_ERRNF(1,I) ** 2.0D0)
    END IF
END DO

END DO

!CHECK FOR CONVERGENCE OF NEUTRON FLUX

ERRMAX_FWD = MAXVAL(ERROR(J_FWDN, J_OLDNF))
PRINT *, ITER, ERRMAX_FWD
ERRMAX_REV = MAXVAL(ERROR(J_REVN, J_OLDNR))
PRINT *, ITER, ERRMAX_REV
CONVERGED = ((ERRMAX_FWD <= TOLERANCE) .AND. (ERRMAX_REV <= TOLERANCE))

IF (CONVERGED) EXIT
    J_OLDNF = J_FWDN
    J_OLDNR = J_REVN
    ITER = ITER + 1
END DO

J_FWDN = J_FWDN * SRC_NORM
J_REVN = J_REVN * SRC_NORMREV

ITER = 0
!CALCULATE THE PHOTON CURRENT
DO
    !CALCULATE RIGHT DIRECTIONAL PHOTON CURRENT
    J_FWDP = MATMUL(J_REVP, SOL_FWDP) + SRC_FWDP

    X = 0
    DO I=0, ZONES
        J_FWDP(1,I) = J_FWDP(1,I) * EXP(0.0235 * X)/1.11
        X = X + REG_DIM(1,I)
    END DO

    !CALCULATE THE ERROR FOR THE CALCULATIONS FORWARD
    DO I=0, ZONES
        TEMP_ERR = J_ERRPF(1,I)
    END DO

```

```

        DO J=0, ZONES
            TEMP_ERR = SQRT(TEMP_ERR ** 2.0D0 + &
                           ERR_FWDP(I,J) ** 2.0D0)
        END DO
        J_ERRPF(1,I) = TEMP_ERR
    END DO

    !CALCULATE LEFT DIRECTIONAL PHOTON FLUX
    J_REVP = MATMUL(J_FWDP, SOL_REVP)
    X = 0
    DO I=0, ZONES
        J_REVP(1,I) = (J_REVP(1,I) * EXP(0.0334 * X))
        X = X + REG_DIM(1,I)
    END DO

    !CALCULATE THE ERROR FOR THE CALCULATIONS BACKWARD
    DO I=0, ZONES
        TEMP_ERR = J_ERRPR(1,I)
        DO J=0, ZONES
            TEMP_ERR = SQRT(TEMP_ERR ** 2.0D0 + &
                           ERR_REVP(I,J) ** 2.0D0)
        END DO
        J_ERRPR(1,I) = TEMP_ERR
    END DO

    !CHECK FOR CONVERGENCE OF PHOTON FLUX
    ERRMAX_FWD = MAXVAL(ERROR(J_FWDP, J_OLDPF))
    PRINT *, ITER, ERRMAX_FWD
    ERRMAX_REV = MAXVAL(ERROR(J_REVP, J_OLDPR))
    PRINT *, ITER, ERRMAX_REV
    CONVERGED = ((ERRMAX_FWD <= TOLERANCE) &
                 .AND. (ERRMAX_REV <= TOLERANCE))
    IF (CONVERGED) EXIT

    J_OLDPF = J_FWDP
    J_OLDPR = J_REVP
    ITER = ITER + 1

END DO

J_FWDP = J_FWDP * SRC_NORM
J_REVP = J_REVP * SRC_NORM

END SUBROUTINE FLUX_CALCULATION

! *****
!
! *****

```

```

SUBROUTINE SHIELD_PROPERTIES

! *****
! TITLE: SHIELD_PROPERTIES
! BY: BEN KOWASH
! DATE: 10 NOV 01
!
! DESCRIPTION: THIS ROUTINE CALCULATES THE TOTAL VOLUME AND THE TOTAL
!              MASS OF THE SHIELD. VOLUMES ARE CALCULATED BASED ON
!              A CONE WITH A VERTEX LOCATED 137 CM FROM THE SOURCE
!              PLANE. THE CONE HAS A HALF CONE ANGLE OPENING OF 22
!              DEGREES.
! V0.1 - CALCULATES SHIELD MASS AND VOLUME
!
! *****
IMPLICIT NONE

INTEGER :: I
REAL(8) :: RAD_LEFT, RAD_RIGHT !RADIUS OF SHIELD ON LEFT AND RIGHT FACES
REAL(8) :: X !POSTION IN SHIELD

!CHECK VOLUME AND MASS ARRAYS FOR ALLOCATION, THEN ALLOCATE
IF (ALLOCATED(VOLUME)) DEALLOCATE(VOLUME)
ALLOCATE(VOLUME(0:ZONES))

IF (ALLOCATED(MASS)) DEALLOCATE(MASS)
ALLOCATE(MASS(0:ZONES))

VOLUME(0) = 0.0
MASS(0) = 0.0
X = 0
RAD_LEFT = (X + 137) * SQRT(0.148)

!CALCULATE THE VOLUME AND MASS OF THE INDIVIDUAL SHIELD SECTIONS
DO I=1, ZONES
    X = X + REG_DIM(1,I)
    RAD_RIGHT = (X + 137) * SQRT(0.148)
    VOLUME(I) = (PI * REG_DIM(1,I) / 3.0D0) * (RAD_LEFT **2.0D0 + &
        (RAD_LEFT * RAD_RIGHT) + RAD_RIGHT ** 2.0D0)
    MASS(I) = VOLUME(I) * REG_DENSITY(I) / 1000.0D0
    RAD_LEFT = RAD_RIGHT
END DO

END SUBROUTINE SHIELD_PROPERTIES

! *****
!
! *****

```

```

ELEMENTAL FUNCTION ERROR(X,Y)

IMPLICIT NONE

REAL(8), INTENT(IN):: X, Y
REAL(8) :: ERROR

IF (X == 0.0 .AND. Y == 0.0) THEN
    ERROR = 0.0
ELSE
    ERROR = 2.0D0 * ABS(X-Y) / (ABS(X) + ABS(Y))
END IF

END FUNCTION ERROR

!*****
!
!*****

SUBROUTINE RESULTS

IMPLICIT NONE

INTEGER :: I
REAL(8) :: POSITION
CHARACTER(1) :: MODE

OPEN (UNIT=10, FILE = SHIELD_NAME, ACTION = 'WRITE', &
      STATUS = 'UNKNOWN')

WRITE(10,100) TRIM(SHIELD_NAME)
100 FORMAT("RESULTS FOR ", A, /, "=====")

WRITE(10,200) SRC_NEUTRON, SRC_PHOTON
200 FORMAT("SOURCE NEUTRON CURRENT = ", ES8.2, /, &
          "SOURCE PHOTON CURRENT = ", ES8.2, /)

MODE = "N"
DO
    WRITE(10,300) MODE
    300 FORMAT("RESULTS FOR MODE = ", A1)
    WRITE(10,400)
    400 FORMAT("POS. [CM]", T15, "MATERIAL", T25, "J_RT [N/S]", &
              T40, "J_LT [N/S]", T55, "VOLUME [CM^3]", T70, MASS &
              KG], /, "=====", T15, "=====", T25, &
              "=====", T40, "=====", T55, &
              "=====", T70, "=====", /)

    POSITION = 0.0D0
    DO I=0, ZONES
        POSITION = POSITION + REG_DIM(1,I)
        IF (MODE == "N") THEN
            WRITE(10,500) POSITION, TRIM(REG_NAME(I)), &
                          J_FWDN(1,I), J_REVN(1,I), &
                          VOLUME(I), MASS(I)

```

```

500 FORMAT(T2, F7.2, T16, A, T25, ES8.2, T40,&
           ES8.2, T55, ES8.2, T70, ES8.2)

ELSE

WRITE(10,600) POSITION, TRIM(REG_NAME(I)), &
              J_FWDP(1,I), J_REVP(1,I), &
              VOLUME(I), MASS(I)
600 FORMAT(T2, F7.2, T16, A, T25, ES8.2, T40,&
           ES8.2, T55, ES8.2, T70, ES8.2)

END IF

END DO

WRITE(10,700) SUM(VOLUME), SUM(MASS)
700 FORMAT(T55, "=====", /, T45, "TOTAL:", &
           T55, ES8.2, T70, ES8.2)
WRITE(10,800)
800 FORMAT(//)

IF (MODE == "P") EXIT
MODE = "P"
END DO

CLOSE(10)

END SUBROUTINE RESULTS

! *****
!
! *****
END MODULE EVAL_SHIELD

```



## Appendix D: “MissDiskProbability” Program

```
Program MissDiskProbability
!*****
!
! Program: MissDiskProbability
! By: K.A. Mathews for Ben Kowash
! Date: 28 Feb 02
!
! Description: This program is used to calculate the probability that a particle born a
!              location on one disk will miss another disk that is separated by some
!              distance delta_z. The program is used to indicate the effectiveness that
!              geometry has in allowing particles to leak from a system. The code used a
!              Monte Carlo technique to perform the estimation of the leakage probability.
!
!
! v.0.1: Implements Monte Carlo method to determine the probability of missing the disk
!        given a half cone angle and location of shields 1 and 2.
!
! v.0.2: Added user interface utility and output of data to file. Added by Ben Kowash.
!
!*****
Implicit None

Integer, Parameter :: dp = Selected_Real_Kind(p=14)
Integer, Parameter :: nBatches = 10, nParticles = 100000
Real(dp), Parameter :: pi = 3.1415926535897932
Integer :: batch, particle
Integer :: missed(1:nBatches)
Real(dp), Dimension(1:3) :: r1, r2, omegaHat
Real(dp) :: Radius1, Radius2, z1, z2, xi, omega, rFrac
Real(dp) :: pAvg, pMissed(1:nBatches)
Real(dp) :: Radius1Sqr, coneAngle, pCenter
Character(12) :: outfile
Character(1) :: calc_again

Write (*,"(A)",Advance = "NO") "Enter the output file name: "
Read (*,*) outfile

Open(Unit=20, File = Trim(outfile), Status = 'Unknown', Action = 'Write')
```

```

Write(20,100)
100 Format("Pos. 1", T10, "Pos 2", T20, "Prob. of Miss", T45, "Prob. of Miss From
      Center", /, &
      "=====", T10, "=====", T20, "=====", T45,
      "=====")
Do

  Write (*,"(A)",Advance = "NO") "Enter the half cone angle of the system [deg]: "
  Read (*,*) coneAngle
  Write (*,"(A)",Advance = "NO") "Enter the location of shield 1 [cm]: "
  Read (*,*) z1
  Write (*,"(A)",Advance = "NO") "Enter the location of shield 2 [cm]: "
  Read (*,*) z2

  missed = 0._dp
  coneAngle = coneAngle * pi / 180._dp
  Radius1 = z1 * tan(coneAngle)
  Radius2 = z2 * tan(coneAngle)
  Radius1Sqr = Radius1 ** 2._dp

  Call Random_Seed()

  Do batch = 1, nBatches

    Do particle = 1, nParticles

      Call Random_Number(xi)
      If (xi <= 1.e-6_dp) then
        missed = missed + 1
        Cycle
      End If

      Call Random_Number(omega)
      omega = 2._dp * pi * omega

      Call Random_Number(rFrac)
      rFrac = Sqrt(rFrac)

      r2 = (/ Radius2 * rFrac, 0._dp, z2 /)
      omegaHat = (/ cos(omega) * sqrt(1 - xi**2._dp), sin(omega) *
        sqrt(1 - xi**2._dp), -xi /)
      r1 = r2 + omegaHat * (z2 - z1) / xi

      If (r1(1)**2._dp + r1(2)**2._dp > Radius1Sqr)
        missed(batch) = missed(batch) + 1

```

```

        End do

        pMissed(batch) = Real(missed(batch),dp) / Real(nParticles,dp)

    End do

    Open(Unit=20, File = Trim(outfile), Status = 'Unknown', Action = 'Write')

    pAvg = Sum(pMissed) / nBatches
    Print *, "Average probability of missing disk 1 from disk 2 = ", pAvg

    pCenter = (z2 - z1) / sqrt((z2 - z1)**2._dp + Radius1Sqr)
    Print *, "Miss probability from center of disk 2 = ", pCenter

    Print *, "Batch results:"
    Do batch = 1, nBatches
        Print *, pMissed(batch)
    End do

    Write(20,200) z1, z2, pAvg, pCenter
    200 Format(F7.2, T10, F7.2, T20, F12.6, T45, F12.6)

    Write (*,"(A)",Advance = "NO") "Would you like to do another calculation [y/n]:
"

    Read (*,*) calc_again

    If (calc_again == 'n' .or. calc_again == 'N') Exit

End do

End Program MissDiskProbability

```

## Bibliography

1. Angelo, J.A. Jr. and D. Buden. *Space Nuclear Power*. Malabar, Florida: Orbit Book Company, Inc, 1985.
2. Aronson, R. and D.L. Yarmush. *Matrix Methods*. Engineering Compendium on Radiation Shielding, Vol I. Berlin/Heidelberg Germany: Springer-Verlag, 1968.
3. Barattino, William John. *Coupled Radiation Transport/Thermal Analysis of the Radiation Shield for a Space Nuclear Reactor*. PhD Dissertation, The University of New Mexico, Albuquerque NM, July 1985.
4. Berga, John O. *The Split Scatter Shield for Space Applications*. MS thesis, AFIT/GNE/61M. School of Engineering, Air Force Institute of Technology, Wright Patterson AFB OH, March 1961.
5. Grotenhuis, M. et al. *Radiation From Secondary Interactions*. Engineering Compendium on Radiation Shielding, Vol I. Berlin/Heidelberg Germany: Springer-Verlag, 1968.
6. Hamer, E.E. et al. *Materials Against Gamma Rays*. Engineering Compendium on Radiation Shielding, Vol II. Berlin/Heidelberg Germany: Springer-Verlag, 1968.
7. Hamer, E.E. et al. *Materials for Shielding Against Neutrons and Gamma Rays*. Engineering Compendium on Radiation Shielding, Vol II. Berlin/Heidelberg Germany: Springer-Verlag, 1968.
8. Jacox, M. et al. *Small Ex-Core Heat Pipe Thermionic Reactor (SEHPTR) Concept Characterization Report*. Idaho Falls ID: EG&G Idaho Inc, October 1991.
9. Keshishian, V. et al. *STAR-C: Thermionic Space Reactor Power System 2<sup>nd</sup> Technical Program Review*. Kirtland AFB NM: Phillips Laboratory, April 9, 1991.
10. Lee, L.W. Jr. *Shielding Analysis of a Small Compact Space Nuclear Reactor*. MS thesis, Air Force Weapons Laboratory, Kirtland AFB NM, August 1987.
11. Lewis, E.E. and W.F. Miller, Jr. *Computational Methods of Neutron Transport*. Illinois: American Nuclear Society Inc, 1993.
12. Mathews, Kirk A. Lecture, NENG 705, Computational Methods for Neutron Transport. Department of Engineering Physics, Air Force Institute of Technology, Wright-Patterson AFB OH, August 2001.

13. Mathews, Kirk A. Professor of Nuclear Engineering, Air Force Institute of Technology, Department of Engineering Physics, Wright-Patterson AFB OH. Personal interview. 29 Oct 01.
14. Mathews, Kirk A. Professor of Nuclear Engineering, Air Force Institute of Technology, Department of Engineering Physics, Wright-Patterson AFB OH. Personal interview. 28 Feb 02.
15. National Institute of Standards and Technology. *XCOM: Photon Cross-Sections Database*. Web program for viewing photon cross-sections.  
<http://physics.nist.gov/PhysRefData/Xcom/html/xcom1.html>. 27 Oct 01.
16. Nuclear Data Evaluation Lab. *ENDFLOT 0.2: Cross-Section Plotter*. Web program for viewing neutron cross-sections.  
<http://hpngp01.kaeri.re.kr/CoN/endlplot.shtml>. 11 Sep 01.
17. RSICC Computer Code Collection. *MCNP<sup>TM</sup> – A General Monte Carlo N-Particle Transport Code: Version 4C*. Los Alamos: Los Alamos National Laboratory, 18 Dec 2000.
18. Walker, W.F et al. *Nuclides and Isotopes Fourteenth Edition: Chart of the Nuclides*. California: GE Nuclear Energy, 1989.

REPORT DOCUMENTATION PAGE					Form Approved OMB No. 0704-0188	
<p>The public reporting burden for this collection of information is estimated to average 1 hour per response, including the time for reviewing instructions, searching existing data sources, gathering and maintaining the data needed, and completing and reviewing the collection of information. Send comments regarding this burden estimate or any other aspect of this collection of information, including suggestions for reducing the burden, to Department of Defense, Washington Headquarters Services, Directorate for Information Operations and Reports (0704-0188), 1215 Jefferson Davis Highway, Suite 1204, Arlington, VA 22202-4302. Respondents should be aware that notwithstanding any other provision of law, no person shall be subject to any penalty for failing to comply with a collection of information if it does not display a currently valid OMB control number.</p> <p><b>PLEASE DO NOT RETURN YOUR FORM TO THE ABOVE ADDRESS.</b></p>						
1. REPORT DATE (DD-MM-YYYY) 04-03-2002		2. REPORT TYPE Master's Thesis			3. DATES COVERED (From - To) Aug 2001 - Mar 2002	
4. TITLE AND SUBTITLE PARAMETER STUDY FOR OPTIMIZING THE MASS OF A SPACE NUCLEAR POWER SYSTEM RADIATION SHIELD					5a. CONTRACT NUMBER	
					5b. GRANT NUMBER	
					5c. PROGRAM ELEMENT NUMBER	
					5d. PROJECT NUMBER	
6. AUTHOR(S) Benjamin R. Kowash, 2nd Lt, USAF					5e. TASK NUMBER	
					5f. WORK UNIT NUMBER	
7. PERFORMING ORGANIZATION NAME(S) AND ADDRESS(ES) Air Force Institute of Technology Graduate School of Engineering and Management (AFIT/EN) 2950 P Street, Building 640 WPAFB OH 45433-7765					8. PERFORMING ORGANIZATION REPORT NUMBER AFIT/GNE/ENP/02M-4	
9. SPONSORING/MONITORING AGENCY NAME(S) AND ADDRESS(ES) N/A					10. SPONSOR/MONITOR'S ACRONYM(S)	
					11. SPONSOR/MONITOR'S REPORT NUMBER(S)	
12. DISTRIBUTION/AVAILABILITY STATEMENT APPROVED FOR PUBLIC RELEASE; DISTRIBUTION UNLIMITED.						
13. SUPPLEMENTARY NOTES						
<b>14. ABSTRACT</b> A parameter study was conducted for a space nuclear reactor radiation shield. The focus of this research was to explore alternatives to current radiation shield designs to reduce the mass while maintaining the same shielding performance. MCNP4C was used to determine the parameters necessary to build an optimum shield. A design known as the split scatter shield offered some potential for reductions in shield mass. In theory, less material is required for this type of shield, which uses thin shield sections to scatter radiation away from the dose plane. The parameters for this shield design are the shield geometry, number of shield sections, and material selection. Split scatter shielding offers a potential for reducing the shield mass by allowing the gamma shield material to be moved closer to the source plane. Further research needs to be conducted on this shielding technique however, to isolate optimum shield values. Once these optima have been identified, a split shield can be developed and compared to the original shield performance. Finally, an energy deposition study indicates that the split scatter shield will absorb less energy than the unit shield, implying that there may be less thermal stress on a scatter shield.						
<b>15. SUBJECT TERMS</b> Radiation Shielding, Space Nuclear Power Systems, Radiation Shield Optimization, Radiation Shield Design, Split Scatter Shielding						
16. SECURITY CLASSIFICATION OF:			17. LIMITATION OF ABSTRACT	18. NUMBER OF PAGES	19a. NAME OF RESPONSIBLE PERSON	
a. REPORT	b. ABSTRACT	c. THIS PAGE			Dr. Ronald F. Tuttle, ENP	
U	U	U	UU	117	19b. TELEPHONE NUMBER (Include area code) (937) 255-3636 ext 4536	